Dipl.-Ing. Elisabeth Rammerstorfer

The Kinetics and Mechanisms of Fouling in Crude Oil Heat Transfer

DISSERTATION

zur Erlangung des akademischen Grades

Doktorin der technischen Wissenschaften

eingereicht an der

Technischen Universität Graz

Betreuer

Univ.-Prof. Dipl.-Ing. Dr.techn. Matthäus Siebenhofer

Institut für chemische Verfahrenstechnik und Umwelttechnik

Graz, März 2018

EIDESSTATTLICHE ERKLÄRUNG

Ich erkläre an Eides statt, dass ich die vorliegende Arbeit selbstständig verfasst, andere als die angegebenen Quellen/Hilfsmittel nicht benutzt, und die den benutzten Quellen wörtlich und inhaltlich entnommenen Stellen als solche kenntlich gemacht habe. Das in TUGRAZonline hochgeladene Textdokument ist mit der vorliegenden Dissertation identisch.

Datum

Unterschrift

Acknowledgement

I would like to thank my supervisor Prof. Siebenhofer for his support.

I am grateful to Prozess Optimal CAP Gmbh and to my colleagues there for their assistance.

I am thankful for my family's strong support. I would like to thank my parents, my parents in law and my daughters. And I specially want to thank my husband for his unfailing support, which I greatly appreciate.

Abstract

The whole energy input for the atmospheric crude oil distillation comes from the crude oil, which is heated in the crude preheat train and a downstream furnace. The crude preheat train usually consists of a set of heat exchangers which have a tendency to become fouled. Fouling is the unwanted buildup of solids and sludge on the heat exchange surface which reduces thermal efficiency.

Asphaltene precipitation, particulate fouling, corrosion fouling and several chemical reactions are relevant for crude oil fouling. Since combination of mechanisms is responsible for deposition, crude oil fouling is generally referred to as mixed fouling.

Crude oil fouling can be caused by the following steps: chemical reaction, corrosion or asphaltene precipitation in the bulk, the film or on the surface; transport in the film and to the heat exchanger surface; adsorption of fluid constituents; desorption of the fouling products; transport of the fouling product to the bulk liquid, all steps in series. By assuming the single step to be rate controlling, fouling rate equations were developed which show the influence of the main variables fluid velocity and temperature on the fouling rate dR_f/dt.

By comparing experimental data with the modeled results, the rate equations investigated in this PhD thesis were used to determine the controlling step of fouling. The results showed, that no matter, what the fouling mechanism was, the effects of velocity and temperature on fouling rates dR_f/dt could best be described with the developed equations for fouling controlled by adsorption. This leads to the assumption, that either single steps or binary combinations of steps affect the fouling process, with adsorption always being a decisive step.

A couple of semi-empirical models for the prediction of time depending fouling in crude oil have been developed in recent years. Five of them were used to compare the results of modelling with these approaches.

The findings from kinetic modelling were used to summarize variables affecting fouling and to highlight possibilities to mitigate fouling by prevention or restriction of adsorption, minimization of particles initially present in the oil and minimization of production of new particles by corrosion, chemical reaction or asphaltene precipitation.

Table of contents

1 Problem definition

Atmospheric crude oil distillation is the first step in oil refining. The whole energy demand for the distillation process is covered by the crude oil, which is heated in the crude preheat train and a downstream furnace. The crude preheat train usually consists of a set of heat exchangers which transfer energy from processed bottoms of the crude oil distillation column to the feed (see figure 1).

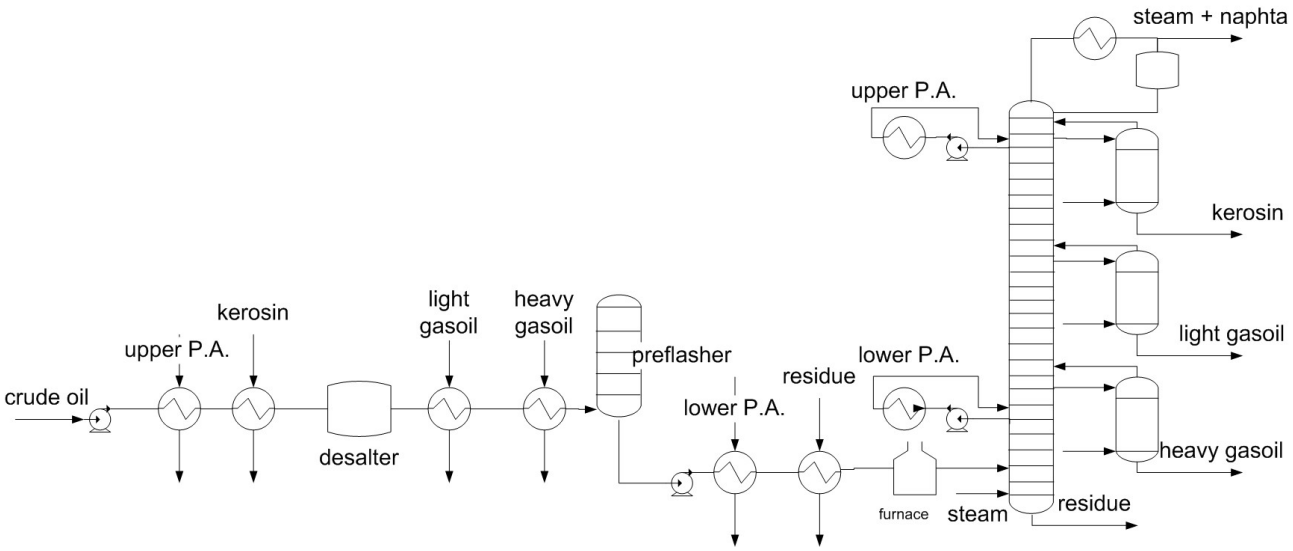

figure 1: preheat train and atmospheric crude distillation

Heat exchangers in the crude preheat train have a tendency to become fouled. Fouling is the unwanted buildup of material on the thermal exchange surface which reduces thermal efficiency.

1.1 Locations of crude oil fouling

Fouling is found in the whole preheat train but is severest for the last heat exchangers where temperatures are highest. The crude oil is usually heated up to about 200°C in the crude oil heat exchanger. Crude oil fouling also affects furnaces and atmospheric distillation columns. Figure 2 shows the units with an indication of hot spots with distinct tendency to severe fouling.

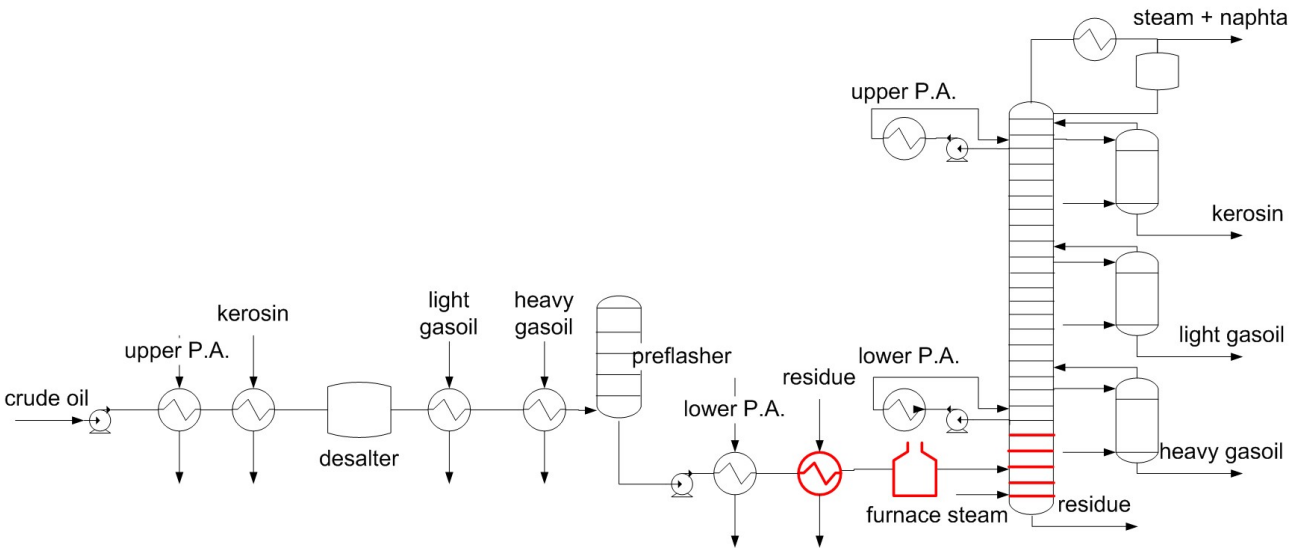

figure 2: preheat train and atmospheric crude distillation, units with a tendency to severe fouling are highlighted

Tube type heat exchangers are commonly used in the preheat train, with the crude oil usually being led tube side. Fouling can affect tube-side and shell-side. [Coletti and Hewitt 2015, S. 10] describe fouling on shell-side in low velocity zones in the vicinity of baffles as well as on the outsides of the tubes.

The transfer temperature to the distillation unit after the furnace is 370°C to 480°C. The crude oil is partly vaporized in the furnace. [Morales-Fuentes 2012] concludes that the fouling in the furnace is heaviest and argues that fouling rates depend on shear stress.

[Doug 2015] states that particularly tower trays in the lower section of the tower are prone to fouling. Like the fouling in the preheat train the deposits consist of organic and inorganic deposits. Fouling can also affect upper trays, especially for sour heavy crudes.

[Wang and Watkinson 2011] published a table containing the deposit composition of four crude oils from laboratory scale experiments. The data shows mixed organic and inorganic deposits. The carbon content ranges from 23% to 46%, the sulphur content between 12% and 22% and the iron content between 21-49%. This clearly shows, that inorganic fouling and organic fouling occur.

1.2 Impact of crude oil fouling

Fouling has a substantial economic and environmental impact. [ESDU 2000] estimates the costs of crude oil fouling in the western world with 4500 million USD per year. [Müller-Steinhagen et al. 2009] estimates, that fouling in refineries was responsible for 2,5% of total worldwide anthropogenic emissions in 2009.

2 Current design methods for heat exchangers

Heat transfer resistances (k) for shell and tube type heat exchangers are generally calculated with inner and outer heat transfer coefficients ($\alpha_{i,o}$), heat conductivity of the pipe (λ) and inner and out fouling resistances ($R_{fi,o}$), see figure 3 and equation 1.

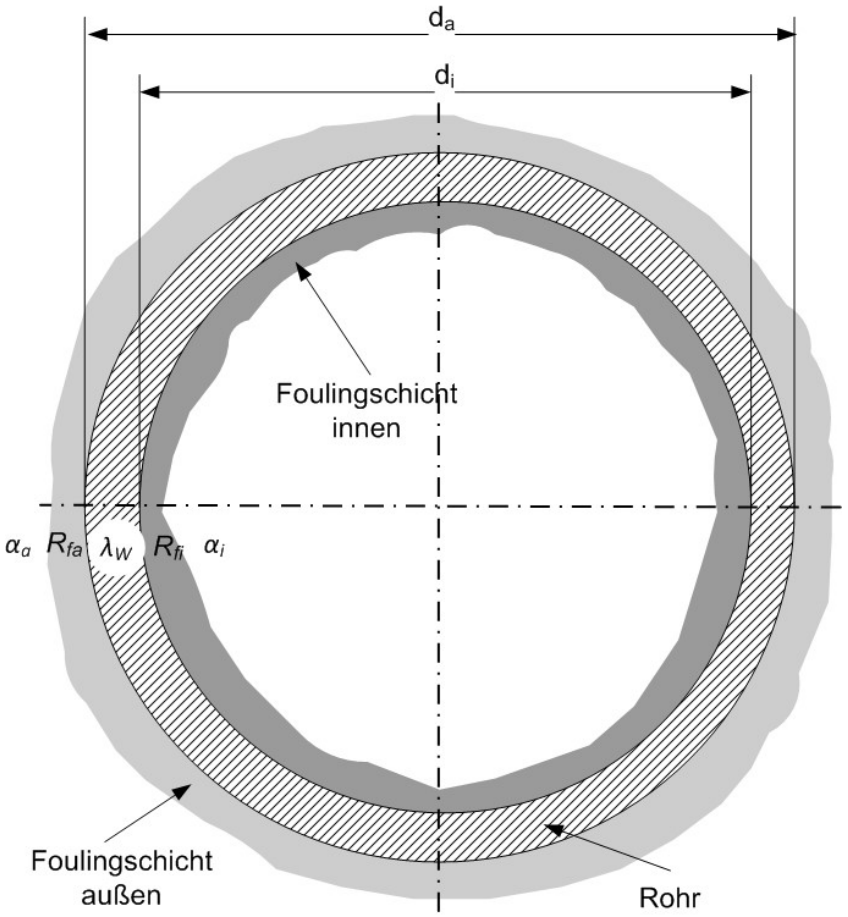

figure 3: inner and outer fouling layer in a heat exchanger tube

equation 1 $$\frac{1}{k} = \left(\frac{1}{\alpha_i} + R_{fi}\right)\frac{d_o}{d_i} + \frac{d_o \cdot ln(d_o/d_i)}{2 \cdot \lambda \cdot \pi} + \frac{1}{\alpha_o} + R_{fo}$$

Fouling resistances are traditionally assumed to be constant and rely on empirical fouling factors. Fouling factors should compensate the higher heat transfer resistance from losing performance over time due to fouling. These fouling factors don't consider the actual fouling dynamics. They merely act as safety factors and provide additional heat transfer area. Therefore, heat exchangers are oversized.

2.1 TEMA standard

The leading standard for the design of shell and tube type heat exchangers is "Standards of the tubular exchanger manufactures association" [TEMA 1999]. TEMA recommends constant fouling factors as state of the art practice and lists these factors in tables for different fluids.

TEMA fouling factors for crude oil are listed in table 1 and for crude oil distillation products in table 2. The fouling factors for crude oil take into account, that there is a dependency of fouling on heat exchanger temperature and velocity. Fouling factors increase with rising heat exchanger temperature and decrease with rising velocity. TEMA fouling factors for crude oil are listed for crude oil bearing salty water and desalted crude oil. At moderate temperatures fouling factors for crude oil bearing salty water are the same like the numbers for desalted crude oil, but are up to 100% higher at elevated temperatures.

	crude oil bearing salty water			
	< 120°C	120°C - 180°C	180°C - 230°C	> 230°C
< 6,5 m/s	0.00053	0.00088	0.00105	0.00123
6,5 - 26,0 m/s	0.00035	0.0007	0.00088	0.00106
> 26 m/s	0.00035	0.0007	0.0007	0.00088

	desalted crude oil			
	< 120°C	120°C - 180°C	180°C - 230°C	> 230°C
< 6,5 m/s	0.00053	0.00053	0.0007	0.00088
6,5 - 26,0 m/s	0.00035	0.00035	0.00053	0.0007
> 26 m/s	0.00035	0.00035	0.00035	0.00053

table 1: TEMA fouling factors [m^2K/W] for crude oil

gasoline	0.00018
naphta and light distillates	0,00018 -0,00053
kerosene	0,00018 -0,00053
light gas oil	0,00018 -0,00053
heavy gas oil	0,00053-0,00088
heavy fuel oil	0,00088-0,00123
atmosphere tower bottoms	0.00176
vaccum tower bottoms	0.00123

table 2: TEMA fouling factors [m^2K/W] for oil refinery products

2.2 VDI standard

VDI-Wärmeatlas [VDI 2006] is the leading standard in Germany for the calculation of shell and tube type heat exchangers. [VDI 2006] criticises the constant TEMA fouling factor approach. VDI-Wärmeatlas lists factors influencing the fouling factors:

- Fouling is related to the concentration of components which are responsible for fouling.
- Fouling decreases with rising shear stress and therefore increasing velocity, because of increasing removal, see equation 2.
  equation 2 $R_f \sim u^{-1,5}$
- Fouling rises exponential with heat transfer surface temperature, see equation 3.
  equation 3 $R_f \sim \exp\left(\frac{-E}{R \cdot T}\right)$
- Fouling rises with heat transfer surface roughness.

VDI-Wärmeatlas also underlines, that up to now even these simple dependencies are not considered in the design of heat exchangers. Nevertheless, VDI-Wärmeatlas recommends the use of TEMA fouling factors, as in practice are no alternatives available.

2.3 Summary

Constant fouling factors don't take into account the variables, that influence fouling, like temperature and velocity. Constant fouling factors additionally don't give any information about the period of time it takes to reach this fouling factors.

TEMA fouling factors are mainly available for streams in refineries and for water. A widespread criticism of constant TEMA fouling factors is that these factors don't consider the actual fouling dynamics. Fouling factors merely act as safety factors and contribute to additional heat transfer area. For clean service the heat exchangers are therefore oversized. [VDI 2006] observes that normally inlet an outlet temperature and mass flow of the product stream as well as inlet temperature of the heating or cooling medium are specified. The heat flow can therefore only be controlled by the velocity of the heating or cooling medium. For cleaning services, the velocity of the heating or cooling medium has to be decreased significantly. Lower velocities lead to less shear stress and reduced removal. Hence constant fouling factors can lead to increased fouling.

3 Analogies/demarcation

Fouling isn't limited to crude oil heat exchangers. It is present in nearly all processes where heat is exchanged; it has an important role in deactivating catalysts (chapter 3.1) and membrane blocking (chapter 3.2).

3.1 Catalyst deactivation

The activity of catalysts normally decreases over time. [Levenspiel 1999] distinguishes between:

- rapid deactivation, which is caused by deposition on the surface, for example carbon deposition in a catalytic cracking process; so called fouling, which can be removed by regeneration.
- slowly modifying catalyst surface by chemisorption, which is commonly referred to as poisoning, which can be removed partly by reactivation.

Both deactivation and poisoning are caused by the deposition of reaction products, side products or impurities in the feed.

In the field of heat exchanger fouling no distinction between fouling and poisoning is made. Both phenomena are applied under the same name, namely fouling.

3.2 Membrane fouling/scaling

In membrane filtration the precipitation or crystallisation of particles on the membrane surface, which results in a cover on the membrane surface, is in large parts responsible for the membrane performance. [Rautenbach 2007] distinguishes between particles on the membrane surface originally from

- suspended pollutants in the feed (fouling).
- dissolved substances, who start to precipitate or crystallize after exceeding the solubility limit (scaling).

In the field of heat exchanger fouling no distinction between fouling and scaling is made. Scaling is commonly referred to as crystallisation fouling.

4 Basics

Several fouling mechanisms are mentioned in the literature. While biofouling and crystallization fouling don't play an important role in crude oil fouling, asphaltene precipitation, particulate fouling, corrosion fouling and several chemical reactions are relevant for crude oil fouling, see table 3 and chapter 4.1 to 4.5. As a combination of mechanisms is responsible for deposition, crude oil fouling is generally referred to as mixed fouling, see chapter 4.6.

	Fouling Mechanisms
Corrosion Fouling	x
Fouling based on Solubility Changes	
Asphaltene Precipitation	x
Crystallisation Fouling	
Wax Crystallisation Fouling	
Chemical Reaction Fouling	
Autoxidation	x
Polymerization	x
Thermal Cracking	x
Particualte Fouling	x
Biofouling	

table 3: Fouling mechanisms relevant for crude oil fouling

4.1 Corrosion fouling

In crude oils corrosion fouling is one of the major fouling mechanism. [Somerscales 1997] reviewed the mechanism of corrosion fouling for oxygenated water. In crude oil oxygen is only found in traces. The mechanism in absence of oxygen differs considerably from the mechanism in presence of oxygen. [Wang and Watkinson 2011] describe three steps for corrosion in crude oils in the absence of oxygen, namely: corrosion of iron by organic acids (step 1a and 1b), thermal decomposition of acids salts (step 2) and reaction of iron oxide with organic sulphur or H_2S (step 3).

equation 4 $(step\ 1a)\quad 2RCH_2COOH + Fe \rightarrow (RCH_2COOH)_2Fe + H_2$

$(step\ 1b)\quad 2RCH_2COOH + Fe^{2+} \rightarrow (RCH_2COOH)_2Fe + 2H^+$

$(step\ 2)\quad (RCH_2COOH)_2Fe \rightarrow RCH_2COCH_2R + FeO + CO_2$

$(step\ 3a)\quad FeO + R' - S - R'' \rightarrow FeS + R' - O - R''$

$(step\ 3b)\quad FeO + H_2S \rightarrow FeS + H_2O$

All steps contribute to fouling on the surface of the heat exchanger. Step 1a can also occur in the bulk fluid. Reactions taking place on the surface will result in FeS films, reactions taking place in the bulk fluid will result in particulate FeS which can deposit elsewhere.

Formation of FeS is a governing fouling mechanism, especially at low temperatures and for sour crude oils [Wang and Watkinson 2011]. Fouling rates of corrosion fouling increase with temperature [Hazelton et al. 2015], but with rising temperatures fouling rates of other mechanism also increase.

Surface condition (especially roughness) and material as well as crude oil impurities influence corrosion fouling. In particular ammonia and hydrogen chloride can contribute to corrosion [Speight 2015, S. 10].

4.2 Fouling based on solubility limits

4.2.1 Asphaltene precipitation

Asphaltenes are defined as the n-heptane insoluble part of the crude oil, therefore the part which precipitates in n-heptane. To quantify the asphaltene concentration an anti-solvent is added to the hydrocarbon system. This measurement is in fact a so called antisolvent crystallization. Asphaltenes are shiny black solids with molecular weight between 1 000 to 100 000, with a high aromaticity and high concentrations of sulphur, nitrogen, nickel and vanadium [Wauquier 1995]. An average 3.000 molecular weight asphaltene can be modelled as $C_{205}H_{236}S_7O_3N_2$ [Wiehe 2012]. Because of the large molecules, the structure of asphaltenes varies widely.

Crude oils are often blended prior to processing in atmospheric crude oil distillation. Mixtures of incompatible crude oils are responsible for significant fouling due to asphaltene precipitation. [Saleh et al. 2005] and [Mason and Lin 2003] have reported that asphaltenes start to flocculate and the subsequent precipitation can cause significant fouling. [Watkinson 2005] states that for unstable oil blends the fouling deposits are similar to the precipitated asphaltenes. [Asomaning and Watkinson 2000] defined a colloidal instability index (C.I.I.) which quantifies crude oil

compatibility (equation 5). C.I.I. less than 1 means that asphaltenes are kept in dispersion, while C.I.I. above 1 means that asphaltene precipitation can be expected.

equation 5 $$C.I.I. = \frac{Saturates + Asphaltenes}{Aromatics + Resin}$$

Fouling caused by asphaltene precipitation is not limited to incompatible oils. Compatible oils as well may cause problems due to asphaltene precipitation [Wiehe et al. 2001]. Fouling can even be caused by self-incompatible crude oils, oils which do not have to be blended at all to lead to fouling caused by asphaltene precipitation. This indicates, that crude oil blending is not the only reason for fouling due to asphaltene precipitation.

Asphaltene precipitation is one of the main fouling mechanisms [Wang and Watkinson 2011], especially for unstable heavy oil systems [Watkinson 2005].

4.2.2 Crystallisation fouling

Crystallisation fouling is observed when liquids containing dissolved salts reach supersaturation due to temperature or pressure changes.

NaCl, $CaCl_2$ and $MgCl_2$ are common inorganic salts in crude oils [Bai and Wang 2007]. Every preheat train contains a desalter to reduce the concentration of dissolved salts. The removal of salts also retards corrosion. Crystallisation fouling can occur in crude oil heat exchangers downstream of the desalters, although it is not likely to be a dominant fouling mechanism.

4.2.3 Wax crystallisation fouling

Organic systems like crude oils contain dissolved wax components. These wax components will form wax crystals when the temperature falls below the cloud point temperature [Bott 1997]. Fouling is severest for heat exchangers with high temperature on tube and shell side exchanger temperatures, significantly exceeding cloud points. Therefore wax crystallisation fouling is not likely to be a major fouling mechanism.

4.3 Chemical reaction fouling

4.3.1 Autoxidation

Oxygen is usually present in very low concentration in crude oil. Autoxidation takes place in the presence of oxygen and leads to the formation of unwanted gums. These gums are not soluble in the surrounding crude oil and start to precipitate.

[Watkinson and Wilson 1997] describe autoxidation by a complex set of radical chain reactions (see equation 6). The initiation of the chain reaction is the abstraction of hydrogen from an organic molecule (RH) because of thermal decomposition (step 1). Initiation can also be caused by reaction with chemical initiators, metal ions or ultraviolet light. The free radical R· starts the chain reaction, it reacts with oxygen to the peroxy radical RO_2. (step 2), which creates a new free radical R· and hyrdoperoxide ROOH by consumption of another organic molecule (step 3). The chain reaction can terminate via step 4.

equation 6

$$\boldsymbol{Initiation}$$

$$(step\ 1)\ \ RH \xrightarrow{Initiator} R\cdot$$

$$\boldsymbol{Chain\ reaction}$$

$$(step\ 2)\ \ R\cdot + O_2 \rightarrow RO_2\cdot$$

$$(step\ 3)\ \ RO_2\cdot + RH \rightarrow ROOH + R\cdot$$

$$\boldsymbol{Termination}$$

$$(step\ 4)\ \ RO_2\cdot + RO_2\cdot \rightarrow ROOR + O_2$$

Step 3 can be catalysed by trace amounts of metal salts, especially of cobalt, manganese, iron, copper, chromium, lead and nickel [Coletti and Hewitt 2015, S. 29].

Autoxidation seems to be one of the main fouling mechanisms for low sulphur light crude oil [Watkinson 2005].

4.3.2 Polymerization

Polymerization fouling is a secondary effect of polymerization, a chemical reaction of monomers condensing to large polymers. Some of these large macromolecules are not soluble in the surrounding crude oil and start to precipitate. Polymerization can be expected when alkenes are present in the oil mixture, therefore it is restricted to crude oils blended with cracked feedstock [Coletti and Hewitt 2015, S. 29].

4.3.3 Thermal cracking

Above cracking temperature (about 350°C) cracking is the relevant fouling mechanism [Hazelton et al. 2015]. Fouling rates of thermal cracking fouling increase with temperature. High molecular weight hydrocarbons start to break into small hydrocarbon fractions by cleaving carbon bonds. The reaction produces coke. Thermal cracking starts at about 350°C. It will therefore mainly occur in the crude distillation furnace. But thermal cracking might still play a role in the aging of deposits, when fouling deposits remain for a long time on hot surfaces, with the temperature increasing as fouling proceeds [Coletti and Hewitt 2015, S. 30].

A synergistic relationship seems to exist between cracking and corrosion fouling. Fouling above cracking temperature starts with corrosion and shifts to coking [Hazelton et al. 2015].

Coking is strongly influenced by asphaltene stability [Derakhshesh 2013]. As the stability of asphaltenes in oil blends decreases, thermal cracking increases.

4.4 Particulate fouling

Particulate fouling for small particles or sedimentation for larger particles can play a role in crude oil fouling. It can occur when particles like dirt, clay or corrosion products formed elsewhere are transported with the crude oil. [Karabelas et al. 1997] conducted experiments with $CaCO_3$ particles in demineralised water to study particulate fouling. He found that the fouling resistance is asymptotic and is strongly affected by velocity. Therefore, he assumes that particulate fouling is adsorption controlled because this behaviour suggests that particle detachment has a dominant role. [Oliveira 1997] points out the importance of heat exchanger surfaces in connection with particulate fouling.

Particulate fouling seems to be a main fouling mechanism for low sulphur light crude oil [Watkinson 2005].

4.5 Biofouling

Biofouling covers fouling caused by bacteria and algae. It can be small for bacteria caused fouling or large when caused by algae or mussels. Although biofouling is an important issue for heat exchangers especially in aqueous systems [Melo and Bott 1997], biofouling does not play a role in crude oil fouling [Coletti and Hewitt 2015, S. 25].

4.6 Mixed fouling

Because of the varying composition of the processed crude oil and the wide temperature range several fouling mechanisms play an important role in crude oil fouling. As a combination of mechanisms is responsible for deposition, crude oil fouling is generally referred to as mixed fouling.

The fouling mechanism can be descried with three irreversible reactions in series (see equation 7). In the first step reactant A forms a precursor. Precursor B reacts to foulant C. High surface temperatures then lead to step three, the ageing of the foulant. The first two steps, the generation of precursors and the formation of the foulant, can take place either in the bulk, the boundary layer or the wall surface, see figure 4. Despite all the research activities of the last years in this field it is still not clear, where the reactions finally take place.

equation 7 $$Reactant\ A \rightarrow Precursor\ B \rightarrow Foulant\ C \rightarrow Aged\ deposit\ D$$

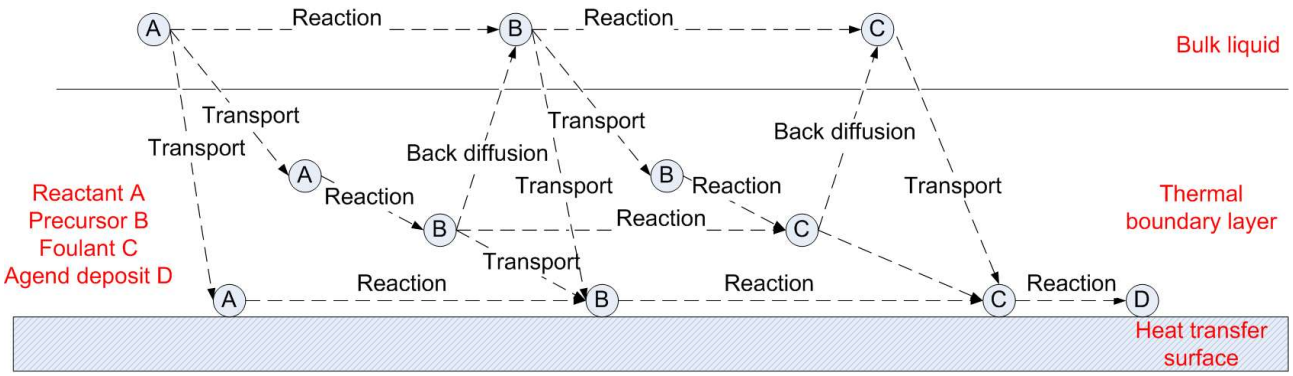

figure 4: Steps of generalized reaction fouling mechanisms. The generation of precursors and the formation of the foulant, can take place either in the bulk, the boundary layer or the heat exchanger surface. Adapted from [Coletti and Hewitt 2015, S. 35].

5 Fouling sequence

Fouling can be described by initiation, deposition, removal and aging, see figure 5. These steps can operate in parallel. The following chapters describe the different processes. The fouling resistance can be linear, descend asymptotically or follow a sawtooth rate, where significant removal takes place, see figure 5. The shape of the fouling curve depends mainly on the prevailing fouling mechanisms and the process conditions.

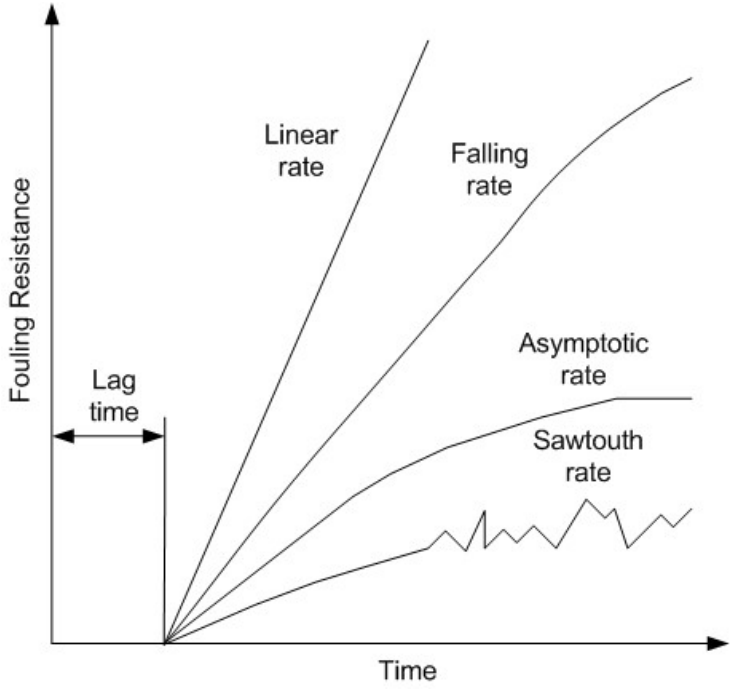

figure 5: Possible fouling curves.

5.1 Initiation

For a clean heat exchanger, the fouling sequence generally starts with an initiation period. After a lag time for the clean heat exchanger the fouling resistance starts growing. In this period little or no fouling can be observed, see figure 5. This period can last up to several days.

Surface temperature, fluid velocity and the heat exchanger surface affect the length of the initiation period. The initiation period is not well understood.

[Yang et al. 2011] proposed a model which can describe the fouling process from the induction period up to the steady fouling period. The model describes the influence of the surface temperature and shows, that an increase in surface temperature leads to a shorter induction period. It also shows, that shorter induction periods can be expected for initially not clean heat exchanger surfaces.

5.2 Deposition

The precursor or the foulant has to be transported from the bulk liquid or the thermal boundary layer to the heat transfer surface, see figure 4.

The transportation step is followed by an adsorption step in which the foulant or precursor becomes attached to the heat transfer surface. The transport of suspended particles can be described as diffusion. As diffusion increases with temperature, transport should therefore increase with surface and bulk temperature. When the transport step is the controlling step, fouling rates should increase linearly in turbulent flow because more particles are transported to the heat transfer surface. In laminar flow fouling rates should increase less because of the velocity boundary layer.

The adsorption step is temperature sensitive, increasing temperature should therefore lead to increased fouling rates, if adsorption is the controlling step. Higher velocities lead to reduced contact time, which means, that fouling rates should decrease.

5.3 Removal

The removal of deposited material generally occurs by shear stress or thermal stress or by diffusion, if the deposited material is soluble in the chemical bulk. Removal is observed for particles or particle clusters or deposit fragments. Removal mechanisms are not well understood, but removal is generally assumed to be dependent on shear stress and therefore on velocity.

[Yiantsios and Karabelas 1994] established a model for the removal kinetics of fouling of tube surfaces. They found in agreement with experimental results, that an increase in velocity results in a smaller asymptotic fouling resistance which is reached more rapidly. According to their model, the deposition rate does not affect the final deposit mass, but merely controls the time-scale. They suggested that the final deposit mass is controlled by the removal and not by the deposition step.

5.4 Aging

After the fouling the heat exchanger surface the deposited material is transformed to a usually more cohesive form. Transformation changes the chemical and physical nature of the deposit and therefore influences the thermal and hydraulic behaviour of the heat exchanger. It also influences

the dynamics of the fouling process itself and the ease with which the fouling layer can be removed.

Crude oil fouling is most likely a molecular transformation, when coking plays an important role [Wilson et al. 2009]. Aging impacts the fouling resistance [Coletti et al. 2010].

6 Kinetic modelling

Crude oil fouling can be approached by the following steps:

- chemical reaction, corrosion and asphaltene precipitation in the bulk;
- transport (diffusion) to the film;
- chemical reaction, corrosion and asphaltene precipitation in the film;
- transport (diffusion) to the heat transfer surface;
- adsorption;
- chemical reaction, corrosion and asphaltene precipitation on the heat transfer surface;
- desorption of the fouling product;
- transport (back diffusion) of the fouling product to the bulk liquid.

All steps are assumed to occur in series. Therefore for quasi steady state fouling, when the fouling layer is not growing, the overall rate of fouling r_f is equal the rate of diffusion r_{Di}, the rate of adsorption r_{Ad}, the rate of chemical reaction r_{Re}, the rate of corrosion r_{FeS} and the rate of asphaltene precipitation r_a, the rate of desorption r_{De}, the rate of back diffusion r_{BDi} , with all steps related to unit surface area, see equation 8.

equation 8 $$r_f = r_{Di} = r_{Ad} = r_{Re} = r_{FeS} = r_a = -r_{De} = -r_{BDi}$$

For the development of rate equations to describe fouling, it is assumed that the fouling layer is steadily developing. For the further discussion it is assumed, that the different steps like diffusion, adsorption and reaction do not interact. By assuming the single steps to be rate controlling, fouling rate equations were developed which show the influence of the main variables fluid velocity and temperature on the fouling rate.

Fouling will cause increasing heat transfer resistance through a growing deposit lawyer. Fouling resistance thus is related to the deposit thickness s_f or deposit mass per unit area m (equation 9).

equation 9 $$R_f = \frac{s_f}{\lambda_f} = \frac{m}{\lambda_f \cdot \rho_f}$$

From equation 9 the rate of fouling is obtained according to equation 10. The rate equation is valid for a flat wall. It can also be applied for fouling in pipes if the deposit thickness is considered to be very small in comparison to the pipe diameter, and when curvature effects can be neglected.

equation 10 $$\frac{dR_f}{dt} = \frac{ds_f}{dt} \cdot \frac{1}{\lambda_f}$$

$$\frac{dR_f}{dt} = \frac{dm}{dt} \cdot \frac{1}{\rho_f \cdot \lambda_f}$$

This approach can be further transformed, so that the fouling rate dR_f/dt becomes a function of the overall fouling rate r_f per unit surface area (see equation 11).

equation 11 $$\frac{dR_f}{dt} = \frac{dm}{dt} \cdot \frac{1}{\rho_f \cdot \lambda_f} = \frac{dn}{dt} \cdot \frac{M_f}{\rho_f \cdot \lambda_f}$$

$$\frac{dn}{dt} = r_f$$

$$\frac{dR_f}{dt} = r_f \cdot \frac{M_f}{\rho_f \cdot \lambda_f}$$

In industrial application the net fouling resistance is strongly dependent on the removal of the fouling layer because of shear stress. This influence cannot be considered in the kinetic model, as mechanical abrasion is not accessible by time dependent phenomena.

The kinetic model neglects the influence of surface roughness and changes in surface roughness. The fouling layer is considered as homogeneous. The shape of deposits is not considered. Change in flow velocity with changing cross-sectional area due to fouling is neglected.

Chapter 6.1 to 6.5 describe the kinetic modelling for the single controlling steps (diffusion, sorption, chemical reaction, corrosion and asphaltene precipitation).

6.1 Transport (diffusion) is rate controlling

6.1.1 Transport (diffusion) in the film and to the heat transfer surface is rate controlling

In a stagnant film the rate of diffusion or rate of mass transfer from the bulk fluid to a physical boundary can be described with the mass transfer coefficient k_{Di} and the concentration difference between bulk c_{Ab} and surface or film c_{As}. For surface related steps like adsorption, the concentration is normally given per m^2. Therefore, the concentration on the surface c_{As} has to be multiplied with the surface area per reactor volume a_s, see equation 12.

equation 12 $$\mathrm{r_{Di}} = \mathrm{k_{Di}} \cdot (\mathrm{c_{Ab}} - \mathrm{c_{As}} \cdot \mathrm{a_s}) = \mathrm{k_{Di}} \cdot \left(\mathrm{c_{Ab}} - \mathrm{c_{As}} \cdot \frac{\mathrm{A}}{\mathrm{V}}\right)$$

The mass transfer coefficient k_{Di} can be approached by the Sherwood number, see equation 13, where d is a characteristic length (the pipe diameter) and D_{AB} is the mass diffusivity.

equation 13 $$Sh = \frac{k_{Di} \cdot d}{D_{AB}}$$

Substituting mass transfer coefficient k_{Di} by the Sherwood number leads to equation 14.

equation 14 $$\mathrm{r_{Di}} = \frac{\mathrm{Sh} \cdot \mathrm{D_{AB}}}{\mathrm{d}} \cdot \left(\mathrm{c_{Ab}} - \mathrm{c_{As}} \cdot \frac{\mathrm{A}}{\mathrm{V}}\right)$$

To develop equations for transport in the film and to the heat transfer surface as controlling step, heat and mass transfer analogously was used to obtain Sherwood numbers from Nusselt numbers, see table 4.

Constant Nusselt numbers have been used for the development of the mass transfer coefficient for fully developed laminar flow, although strictly speaking this is only true for large numbers of Re·Pr·d/l.

For Nusselt numbers of fully turbulent flow in pipes the Dittus Boelter equation can be used to obtain the mass transfer coefficient necessary for the rate of diffusion.

Fully developed laminar flow in pipes	**Fully developed turbulent flow in pipes**
Nusselt number for constant surface temperature: $Nu = \frac{\alpha \cdot d}{\lambda} = 3.66$ (T_s=const.) Nusselt number for constant heat flow density: $Nu = \frac{\alpha \cdot d}{\lambda} = 4.364$ (q_w=const.)	Nusselt number from Dittus Boelter: $Nu = \frac{\alpha \cdot d}{\lambda} = 0.023 \cdot Re^{0.8} \cdot Pr^{0.4}$
Sherwood number with heat and mass transfer analogousy: $Sh = \frac{k_{Di} \cdot d}{D_{AB}} = 3.66$ (T_s=const.) $Sh = \frac{k_{Di} \cdot d}{D_{AB}} = 4.364$ (q_w=const.)	Sherwood number with heat and mass transfer analogousy: $Sh = \frac{k_{Di} \cdot d}{D_{AB}} = 0.023 \cdot Re^{0.8} \cdot Sc^{0.4}$

table 4: Sherwood number for fully developed laminar and turbulent flow in pipes

Sherwood number for fully developed turbulent flow in pipes is related to Reynolds and Schmidt number (equation 15 and equation 16).

equation 15 $Re = \frac{d \cdot u}{\nu}$

equation 16 $Sc = \frac{\nu}{D_{AB}}$

Using Sherwood number for the fully developed turbulent flow leads to the equations developed in table 5.

Fully developed laminar flow in pipes	**Fully developed turbulent flow in pipes**
$r_{Di} = 3.66 \cdot \left(c_{Ab} - c_{As} \cdot \frac{A}{V}\right)$ (T_w=const.) $r_{Di} = 4.364 \cdot \left(c_{Ab} - c_{As} \cdot \frac{A}{V}\right)$ (q_w=const.)	$r_{Di} = \frac{0.023 \cdot Re^{0.8} \cdot Sc^{0.4} \cdot D_{AB}}{d} \cdot \left(c_{Ab} - c_{As} \cdot \frac{A}{V}\right)$ $r_{Di} = \frac{0.023 \cdot \left(\frac{d \cdot u}{\nu}\right)^{0.8} \cdot \left(\frac{\nu}{D_{AB}}\right)^{0.4} \cdot D_{AB}}{d} \cdot \left(c_{Ab} - c_{As} \cdot \frac{A}{V}\right)$ $r_{Di} = 0.023 \cdot \frac{u^{0.8} \cdot {D_{AB}}^{0.6}}{d^{0.2} \cdot \nu^{0.4}} \cdot \left(c_{Ab} - c_{As} \cdot \frac{A}{V}\right)$

table 5: rate of diffusion per unit surface area r_{Di}

In case of diffusion control the overall fouling rate per unit surface area r_f is equal to the rate of diffusion per unit surface area r_{Di} (equation 17), which leads to the equations for the fouling rate dR_f/dt developed in table 6.

equation 17 $r_f = r_{Di}$

Fully developed laminar flow in pipes	**Fully developed turbulent flow in pipes**
$\frac{dR_f}{dt} = 3.66 \cdot \left(c_{Ab} - c_{As} \cdot \frac{A}{V}\right) \cdot \frac{M_f}{\rho_f \cdot \lambda_f}$ (T_w=const.) $\frac{dR_f}{dt} = 4.364 \cdot \left(c_{Ab} - c_{As} \cdot \frac{A}{V}\right) \cdot \frac{M_f}{\rho_f \cdot \lambda_f}$ (q_w=const.)	$\frac{dR_f}{dt} = 0.023 \cdot \frac{u^{0.8} \cdot {D_{AB}}^{0.6}}{d^{0.2} \cdot \nu^{0.4}} \cdot \left(c_{Ab} - c_{As} \cdot \frac{A}{V}\right) \cdot \frac{M_f}{\rho_f \cdot \lambda_f}$

table 6: fouling rate dR_f/dt for fouling controlled by diffusion

6.1.1.1 Temperature dependency of fouling controlled by diffusion

Assuming constant velocity and concentration the temperature dependency of diffusion controlled fouling can be described with the temperature dependency of the diffusivity D_{AB}. [Fogler 2006] specifies the following relationship, see equation 18.

equation 18 $D_{AB}(T_2) = D_{AB}(T_1) \cdot \frac{\mu_1}{\mu_2} \cdot \frac{T_{f,2}}{T_{f,1}}$

Typical physical property parameters of crude oil and their dependency of temperature are indicated by [Polley et al. 2002], see equation 19.

equation 19 $\rho = 917 - 0.833 \cdot T$

$$\mu = \nu \cdot \rho = 0.0985 \cdot \exp\left(\frac{406}{T}\right)$$

By using these relationships, the temperature dependency develops to the equations summarized in table 6. The equations show, that for fouling controlled by diffusion for fully developed laminar flow in pipes there is no temperature dependency and the temperature dependency for fully developed turbulent flow is very small, see equation 20 for an example and figure 6. Temperature effects are plotted as the logarithm of the initial fouling rate dR_f/dt versus the reciprocal of the temperature. This so called "fouling Arrhenius" plot is commonly used in the related literature.

Fully developed laminar flow in pipes	**Fully developed turbulent flow in pipes**
$\frac{dR_{f,2}}{dt} \sim \frac{dR_{f,1}}{dt}$	$\frac{dR_{f,2}}{dt} \sim \frac{dR_{f,1}}{dt} \cdot \left(\frac{T_{f,2}}{T_{f,1}}\right)^{0.6} \cdot \left(\frac{\mu_1}{\mu_2}\right)^{0.2} \cdot \left(\frac{\rho_2}{\rho_1}\right)^{0..4}$
	$\frac{dR_{f,2}}{dt} \sim \frac{dR_{f,1}}{dt} \cdot \left(\frac{T_{f,2}}{T_{f,1}}\right)^{0.6} \cdot \left(\frac{917-0.833*T_{f,2}}{917-0.833*T_{f,1}}\right)^{0.4} \cdot \left(\exp\left(\frac{406}{T_{f,1}} - \frac{406}{T_{f,2}}\right)\right)^{0.2}$

table 7: temperature dependency of fouling rate dR_f/dt for fouling controlled by diffusion

equation 20 $\frac{dR_{f,500K}}{dt} \sim \frac{dR_{f,400K}}{dt} \cdot 1.12$

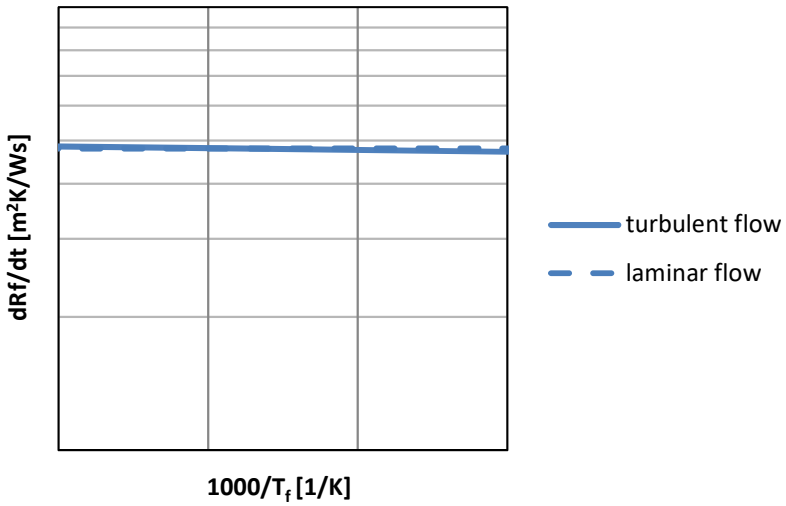

figure 6: temperature dependency of fouling rate dR_f/dt for diffusion controlled fouling, for fully developed laminar and turbulent flow

6.1.1.2 Velocity dependency of fouling controlled by diffusion

Assuming constant temperature and concentration the rate dependency of fouling controlled by diffusion can be described with the equations given in table 8. For fully developed laminar flow in pipes there is no velocity dependency, for fully developed turbulent flow the fouling rate dR_f/dt rises with increasing velocity to the power of 0.8. Temperature effects are plotted in figure 7.

Laminar flow in pipes	**Fully developed turbulent flow in pipes**
$\frac{dR_{f,2}}{dt} \sim \frac{dR_{f,1}}{dt}$	$\frac{dR_{f,2}}{dt} \sim \frac{dR_{f,1}}{dt} \cdot \left(\frac{u_2}{u_1}\right)^{0.8}$

table 8: velocity dependency of fouling rate dR_f/dt for fouling controlled by diffusion

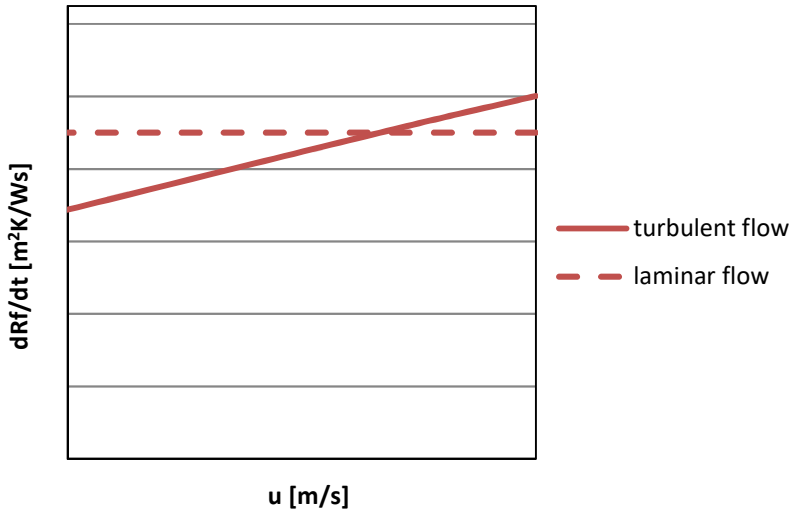

figure 7: velocity dependency of fouling rate dR_f/dt for diffusion controlled fouling

6.1.1.3 Discussion

Chapter 6.1.1.1 and 6.1.1.2 show that fouling rate for diffusion controlled fouling increases weakly for turbulent flow with temperature, because diffusion is favored at higher temperatures. For laminar flow there is no influence of temperature on diffusion.

For increasing velocity fouling rates increase linearly in turbulent flow because of increasing turbulent diffusion while for laminar flow fouling rates remain constant.

6.1.2 Back diffusion is rate controlling

The rate of diffusion per unit surface area r_{BDI} can be developed analogously to diffusion (see chapter 6.1). The results are summarized in table 9.

Fully developed laminar flow in pipes	**Fully developed turbulent flow in pipes**
$\mathrm{r_{BDi}} = 3.66 \cdot \left(c_{Fs} \cdot \frac{A}{V} - c_{Fb}\right)$ (T_s=const.) $\mathrm{r_{BDi}} = 4.364 \cdot \left(c_{Fs} \cdot \frac{A}{V} - c_{Fb}\right)$ (q_w=const.)	$\mathrm{r_{BDi}} = 0.023 \cdot \frac{u^{0.8} \cdot {D_{AB}}^{0.6}}{d^{0.2} \cdot \nu^{0.4}} \cdot \left(c_{Fs} \cdot \frac{A}{V} - c_{Fb}\right)$

table 9: rate of diffusion per unit surface area r_{BDI}

In case back diffusion is controlling the overall fouling rate per unit surface area r_f is equal to the negative rate of back diffusion per unit surface area r_{De} (equation 21), which leads to the equations for the fouling rate dR_f/dt developed in table 10.

equation 21 $r_f = -\mathrm{r_{BDi}}$

Fully developed laminar flow in pipes	**Fully developed turbulent flow in pipes**
$\frac{dR_f}{dt} = -3.66 \cdot \left(c_{Fs} \cdot \frac{A}{V} - c_{Fb}\right) \cdot \frac{M_f}{\rho_f \cdot \lambda_f}$ (T_s=const.) $\frac{dR_f}{dt} = -4.364 \cdot \left(c_{Fs} \cdot \frac{A}{V} - c_{Fb}\right) \cdot \frac{M_f}{\rho_f \cdot \lambda_f}$ (q_w=const.)	$\frac{dR_f}{dt} = -0.023 \cdot \frac{u^{0.8} \cdot {D_{AB}}^{0.6}}{d^{0.2} \cdot \nu^{0.4}} \cdot \left(c_{Fs} \cdot \frac{A}{V} - c_{Fb}\right) \cdot \frac{M_f}{\rho_f \cdot \lambda_f}$

table 10: fouling rate dR_f/dt of fouling controlled by back diffusion

6.1.2.1 Temperature dependency of fouling controlled by back diffusion

Assuming constant velocity and concentration the temperature dependency of fouling controlled by back diffusion can be developed by taking into account the temperature dependency of diffusivity and typical physical properties according to chapter 6.1.1. The results are summarized in table 11 and figure 8. The equations show, that for fouling controlled by back diffusion for fully developed laminar flow in pipes there is no temperature dependency and the temperature dependency for fully developed turbulent flow is very small.

Fully developed laminar flow in pipes	Fully developed turbulent flow in pipes
$-\frac{dR_{f,2}}{dt} \sim -\frac{dR_{f,1}}{dt}$	$-\frac{dR_{f,2}}{dt} \sim -\frac{dR_{f,1}}{dt} \cdot \left(\frac{T_{f,2}}{T_{f,1}}\right)^{0.6} \cdot \left(\frac{917-0.833*T_{f,1}}{917-0.833*T_{f,2}}\right)^{0.4} \cdot \left(\exp\left(\frac{406}{T_{f,2}} - \frac{406}{T_{f,1}}\right)\right)^{0.2}$

table 11: temperature dependency of fouling rate dR_f/dt of fouling controlled by back diffusion

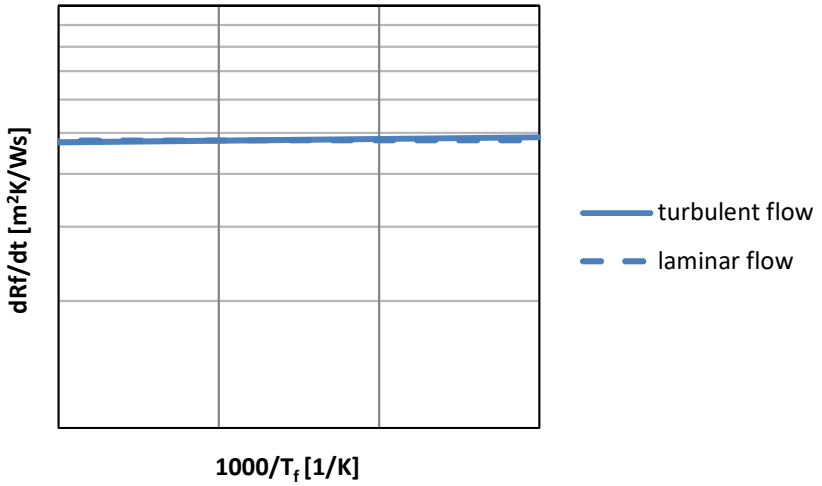

figure 8: temperature dependency of fouling rate dR_f/dt of fouling controlled by back diffusion

6.1.2.2 Velocity dependency of fouling controlled by back diffusion

Assuming constant temperature and concentration the rate dependency of fouling controlled by back diffusion can be described with the temperature equations given in table 12. For fully developed laminar flow in pipes there is no velocity dependency. If diffusion was the controlling mechanism for crude oil fouling, the fouling rate dR_f/dt would drop with increasing velocity, see figure 9.

Fully developed laminar flow in pipes	Fully developed turbulent flow in pipes
$-\frac{dR_{f,2}}{dt} \sim -\frac{dR_{f,1}}{dt}$	$-\frac{dR_{f,2}}{dt} \sim -\frac{dR_{f,1}}{dt} \cdot \left(\frac{u_2}{u_1}\right)^{0.8}$

table 12: velocity dependency of fouling rate dR_f/dt for back diffusion controlled fouling

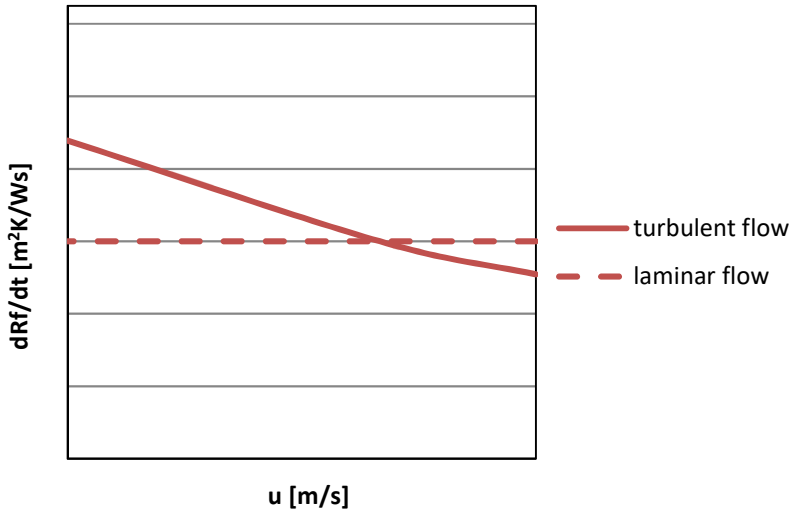

figure 9: velocity dependency of fouling rate dR_f/dt of fouling controlled by back diffusion

6.1.2.3 Discussion

Fouling rate for back diffusion controlled fouling decrease weakly with film temperature for turbulent flow with temperature, because diffusion is favored at higher temperatures. For laminar flow temperature does not have an influence on diffusion. For increasing velocity fouling rates decrease linearly in turbulent flow because of increasing turbulent diffusion while for laminar flow fouling rates remain constant.

6.2 Sorption is rate controlling

Adsorption can be observed as chemisorption or physisorption. Physisorption is mainly caused by van der Waals forces. Physisorption can be expected at relatively low temperatures, no chemical reaction between absorbate and surface takes place. Chemisorption occurs, when some kind of chemical reaction between adsorbate and surface takes place; typical examples are corrosion and heterogeneous catalysis.

Low binding energies of the absorbate to the surface indicate physisorption, high binding energies indicate chemisorption. For crude oil fouling chemisorption is likely to be the relevant mechanism.

Generally, adsorption data is reported with adsorption isotherms. An adsorption isotherm gives the amount of absorbed material for different pressures at equilibrium and for constant temperatures. The most widely known adsorption isotherms are the Langmuir isotherm and the Freundlich isotherm.

The Langmuit isotherme is a simple adsorption model, which describes adsorption as a single molecular layer on the surface of the adsorbing material and assumes, that all sites are equal accessible, and no interactions between sites and adsorbed material exist. The Freundlich isotherme describes a heterogeneous surface and takes into account that for heavy loaded surfaces less particles can be adsorbed.

Chapter 6.2.1 describes the kinetic modelling for adsorption as rate controlling step, see chapter 6.2.2 for desorption.

6.2.1 Adsorption is rate controlling

In order to obtain a rate law, adsorption is treated as an elementary chemical reaction, see equation 22 and figure 10, where A is a particle and S a surface site. A*S means, that A is adsorbed on the site S.

equation 22 $A + S = A * S$

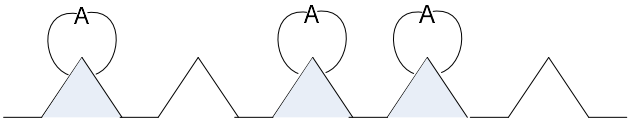

figure 10: vacant and occupied sites

The total number of available sites c_t is the sum of vacant sites c_v and sites, occupied by A, c_{A*S} (equation 23).

equation 23 $c_t = c_v + c_{A*S}$

The rate of adsorption per unit surface area r_{AD} for pseudo first and second order adsorption models is summarized in table 13.

For a pseudo first order model the rate of attachment of A $r_{AD,1}$ is proportional to the number of collisions with a surface active site per time. The collision rate is directly proportional to the concentration on the surface c_{As} and the concentration of vacant sites c_v. The concentration of vacant sites c_v is the difference of the total number of sites at the beginning of adsorption and the sites, occupied by A c_{A*S}.

For a pseudo second order model the rate of attachment of A $r_{AD,2}$ is proportional to the number of collisions with a surface active site per time ($c_{t,0}$ - c_{A*S}) to the second power and the concentration c_{AS}.

Pseudo first order adsorption model	Pseudo second order adsorption model
$r_{AD,1} = \frac{dc_{A*S}}{dt} = k_{AD1} \cdot \left(c_{t,o} - c_{A*S}\right) \cdot c_{AS}$	$r_{AD,2} = \frac{dc_{A*S}}{dt} = k_{AD2} \cdot \left(c_{t,o} - c_{A*S}\right)^2 \cdot c_{AS}$
$r_{AD,1} = \mathrm{A_{AD1}} \cdot \exp\left(\frac{-E}{R \cdot T_S}\right) \cdot \left(c_{t,o} - c_{A*S}\right) \cdot c_{AS}$	$r_{AD,2} = \mathrm{A_{AD2}} \cdot \exp\left(\frac{-E}{R \cdot T_S}\right) \cdot \left(c_{t,o} - c_{A*S}\right)^2 \cdot c_{AS}$

table 13: rate of adsorption per unit surface area r_{AD}

In case of adsorption being controlling the overall fouling rate per unit surface area r_f is equal to the rate of diffusion per unit surface area r_{Ad} (equation 24), which leads to the equations for the fouling rate dR_f/dt developed in table 14.

equation 24 $r_f = r_{Ad}$

Pseudo first order adsorption model	Pseudo second order adsorption model
$\frac{dR_f}{dt} = \frac{M_f}{\rho_f \cdot \lambda_f} \cdot \mathrm{A_{AD1}} \cdot \exp\left(\frac{-E}{R \cdot T_S}\right) \cdot \left(c_{t,o} - c_{A*S}\right) \cdot c_{AS}$	$\frac{dR_f}{dt} = \frac{M_f}{\rho_f \cdot \lambda_f} \cdot \mathrm{A_{AD1}} \cdot \exp\left(\frac{-E}{R \cdot T_S}\right) \cdot \left(c_{t,o} - c_{A*S}\right)^2 \cdot c_{AS}$

table 14: fouling rate dR_f/dt for fouling controlled by adsorption

6.2.1.1 Temperature dependency of fouling controlled by adsorption

Assuming constant velocity and concentration the temperature dependency of fouling controlled by adsorption can be described with the equations developed in table 15. The equations for temperature dependency are the same for pseudo first and second order adsorption models. Temperature effects are plotted in figure 11.

Pseudo first order adsorption model	Pseudo second order adsorption model
$\frac{dR_{f,2}}{dt} \sim \frac{dR_{f,1}}{dt} \cdot \frac{exp(\frac{-E}{R \cdot T_{S,2}})}{exp(\frac{-E}{R \cdot T_{S,1}})}$	$\frac{dR_{f,2}}{dt} \sim \frac{dR_{f,1}}{dt} \cdot \frac{exp(\frac{-E}{R \cdot T_{S,2}})}{exp(\frac{-E}{R \cdot T_{S,1}})}$
$\frac{dR_{f,2}}{dt} \sim \frac{dR_{f,1}}{dt} \cdot exp\left[\frac{E}{R} \cdot \left(\frac{1}{T_{S,1}} - \frac{1}{T_{S,2}}\right)\right]$	$\frac{dR_{f,2}}{dt} \sim \frac{dR_{f,1}}{dt} \cdot exp\left[\frac{E}{R} \cdot \left(\frac{1}{T_{S,1}} - \frac{1}{T_{S,2}}\right)\right]$

table 15: temperature dependency of fouling rate dR_f/dt for adsorption controlled fouling

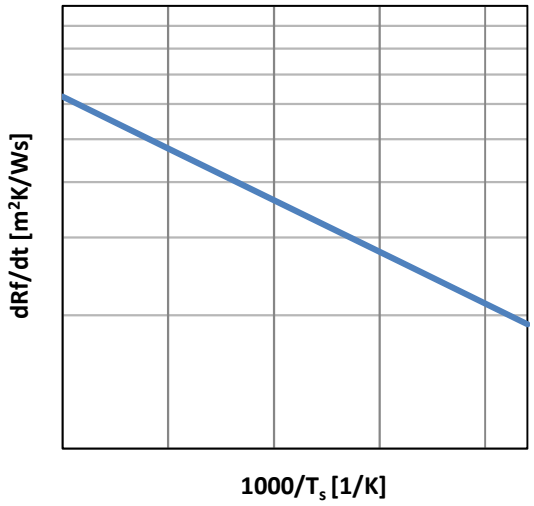

figure 11: temperature dependency of fouling rate dR_f/dt for adsorption controlled fouling

6.2.1.2 Velocity dependency of fouling controlled by adsorption

Assuming constant temperature the rate dependency of fouling controlled by adsorption can be developed by integrating the rate law, see table 16.

Pseudo first order adsorption model	Pseudo second order adsorption model
$\frac{dc_{A*S}}{(c_{t,o}-c_{A*S})} = k_{AD1} \cdot c_{AS} \cdot dt$	$\frac{dc_{A*S}}{(c_{t,o}-c_{A*S})^2} = k_{AD2} \cdot c_{AS} \cdot dt$
$\int \frac{dc_{A*S}}{(c_{t,o}-c_{A*S})} = \int k_{AD1} \cdot c_{AS} \cdot dt$	$\int \frac{dc_{A*S}}{(c_{t,o}-c_{A*S})^2} = \int k_{AD2} \cdot c_{AS} \cdot dt$
$\ln(c_{t,o} - c_{A*s}) + C = k_{AD1} \cdot c_{AS} \cdot t$ t=0: $c_{A*S} = 0$ $C = -\ln(c_{t,o})$ $\ln(c_{t,o} - c_{A*S}) - \ln(c_{t,o}) = k_{AD} \cdot c_{AS} \cdot t$ $\ln\left(\frac{c_{t,o}-c_{A*S}}{c_{t,o}}\right) = k_{AD1} \cdot c_{AS} \cdot t$ $c_{A*S} = c_{t,o} - c_{t,o} * \exp(k_{AD1} \cdot c_{AS} \cdot t)$	$-\frac{1}{(c_{t,o}-c_{A*S})} + C = k_{AD2} \cdot c_{AS} \cdot t$ t=0: $c_{A*S} = 0$ $C = \frac{1}{c_{t,o}}$ $-\frac{1}{c_{t,o}-c_{A*S}} + \frac{1}{c_{t,o}} = k_{AD2} \cdot c_{AS} \cdot t$ $c_{A*S} = c_{t,o} - \frac{1}{\frac{1}{c_{t,o}} - k_{AD2} \cdot c_{AS} \cdot t}$
$r_{AD,1} = k_{AD1} \cdot c_{t,o} * \exp(k_{AD1} \cdot c_{AS} \cdot t) \cdot c_{AS}$	$r_{AD,2} = k_{AD2} \cdot \left(\frac{1}{1-k_{AD2} \cdot c_{AS} \cdot t \cdot c_{t,o}}\right)^2 \cdot c_{AS}$
$\frac{dR_f}{dt} = \frac{M_f}{\rho_f \cdot \lambda_f} \cdot k_{AD1} \cdot c_{t,o} \cdot \exp(k_{AD1} \cdot c_{AS} \cdot t) \cdot c_{As}$	$\frac{dR_f}{dt} = \frac{M_f}{\rho_f \cdot \lambda_f} \cdot k_{AD2} \cdot \left(\frac{1}{1-k_{AD2} \cdot c_{AS} \cdot t \cdot c_{t,o}}\right)^2 \cdot c_{AS}$

table 16: time dependency of fouling rate dR_f/dt for fouling controlled by adsorption, developed by integrating the rate law

Assuming plug flow in the heat exchanger and constant velocity, time t (actually the residence time) can be expressed in terms of the length of the pipe l and the velocity u in the pipe (equation 25). Applying equation 25 to the developed equations for the fouling rate dR_f/dt leads to the equations shown in table 17. Velocity effects are plotted in figure 12.

equation 25 $t = \frac{l}{u}$

Pseudo first order adsorption model	Pseudo second order adsorption model
$\frac{dR_f}{dt} = \frac{M_f}{\rho_f * \lambda_f} \cdot k_{AD1} \cdot c_{t,o} \cdot \exp\left(k_{AD1} \cdot c_{AS} \cdot \frac{l}{u}\right) \cdot c_{AS}$	$\frac{dR_f}{dt} = \frac{M_f}{\rho_f \cdot \lambda_f} \cdot k_{AD2} \cdot \left(\frac{1}{1 - k_{AD2} \cdot c_{AS} \cdot c_{t,o} \cdot \frac{l}{u}}\right)^2 \cdot c_{AS}$
$\frac{dR_{f,2}}{dt} \sim \frac{dR_{f,1}}{dt} \cdot \frac{\exp\left(k_{AD1} \cdot c_{AS} \cdot \frac{l}{u_2}\right)}{ex\ \left(k_{AD1} \cdot c_{AS} \cdot \frac{l}{u_1}\right)}$	$\frac{dR_{f,2}}{dt} \sim \frac{dR_{f,1}}{dt} \cdot \frac{\left(\frac{1}{1 - k_{AD2} \cdot c_{AS} \cdot c_{t,o} \cdot \frac{l}{u_2}}\right)^2}{\left(\frac{1}{1 - k_{AD2} \cdot c_{AS} \cdot c_{t,o} \cdot \frac{l}{u_1}}\right)^2}$
$\frac{dR_{f,2}}{dt} \sim \frac{dR_{f,1}}{dt} \cdot \exp\left(k_{AD1} \cdot c_{AS} \cdot l \cdot \left(\frac{1}{u_2} - \frac{1}{u_1}\right)\right)$	$\frac{dR_{f,2}}{dt} \sim \frac{dR_{f,1}}{dt} \cdot \left(\frac{1 - k_{AD2} \cdot c_{AS} \cdot c_{t,o} \cdot \frac{l}{u_1}}{1 - k_{AD2} \cdot c_{AS} \cdot c_{t,o} \cdot \frac{l}{u_2}}\right)^2$

table 17: velocity dependency of fouling rate dR_f/dt for adsorption controlled fouling

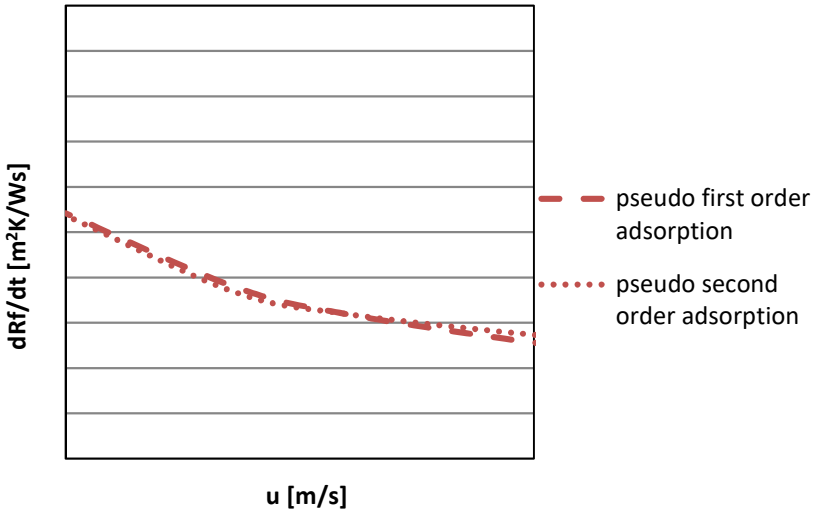

figure 12: velocity dependency of fouling rate dR_f/dt for adsorption controlled fouling

6.2.1.3 Discussion

Fouling rate for adsorption controlled fouling increases with surface temperature, because of the temperature sensitivity of the adsorption process. Fouling rates decrease with increasing velocity because of the reduced contact time for adsorption to occur.

6.2.2 Desorption is rate controlling

In order to obtain a rate law desorption is treated as an elementary chemical reaction, see equation 26 and figure 13, where F is a fouling particle and S a surface site. F*S means, that F is adsorbed on the site S.

equation 26 $F * S = F + S$

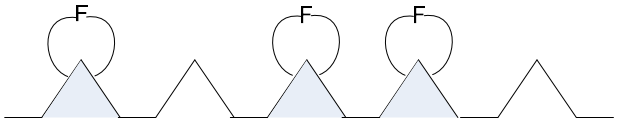

figure 13: vacant and occupied sites

The total number of available sites c_t is the sum of vacant sites c_v and sites, occupied by F, c_{F*S} (equation 27).

equation 27 $c_t = c_v + c_{F*S}$

The rate of desorption per unit surface area r_{De} for pseudo first and second order desorption models is summarized in table 13.

For a pseudo first order model the rate of detachment of F $r_{De,1}$ is proportional to the concentration of the adsorbed material. For a pseudo second order model for desorption the rate of detachment of F is proportional to the concentration of the adsorbed material to the second power.

Pseudo first order desorption model	Pseudo second order desorption model
$r_{De,1} = \frac{dc_F}{dt} = k_{De1} \cdot c_{F*S}$	$r_{De,2} = \frac{dc_F}{dt} = k_{De1} \cdot {c_{F*S}}^2$
$r_{De,1} = \mathrm{A_{De1}} \cdot \exp\left(\frac{-E}{R*T_S}\right) \cdot c_{F*S}$	$r_{De,2} = \mathrm{A_{De2}} \cdot \exp\left(\frac{-E}{R*T_S}\right) \cdot {c_{F*S}}^2$

table 18: rate of adsorption per unit surface area r_{De}

For fouling controlled by desorption the overall fouling rate per unit surface area r_f is equal to the negative rate of diffusion per unit surface area r_{De} (equation 28), which leads to the equations for the fouling rate dR_f/dt developed in table 9.

equation 28 $r_f = -r_{De}$

Pseudo first order desorption model	Pseudo second order desorption model
$\frac{dR_f}{dt} = -\frac{M_f}{\rho_f \cdot \lambda_f} \cdot \mathrm{A_{De1}} \cdot \exp\left(\frac{-E}{R \cdot T_S}\right) \cdot c_{F*S}$	$\frac{dR_f}{dt} = -\frac{M_f}{\rho_f \cdot \lambda_f} \cdot \mathrm{A_{De2}} \cdot \exp\left(\frac{-E}{R \cdot T_S}\right) \cdot {c_{F*S}}^2$

table 19: fouling rate dR_f/dt of fouling controlled by desorption

6.2.2.1 Temperature dependency of fouling controlled by desorption

Assuming constant velocity and concentration the temperature dependency of fouling controlled by desorption according to the rate expressions in table 19 can be described with the equations developed in table 20. The equations for temperature dependency are the same for pseudo first and second order desorption models. Temperature effects are plotted in figure 14.

Pseudo first order desorption model	Pseudo second order desorption model
$-\frac{dR_{f,2}}{dt} \sim -\frac{dR_{f,1}}{dt} \cdot \frac{exp(\frac{-E}{R \cdot T_{s,2}})}{exp(\frac{-E}{R \cdot T_{s,1}})}$	$-\frac{dR_{f,2}}{dt} \sim -\frac{dR_{f,1}}{dt} \cdot \frac{exp(\frac{-E}{R \cdot T_{s,2}})}{exp(\frac{-E}{R \cdot T_{s,1}})}$
$-\frac{dR_{f,2}}{dt} \sim -\frac{dR_{f,1}}{dt} \cdot exp\left[\frac{E}{R} \cdot \left(\frac{1}{T_{s,1}} - \frac{1}{T_{s,2}}\right)\right]$	$-\frac{dR_{f,2}}{dt} \sim -\frac{dR_{f,1}}{dt} \cdot exp\left[\frac{E}{R} \cdot \left(\frac{1}{T_{s,1}} - \frac{1}{T_{s,2}}\right)\right]$

table 20: temperature dependency of fouling rate dR_f/dt of fouling controlled by desorption, for pseudo first and second order desorption models

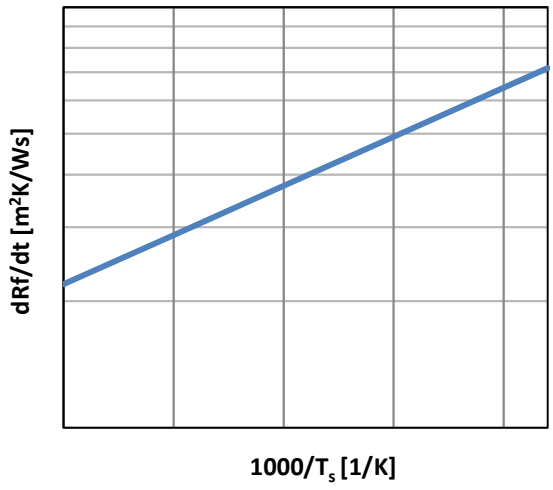

figure 14: temperature dependency of fouling rate dR_f/dt of fouling controlled by desorption, for pseudo first and second order desorption models

6.2.2.2 Velocity dependency of fouling controlled by desorption

Desorption is not a function of the bulk fluid concentration, therefore does not depend on velocity, see table 21 and figure 15.

Pseudo first order desorption model	Pseudo second order desorption model
$\frac{dR_{f,2}}{dt} \sim \frac{dR_{f,1}}{dt}$	$\frac{dR_{f,2}}{dt} \sim \frac{dR_{f,1}}{dt}$

table 21: velocity dependency of fouling rate dR_f/dt of fouling controlled by desorption, for pseudo first and second order desorption models

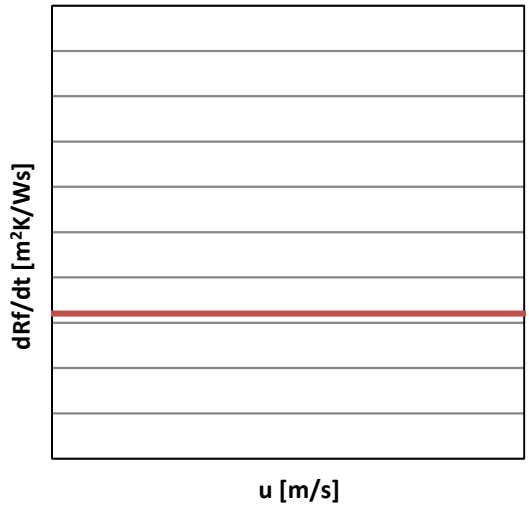

figure 15: velocity dependency of fouling rate dR_f/dt of fouling controlled by desorption, for pseudo first and second order desorption models

6.2.2.3 Discussion

Fouling rate for desorption controlled fouling decreases strongly with surface temperature, because of the temperature sensitivity of the process. Fouling rates do not show dependence from velocity as desorption is not influenced by contact time.

6.3 Chemical reaction is rate controlling

In order to develop equations for kinetic modelling, one has to know the chemical reaction order of the chemical reaction taking place. The reaction order is not forecastable. In a first approach it is assumed, that a specific phenomenological time dependent process may be of first or second order or even a pseudo zero order chemical reaction.

[Watkinson 2005] deduced a significant temperature dependency of fouling rates from experiments. Significant temperature dependency indicates, that a reaction process could govern the fouling rate. Chemical reactions can take place either in the bulk, the film or on the surface. Chapter 6.3.1 to 6.3.3 describe the development of fouling kinetic for all three of them.

6.3.1 Chemical reaction in the bulk is rate controlling

In equation 11 the overall fouling rate was defined per unit surface area, as diffusion, chemical reaction in the film, adsorption, chemical reaction on the heat exchanger surface and desorption depend on the surface area.

If the chemical reaction takes place in the fluid bulk, a chemical reaction rate per unit surface area cannot be applied. The chemical reaction rate in the bulk $r_{Re,b}$ has to be related to the surface area per reactor volume a_s, see equation 29.

equation 29 $$r_{Re} = \frac{r_{Re,b}}{a_S} = r_{Re,b} \cdot \frac{V}{A}$$

The rate of chemical reaction in the bulk $r_{re,b}$ for pseudo zero, first and second order chemical reaction is summarized in table 22.

Pseudo zero order chemical reaction	**First order chemical reaction**	**Second order chemical reaction**
$r_{Re,b,0} = \mathrm{k_{b0}}$	$r_{Re,b,1} = \mathrm{k_{b1}} \cdot \mathrm{c_{Ab}}$	$r_{Re,b,2} = \mathrm{k_{b2}} \cdot \mathrm{c_{Ab}}^2$
$r_{Re,b,0} = \mathrm{A_{b0}} \cdot \exp\left(\frac{-E}{R \cdot T_b}\right)$	$r_{Re,b,1} = \mathrm{A_{b1}} \cdot \exp\left(\frac{-E}{R \cdot T_b}\right) \cdot \mathrm{c_{Ab}}$	$r_{Re,b,2} = \mathrm{A_{b2}} \cdot \exp\left(\frac{-E}{R \cdot T_b}\right) \cdot \mathrm{c_{Ab}}^2$

table 22: rate of chemical reaction in the bulk $r_{Re,b}$ for pseudo zero, first and second order chemical reaction

In case chemical reaction in the bulk is controlling, the overall fouling rate r_f per unit surface area is equal to the rate of chemical reaction in the bulk r_{Re} per unit surface area (equation 30).

equation 30 $$r_f = r_{Re} = r_{Re,b} \cdot \frac{V}{A}$$

Therefore, the fouling rate dR_f/dt can be expressed according to table 23.

Pseudo zero order chemical reaction	First order chemical reaction	Second order chemical reaction
$\frac{dR_f}{dt} = A_{b0} \cdot exp\left(\frac{-E}{R \cdot T_b}\right) \cdot \frac{M_f}{\rho_f \cdot \lambda_f} \cdot \frac{V}{A}$	$\frac{dR_f}{dt} = A_{b1} \cdot exp\left(\frac{-E}{R \cdot T_b}\right) \cdot \frac{M_f}{\rho_f \cdot \lambda_f} \cdot \frac{V}{A} \cdot c_{Ab}$	$\frac{dR_f}{dt} = A_{b2} \cdot exp\left(\frac{-E}{R \cdot T_b}\right) \cdot \frac{M_f}{\rho_f \cdot \lambda_f} \cdot \frac{V}{A} \cdot c_{Ab}{}^2$

table 23: fouling rate dR_f/dt for fouling limited by chemical reaction in the bulk for pseudo zero, first and second order chemical reaction

6.3.1.1 Temperature dependency of fouling controlled by chemical reaction in the bulk

Assuming constant velocity and concentration the temperature dependency of fouling according to table 23, controlled by chemical reaction in the bulk can be described with the equations developed in table 24. The equations for temperature dependency are the same for pseudo zero, first and second order chemical reaction. Temperature effects are plotted in figure 16.

Pseudo zero order chemical reaction	First order chemical reaction	Second order chemical reaction
$\frac{dR_{f,2}}{dt} \sim \frac{dR_{f,1}}{dt} \cdot \frac{exp(\frac{-E}{R \cdot T_{b,2}})}{exp(\frac{-E}{R \cdot T_{b,1}})}$	$\frac{dR_{f,2}}{dt} \sim \frac{dR_{f,1}}{dt} \cdot \frac{exp(\frac{-E}{R \cdot T_{b,2}})}{exp(\frac{-E}{R \cdot T_{b,1}})}$	$\frac{dR_{f,2}}{dt} \sim \frac{dR_{f,1}}{dt} \cdot \frac{exp(\frac{-E}{R \cdot T_{b,2}})}{exp(\frac{-E}{R \cdot T_{b,1}})}$
$\frac{dR_{f,2}}{dt} \sim \frac{dR_{f,1}}{dt} \cdot exp\left[\frac{E}{R} \cdot \left(\frac{1}{T_{b,1}} - \frac{1}{T_{b,2}}\right)\right]$	$\frac{dR_{f,2}}{dt} \sim \frac{dR_{f,1}}{dt} \cdot \exp\left[\frac{E}{R} \cdot \left(\frac{1}{T_{b,1}} - \frac{1}{T_{b,2}}\right)\right]$	$\frac{dR_{f,2}}{dt} \sim \frac{dR_{f,1}}{dt} \cdot exp\left[\frac{E}{R} \cdot \left(\frac{1}{T_{b,1}} - \frac{1}{T_{b,2}}\right)\right]$

table 24: temperature dependency of fouling rate dR_f/dt of fouling controlled by chemical reaction in the bulk, for pseudo zero, first and second order chemical reaction

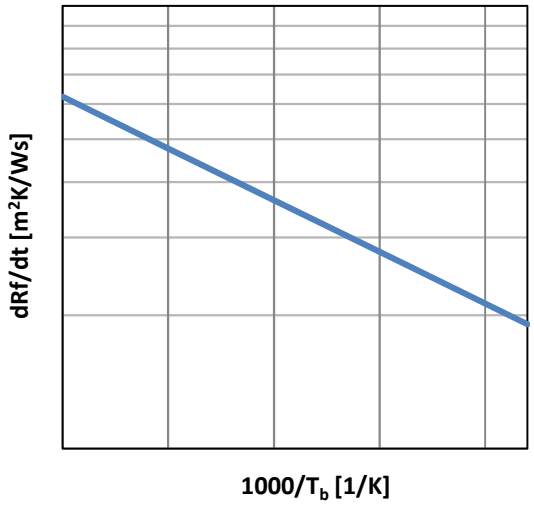

figure 16: temperature dependency of fouling rate dR_f/dt of fouling controlled by chemical reaction in the bulk

6.3.1.2 Velocity dependency of fouling controlled by chemical reaction in the bulk

Unlike pseudo zero order chemical reactions fouling rate for first order and second order chemical reactions are influenced by the concentration of A in the bulk c_{Ab}.

The rate dependency of fouling controlled by chemical reaction in the bulk can be developed by integrating the rate law, see table 25.

Pseudo zero order chemical reaction	**First order chemical reaction**	**Second order chemical reaction**
$-\frac{dc_{Ab}}{dt} = \mathrm{k_{b0}}$	$-\frac{dc_{Ab}}{dt} = \mathrm{k_{b1} \cdot c_{Ab}}$	$-\frac{dc_{Ab}}{dt} = \mathrm{k_{b2} \cdot c_{Ab}}^2$
$\int_{c_{Ab0}}^{c_{Ab}} dc_A = -\mathrm{k_{b0}} \cdot \int_0^t \mathrm{dt}$	$\int_{c_{Ab0}}^{c_{Ab}} \frac{dc_{Ab}}{c_{Ab}} = -\mathrm{k_{b1}} \cdot \int_0^t \mathrm{dt}$	$\int_{c_{Ab0}}^{c_A} \frac{dc_{Ab}}{{c_{Ab}}^2} = -\mathrm{k_{b2}} \cdot \int_0^t \mathrm{dt}$
$c_{Ab}/_{c_{Ab0}}^{c_{Ab}} = -\mathrm{k_{b0}} \cdot t/_0^t$ $c_{Ab} - c_{Ab0} = -\mathrm{k_{b0}} \cdot \mathrm{t}$ $c_{Ab} = c_{Ab} \ - \mathrm{k_{b0}} \cdot \mathrm{t}$	$\ln c_{Ab}\,/_{c_{Ab}}^{c_{Ab}} = -\mathrm{k_{b1}} \cdot t/_0^t$ $\ln c_{Ab} - \ln c_{Ab0} = -\mathrm{k_{b1}} \cdot \mathrm{t}$ $\ln \frac{c_{Ab}}{c_{Ab}} = -\mathrm{k_{b1}} \cdot \mathrm{t}$ $c_{Ab} = c_{Ab0} \cdot exp(-\mathrm{k_{b1}} \cdot \mathrm{t})$	$-\frac{1}{c_{Ab}}/_{c_{Ab}}^{c_{Ab}} = -\mathrm{k_{b2}} \cdot t/_0^t$ $\frac{1}{c_{Ab}} - \frac{1}{c_{Ab}} = \mathrm{k_{b2}} \cdot \mathrm{t}$ $c_{Ab} = \frac{c_{Ab0}}{c_{Ab} \cdot \mathrm{k_{b2}} \cdot \mathrm{t}+1}$

table 25: integrated rate laws for pseudo zero order, first order and second order chemical reaction

For liquid flow the velocity can be assumed to be constant, time t can be expressed in terms of the length of the pipe l and the velocity u in the pipe. This leads to the equations stated in table 17. Velocity effects are plotted in figure 17.

Pseudo zero order chemical reaction	**First order chemical reaction**	**Second order chemical reaction**
$c_{Ab} = c_{Ab0} - \mathrm{k_{b0}} \cdot \frac{\mathrm{l}}{\mathrm{u}}$	$c_{Ab} = c_{Ab0} \cdot exp\left(-\mathrm{k_{b1}} \cdot \frac{\mathrm{l}}{\mathrm{u}}\right)$	$c_{Ab} = \frac{c_{Ab0}}{c_{Ab0} \cdot \mathrm{k_{b2}} \cdot \frac{\mathrm{l}}{\mathrm{u}} + 1}$
$\frac{\mathrm{dR_f}}{\mathrm{dt}} = \mathrm{k_{b0}} \cdot \frac{M_f}{\rho_f * \lambda_f} \cdot \frac{V}{A}$	$\frac{dR_f}{dt} = \mathrm{k_{b1}} \cdot \frac{M_f}{\rho_f \cdot \lambda_f} \cdot \frac{V}{A} \cdot c_{Ab0} \cdot exp\left(-\mathrm{k_{b1}} \cdot \frac{\mathrm{l}}{\mathrm{u}}\right)$	$\frac{dR_f}{dt} = \mathrm{k_{b2}} \cdot \frac{M_f}{\rho_f \cdot \lambda_f} \cdot \frac{V}{A} \cdot \left(\frac{c_{Ab0}}{c_{Ab0} \cdot \mathrm{k_{b2}} \cdot \frac{\mathrm{l}}{\mathrm{u}} + 1}\right)^2$
$\frac{dR_{f,2}}{dt} \sim \frac{dR_{f,1}}{dt}$	$\frac{dR_{f,2}}{dt} \sim \frac{dR_{f,1}}{dt} \cdot \frac{exp(\frac{-\mathrm{k_{b1}} \cdot \mathrm{l}}{u_2})}{exp(\frac{-\mathrm{k_{b1}} \cdot \mathrm{l}}{u_1})}$ $\frac{dR_{f,2}}{dt} \sim \frac{dR_{f,1}}{dt} \cdot exp\left[\mathrm{k_{b1}} \cdot \mathrm{l} \cdot \left(\frac{1}{u_1} - \frac{1}{u_2}\right)\right]$	$\frac{dR_{f,2}}{dt} \sim \frac{dR_{f,1}}{dt} \cdot \left(\frac{\frac{c_{Ab0}}{c_{Ab} \cdot \mathrm{k_{b2}} \cdot \frac{\mathrm{l}}{u_2} + 1}}{\frac{c_{Ab0}}{c_{Ab0} \cdot \mathrm{k_{b2}} \cdot \frac{\mathrm{l}}{u_1} + 1}}\right)^2$ $\frac{dR_{f,2}}{dt} \sim \frac{dR_{f,1}}{dt} \cdot \left(\frac{c_{Ab} \cdot \mathrm{k_{b2}} \cdot \frac{\mathrm{l}}{u_1} + 1}{c_{Ab0} \cdot \mathrm{k_{b2}} \cdot \frac{\mathrm{l}}{u_2} + 1}\right)^2$

table 26: velocity dependency of fouling rate dR_f/dt of fouling controlled by chemical reaction in the bulk

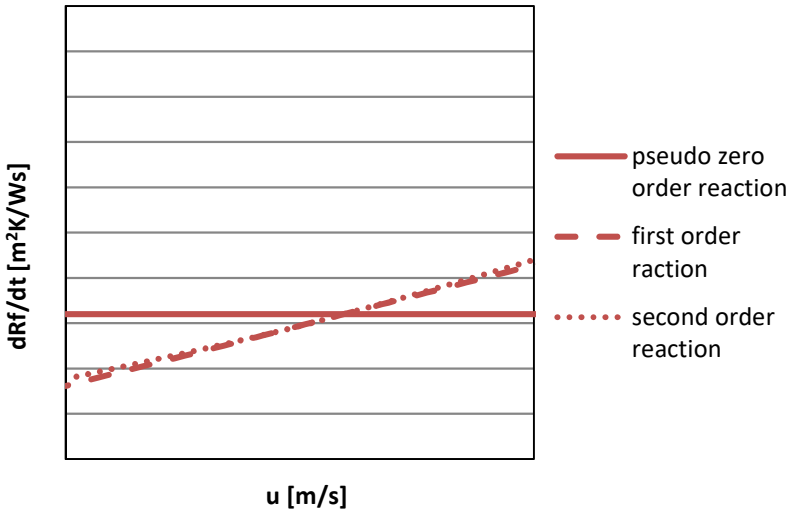

figure 17: velocity dependency of fouling rate dR_f/dt of fouling controlled by chemical reaction in the bulk

Initial fouling is not rate dependent, see table 27 and figure 18.

Pseudo zero order chemical reaction	First order chemical reaction	Second order chemical reaction
$\frac{dR_{f,2}}{dt} \sim \frac{dR_{f,1}}{dt}$	$\frac{dR_{f,2}}{dt} \sim \frac{dR_{f,1}}{dt}$	$\frac{dR_{f,2}}{dt} \sim \frac{dR_{f,1}}{dt}$

table 27: velocity dependency of fouling rate dR_f/dt of fouling controlled by chemical reaction in the bulk, for pseudo zero, first and second order chemical reaction, for initial fouling

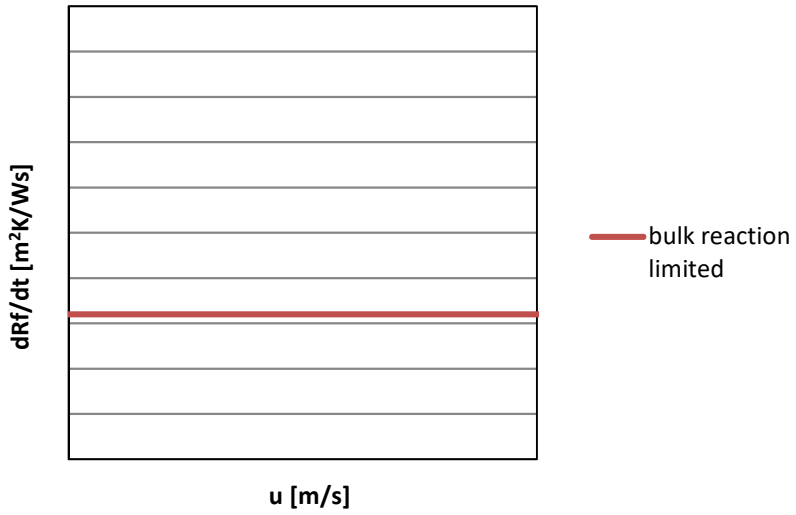

figure 18: velocity dependency of fouling rate R_f/dt of fouling controlled by chemical reaction in the bulk, for initial fouling

6.3.1.3 Discussion

Fouling rate for fouling controlled by chemical reaction in the bulk increases strongly with bulk temperature, because of the temperature sensitivity of reaction processes.

The fouling rate of pseudo zero order chemical reactions shows no dependency of the concentration of A in bulk c_{Ab}. For the fouling rate for first order and second order fouling this is different. At low velocity the fluid spends more time in the heat exchanger and the concentration of A in the bulk depletes according to the order of the constituent involved while the fluid passes the heat exchanger.

For initial fouling, before concentration in the bulk has changed, there is no dependency of concentration and therefore of velocity.

6.3.2 Chemical reaction in the film is rate controlling

The rate of chemical reaction in the film per unit surface area $r_{Re,f}$ for pseudo zero, first and second order chemical reaction is summarized in table 28.

Pseudo zero order chemical reaction	First order chemical reaction	Second order chemical reaction
$r_{Re,f,0} = \mathrm{k_{f0}}$	$r_{Re,f,1} = \mathrm{k_{f1}} \cdot \mathrm{c_{Af}}$	$r_{Re,f,2} = \mathrm{k_{f2}} \cdot \mathrm{c_{Af}}^2$
$r_{Re,f,0} = \mathrm{A_{f0}} \cdot \exp\left(\frac{-E}{R \cdot T_f}\right)$	$r_{Re,f,1} = \mathrm{A_{f1}} \cdot \exp\left(\frac{-E}{R \cdot T_f}\right) \cdot \mathrm{c_{Af}}$	$r_{Re,f,2} = \mathrm{A_{f2}} \cdot \exp\left(\frac{-E}{R \cdot T_f}\right) \cdot \mathrm{c_{Af}}^2$

table 28: rate of chemical reaction in the film per unit surface area r_{Re} for pseudo zero, first and second order chemical reaction

In case that chemical reaction in the film is controlling the overall fouling rate per unit surface area r_f is equal to the rate of chemical reaction in the film per unit surface area $r_{Re,f}$ (equation 31), which leads to the equations for the fouling rate dR_f/dt developed in table 29.

equation 31 $r_f = r_{Re,f}$

Pseudo zero order chemical reaction	First order chemical reaction	Second order chemical reaction
$\frac{dR_f}{dt} = A_{f0} \cdot exp\left(\frac{-E}{R \cdot T_f}\right) \cdot \frac{M_f}{\rho_f \cdot \lambda_f}$	$\frac{dR_f}{dt} = A_{f1} \cdot exp\left(\frac{-E}{R \cdot T_f}\right) \cdot \frac{M_f}{\rho_f \cdot \lambda_f} \cdot c_{Af}$	$\frac{dR_f}{dt} = A_{f2} \cdot exp\left(\frac{-E}{R \cdot T_f}\right) \cdot \frac{M_f}{\rho_f \cdot \lambda_f} \cdot {c_{Af}}^2$

table 29: fouling rate dR_f/dt of fouling controlled by chemical reaction in the film, for pseudo zero, first and second order chemical reaction

6.3.2.1 Temperature dependency of fouling controlled by chemical reaction in the film

Assuming constant velocity and concentration the temperature dependency of fouling controlled by chemical reaction in the film can be described with the equations developed in table 30. The equations for temperature dependency are the same for pseudo zero, first and second order chemical reaction. Temperature effects are plotted in figure 19.

Pseudo zero order chemical reaction	First order chemical reaction	Second order chemical reaction
$\frac{dR_{f,2}}{dt} \sim \frac{dR_{f,1}}{dt} \cdot \frac{exp(\frac{-E}{R \cdot T_{f,2}})}{exp(\frac{-E}{R \cdot T_{f,1}})}$	$\frac{dR_{f,2}}{dt} \sim \frac{dR_{f,1}}{dt} \cdot \frac{exp(\frac{-E}{R \cdot T_{f,2}})}{exp(\frac{-E}{R \cdot T_{f,1}})}$	$\frac{dR_{f,2}}{dt} \sim \frac{dR_{f,1}}{dt} \cdot \frac{exp(\frac{-E}{R \cdot T_{f,2}})}{exp(\frac{-E}{R \cdot T_{f,1}})}$
$\frac{dR_{f,2}}{dt} \sim \frac{dR_{f,1}}{dt} \cdot exp\left[\frac{E}{R} \cdot \left(\frac{1}{T_{f,1}} - \frac{1}{T_{f,2}}\right)\right]$	$\frac{dR_{f,2}}{dt} \sim \frac{dR_{f,1}}{dt} \cdot exp\left[\frac{E}{R} \cdot \left(\frac{1}{T_{f,1}} - \frac{1}{T_{f,2}}\right)\right]$	$\frac{dR_{f,2}}{dt} \sim \frac{dR_{f,1}}{dt} \cdot exp\left[\frac{E}{R} \cdot \left(\frac{1}{T_{f,1}} - \frac{1}{T_{f,2}}\right)\right]$

table 30: temperature dependency of fouling rate dR_f/dt of fouling controlled by chemical reaction in the film, for pseudo zero, first and second order chemical reaction

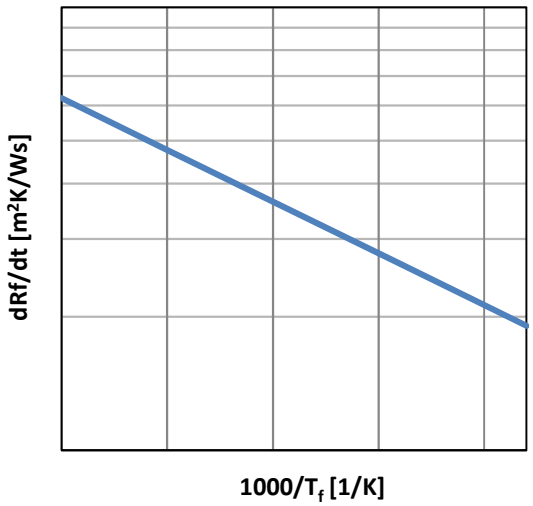

figure 19: temperature dependency of fouling rate dR_f/dt of fouling controlled by chemical reaction in the film

6.3.2.2 Velocity dependency of fouling controlled by chemical reaction in the film

The velocity dependency of chemical reaction in the bulk controlled fouling can be developed by assuming, that the rate of fouling per unit surface area $r_{Re,f}$ is equal to the rate of diffusion per unit surface area r_{Di} for slow chemical reaction in the film (see equation 32 and table 31). For surface related steps the concentration is normally given per m^2. Therefore, the concentration in the film c_{Af} has to be multiplied with the surface area per reactor volume a_s.

equation 32 $r_{Di} = k_{Di} \cdot \left(c_{Ab} - c_{Af} \cdot a_s\right) = k_{Di} \cdot \left(c_{Ab} - c_{Af} \cdot \frac{A}{V}\right)$

$r_{Re,f} = r_{Di}$

Pseudo zero order chemical reaction	**First order chemical reaction**	**Second order chemical reaction**
$k_{f0} = k_{Di} \cdot \left(c_{Ab} - c_{Af} \cdot \frac{A}{V}\right)$	$k_{f1} \cdot c_{Af} = k_{Di} \cdot \left(c_{Ab} - c_{Af} \cdot \frac{A}{V}\right)$	$k_{f2} \cdot c_{Af}^2 = k_{Di} \cdot \left(c_{Ab} - c_{Af} \cdot \frac{A}{V}\right)$
$c_{Af} = \frac{k_{Di} \cdot c_{Ab} - k_0}{k_{Di}} = \left(c_{Ab} - \frac{k_{f0}}{k_{Di}}\right) \cdot \frac{V}{A}$	$c_{Af} = \frac{k_{Di} \cdot c_{Ab}}{k_{f1} + k_{Di}} = c_{Ab} \cdot \frac{k_{Di}}{k_{f1} + k_{Di}} \cdot \frac{V}{A}$	for a slow chemical reaction: $k_{f2} \ll k_{Di}$
for a slow chemical reaction: $k_{f0} \ll k_{Di}$	for a slow chemical reaction: $k_{f1} \ll k_{Di}$	$0 = k_{Di} \cdot \left(c_{Ab} - c_{Af}\right)$
$c_{Af} = c_{Ab} \cdot \frac{V}{A}$	$c_{Af} = c_{Ab} \cdot \frac{V}{A}$	$c_{Af} = c_{Ab} \cdot \frac{V}{A}$

table 31: concentration of A in the film of fouling controlled by chemical reaction in the film

The rate dependency of fouling controlled by fouling in the film can be developed by integrating the rate law, see table 33.

Pseudo zero order chemical reaction	First order chemical reaction	Second order chemical reaction
$-\frac{dc_{Af}}{dt} = \mathrm{k_{f0}}$ $-\frac{dc_{Ab}}{dt} = \mathrm{k_{f0}}$	$-\frac{dc_{Af}}{dt} = \mathrm{k_{f1}} \cdot \mathrm{c_{Af}}$ $-\frac{V}{A} \cdot \frac{dc_{Ab}}{dt} = \mathrm{k_{f1}} \cdot \mathrm{c_{Ab}} \cdot \frac{V}{A}$	$-\frac{dc_{Af}}{dt} = \mathrm{k_{f2}} \cdot \mathrm{c_{Af}}^2$ $-\frac{V}{A} \cdot \frac{dc_{Ab}}{dt} = \mathrm{k_{f2}} \cdot \mathrm{c_{Ab}}^2 \cdot \left(\frac{V}{A}\right)^2$
$\int_{c_{Ab0}}^{c_{Ab}} dc_A = -\mathrm{k_{b0}} \cdot \int_0^t \mathrm{dt}$	$\int_{c_{Ab0}}^{c_{Ab}} \frac{dc_{Ab}}{c_{Ab}} = -\mathrm{k_{b1}} \cdot \int_0^t \mathrm{dt}$	$\int_{c_{Ab0}}^{c_A} \frac{dc_{Ab}}{{c_{Ab}}^2} = -\mathrm{k_{b2}} \cdot \frac{V}{A} \cdot \int_0^t \mathrm{dt}$
$c_{Ab}/_{c_{Ab0}}^{c_{Ab}} = -\mathrm{k_{b0}} \cdot t/_0^t$ $c_{Ab} - c_{Ab0} = -\mathrm{k_{b0}} \cdot \mathrm{t}$ $c_{Ab} = c_{Ab0} - \mathrm{k_{b0}} \cdot \mathrm{t}$	$\ln c_{Ab}/_{c_{Ab0}}^{c_{Ab}} = -\mathrm{k_{b1}} \cdot t/_0^t$ $\ln c_{Ab} - \ln c_{Ab0} = -\mathrm{k_{b1}} \cdot \mathrm{t}$ $\ln \frac{c_{Ab}}{c_{Ab0}} = -\mathrm{k_{b1}} \cdot \mathrm{t}$ $c_{Ab} = c_{Ab0} \cdot exp(-\mathrm{k_{b1}} \cdot \mathrm{t})$	$-\frac{1}{c_{Ab}}/_{c_{Ab0}}^{c_{Ab}} = -\mathrm{k_{b2}} \cdot \frac{V}{A} \cdot t/_0^t$ $\frac{1}{c_{Ab}} - \frac{1}{c_{Ab0}} = \mathrm{k_{b2}} \cdot \frac{V}{A} \cdot \mathrm{t}$ $c_{Ab} = \frac{c_{Ab0}}{c_{Ab0} \cdot \mathrm{k_{b2}} \cdot \frac{V}{A} \cdot \mathrm{t}+1}$

table 32: integrated rate laws for pseudo zero, first order and second order reaction

By using the bulk concentration c_{Ab} from table 32, the fouling rate dR_f/dt can be developed (table 33). Velocity effects are plotted in figure 20.

Pseudo zero order chemical reaction	First order chemical reaction	Second order chemical reaction
$c_{Af} = c_{Ab} \cdot \frac{V}{A} =$ $\left(c_{Ab0} - \mathrm{k_{f0}} \cdot \frac{l}{u}\right) \cdot \frac{V}{A}$	$c_{Af} = c_{Ab} \cdot \frac{V}{A} =$ $c_{Ab0} \cdot exp\left(-\mathrm{k_{f1}} \cdot \frac{l}{u}\right) \cdot \frac{V}{A}$	$c_{Af} = c_{Ab} \cdot \frac{V}{A} =$ $\frac{c_{Ab}}{c_{Ab0} \cdot \mathrm{k_{f2}} \cdot \frac{V}{A} \cdot \frac{l}{u}+1} \cdot \frac{V}{A}$
$\frac{dR_f}{dt} = A_{f0} \cdot exp\left(\frac{-E}{R \cdot T_f}\right) \cdot \frac{M_f}{\rho_f \cdot \lambda_f}$	$\frac{dR_f}{dt} = A_{f1} \cdot exp\left(\frac{-E}{R \cdot T_f}\right) \cdot \frac{M_f}{\rho_f \cdot \lambda_f} \cdot$ $c_{Ab} \cdot exp\left(-\mathrm{k_{f1}} \cdot \frac{l}{u}\right) \cdot \frac{V}{A}$	$\frac{dR_f}{dt} = A_{f2} \cdot exp\left(\frac{-E}{R \cdot T_f}\right) \cdot \frac{M_f}{\rho_{f*} \lambda_f} \cdot$ $\left(\frac{c_{Ab0}}{c_{Ab0} \cdot \mathrm{k_{f2}} \cdot \frac{V}{A} \cdot \frac{l}{u}+1} \cdot \frac{V}{A}\right)^2$
$\frac{dR_{f,2}}{dt} \sim \frac{dR_{f,1}}{dt}$	$\frac{dR_{f,2}}{dt} \sim \frac{dR_{f,1}}{dt} \cdot \frac{exp\left(-\mathrm{k_{f1}} \cdot \frac{l}{u_2}\right)}{exp\left(-\mathrm{k_{f1}} \cdot \frac{l}{u_1}\right)}$ $\frac{dR_{f,2}}{dt} \sim \frac{dR_{f,1}}{dt} \cdot$ $exp\left[\mathrm{k_{f1}} \cdot \mathrm{l} \cdot \left(\frac{1}{u_1} - \frac{1}{u_2}\right)\right]$	$\frac{dR_{f,2}}{dt} \sim \frac{dR_{f,1}}{dt} \cdot \left(\frac{\frac{c_{Ab0}}{c_{Ab0} \cdot \mathrm{k_{f2}} \cdot \frac{V}{A} \cdot \frac{l}{u_2}+1}}{\frac{c_{Ab}}{c_{Ab0} \cdot \mathrm{k_{f2}} \cdot \frac{V}{A} \cdot \frac{l}{u_1}+1}}\right)^2$ $\frac{dR_{f,2}}{dt} \sim \frac{dR_{f,1}}{dt} \cdot \left(\frac{c_{Ab} \cdot \mathrm{k_{f2}} \cdot \frac{V}{A} \cdot \frac{l}{u_1}+1}{c_{Ab0} \cdot \mathrm{k_{f2}} \cdot \frac{V}{A} \cdot \frac{l}{u_2}+1}\right)^2$

table 33: velocity dependency of fouling rate dR_f/dt of fouling controlled by chemical reaction in the film

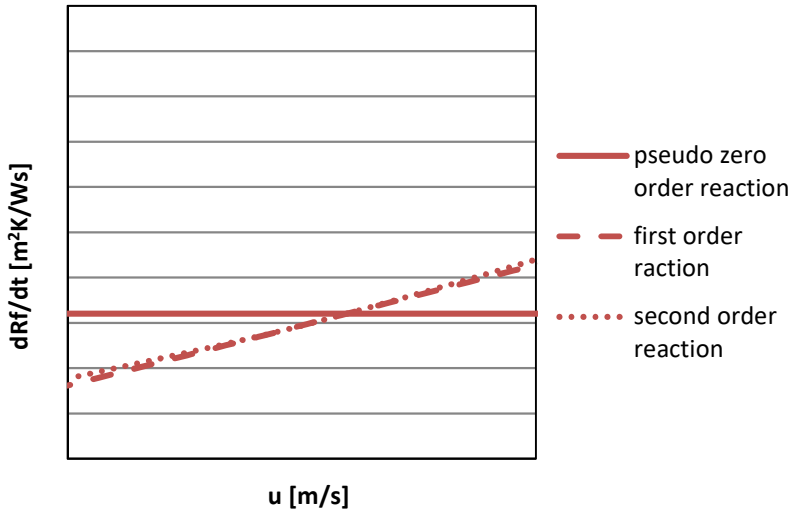

figure 20: velocity dependency of fouling rate dR_f/dt of fouling controlled by chemical reaction in the film

Initial fouling is not rate dependent, see table 34 and figure 21.

Pseudo zero order chemical reaction	First order chemical reaction	Second order chemical reaction
$\frac{dR_{f,2}}{dt} \sim \frac{dR_{f,1}}{dt}$	$\frac{dR_{f,2}}{dt} \sim \frac{dR_{f,1}}{dt}$	$\frac{dR_{f,2}}{dt} \sim \frac{dR_{f,1}}{dt}$

table 34: velocity dependency of fouling rate dR_f/dt of fouling controlled by chemical reaction in the film, for initial fouling

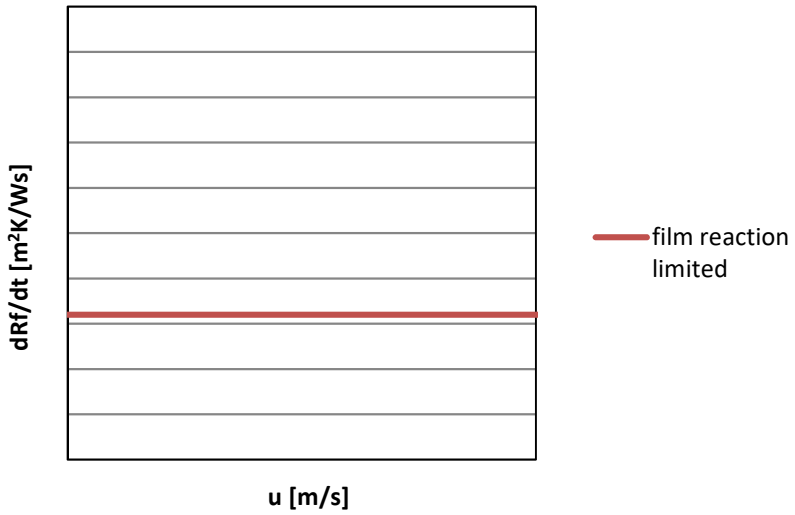

figure 21: velocity dependency of fouling rate dR_f/dt of fouling controlled by chemical reaction in the film, for initial fouling

6.3.2.3 Discussion

Fouling rate for fouling controlled by chemical reaction in the film increases strongly with film temperature, because of the temperature sensitivity of reaction processes.

The fouling rate of pseudo zero order chemical reactions shows no dependency of the concentration of A in bulk c_{Ab}. For the fouling rate for first order and second order fouling this is different. At low velocity the fluid spends more time in the heat exchanger and the concentration of A in the bulk depletes according to the order of the constituents involved while the fluid passes the heat exchanger.

For initial fouling, before concentration in the bulk has changed, there is no dependency of concentration and therefore of velocity.

6.3.3 Chemical reaction on the surface is rate controlling

The equations for fouling controlled by chemical reaction on the surface can be developed analogous to the equations for chemical reaction in the film. The temperature of the film has to be substituted by the temperature on the surface, see table 35.

Pseudo zero order chemical reaction	First order chemical reaction	Second order chemical reaction
$\frac{dR_f}{dt} = A_{s0} \cdot exp\left(\frac{-E}{R \cdot T_s}\right) \cdot \frac{M_f}{\rho_f \cdot \lambda_f}$	$\frac{dR_f}{dt} = A_{s1} \cdot exp\left(\frac{-E}{R \cdot T_s}\right) \cdot \frac{M_f}{\rho_f * \lambda_f} \cdot c_{As}$	$\frac{dR_f}{dt} = A_{s2} \cdot exp\left(\frac{-E}{R \cdot T_s}\right) \cdot \frac{M_f}{\rho_f \cdot \lambda_f} \cdot {c_{As}}^2$

table 35: fouling rate dR_f/dt of fouling controlled by chemical reaction on the surface, for pseudo zero, first and second order chemical reaction

6.3.3.1 Temperature dependency of fouling controlled by chemical reaction on the surface

Assuming constant velocity and concentration the temperature dependency of fouling controlled by chemical reaction on the surface can be described with the equations in table 36. The equations for temperature dependency are the same for pseudo zero, first and second order chemical reaction. Temperature effects are plotted in figure 22.

Pseudo zero order chemical reaction	First order chemical reaction	Second order chemical reaction
$\frac{dR_{f,2}}{dt} \sim \frac{dR_{f,1}}{dt} \cdot exp\left[\frac{E}{R} \cdot \left(\frac{1}{T_{s,1}} - \frac{1}{T_{s,2}}\right)\right]$	$\frac{dR_{f,2}}{dt} \sim \frac{dR_{f,1}}{dt} \cdot exp\left[\frac{E}{R} \cdot \left(\frac{1}{T_{s,1}} - \frac{1}{T_{s,2}}\right)\right]$	$\frac{dR_{f,2}}{dt} \sim \frac{dR_{f,1}}{dt} \cdot exp\left[\frac{E}{R} \cdot \left(\frac{1}{T_{s,1}} - \frac{1}{T_{s,2}}\right)\right]$

table 36: temperature dependency of fouling rate dR_f/dt of fouling controlled by chemical reaction on the surface, for pseudo zero, first and second order chemical reaction

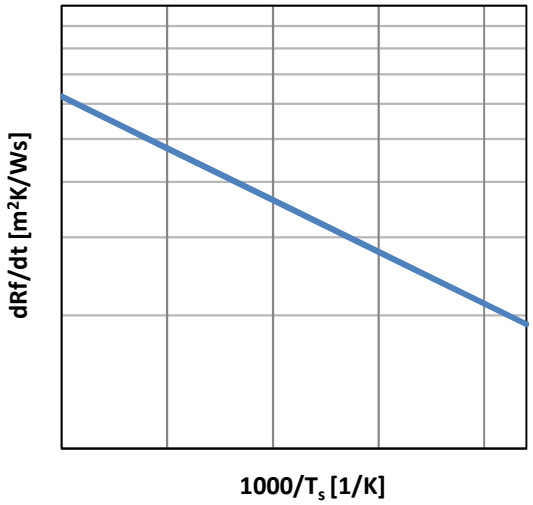

figure 22: temperature dependency of fouling rate dR_f/dt of fouling controlled by chemical reaction on the surface, for pseudo zero, first and second order chemical reaction

6.3.3.2 Velocity dependency of fouling controlled by chemical reaction on the surface

The rate dependency of fouling controlled by chemical reaction on the surface is summarized in table 37 and plotted in figure 23.

Pseudo zero order chemical reaction	First order chemical reaction	Second order chemical reaction
$\frac{dR_{f,2}}{dt} \sim \frac{dR_{f,1}}{dt}$	$\frac{dR_{f,2}}{dt} \sim \frac{dR_{f,1}}{dt} \cdot exp\left[k_{s1} \cdot l \cdot \left(\frac{1}{u_1} - \frac{1}{u_2}\right)\right]$	$\frac{dR_{f,2}}{dt} \sim \frac{dR_{f,1}}{dt} \cdot \left(\frac{c_{Ab0} \cdot k_{f2} \cdot \frac{V}{A} \cdot \frac{1}{u_1} + 1}{c_{Ab} \cdot k_{f2} \cdot \frac{V}{A} \cdot \frac{1}{u_2} + 1}\right)^2$

table 37: velocity dependency of fouling rate R_f/dt of fouling controlled by chemical reaction on the surface

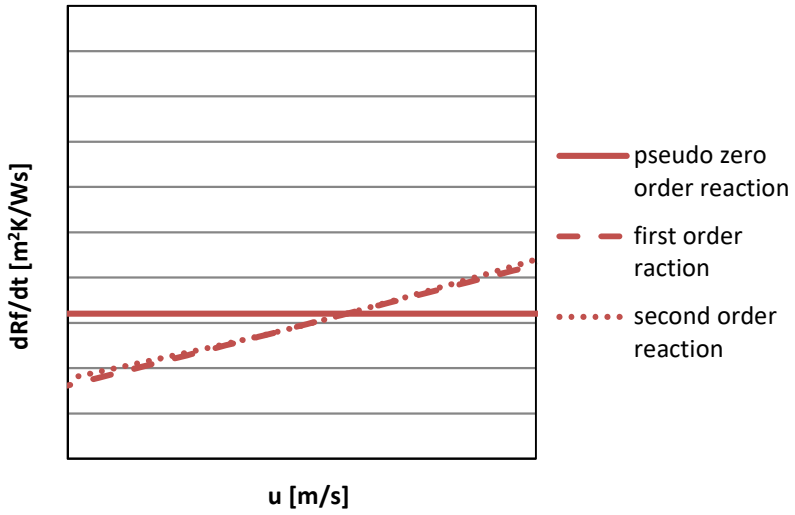

figure 23: velocity dependency of fouling rate dR_f/dt of fouling controlled by chemical reaction on the surface

Initial fouling is not rate dependent, see table 38 and figure 24.

Pseudo zero order chemical reaction	First order chemical reaction	Second order chemical reaction
$\frac{dR_{f,2}}{dt} \sim \frac{dR_{f,1}}{dt}$	$\frac{dR_{f,2}}{dt} \sim \frac{dR_{f,1}}{dt}$	$\frac{dR_{f,2}}{dt} \sim \frac{dR_{f,1}}{dt}$

table 38: velocity dependency of fouling rate dR_f/dt of fouling controlled by chemical reaction on the surface, for initial fouling

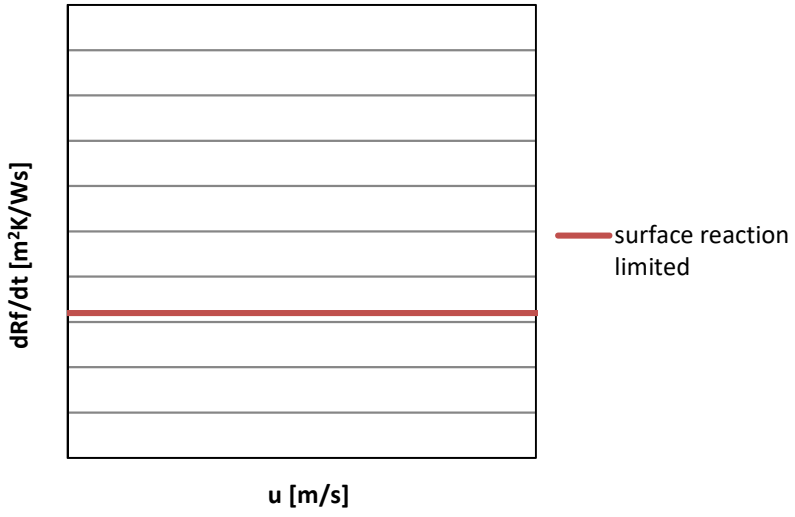

figure 24: velocity dependency of fouling rate dR_f/dt of fouling controlled by chemical reaction on the surface, for initial fouling

6.3.3.3 Discussion

Fouling rate for fouling controlled by chemical reaction on the surface increases strongly with surface temperature, because of the temperature sensitivity of reaction processes.

The fouling rate of pseudo zero order chemical reactions shows no dependency of the concentration of A in bulk c_{Ab}. For the fouling rate of first order and second order fouling this is different. At low velocity the fluid spends more time in the heat exchanger and the concentration of A in the bulk depletes according to the order of the constituents involved while the fluid passes the heat exchanger.

For initial fouling, before concentration in the bulk has changed, there is no dependency of concentration and therefore of velocity.

6.4 Corrosion is rate controlling

In the further discussion it will be assumed that corrosion exemplarily takes place as a reaction of iron oxide with organic sulphur or H_2S (equation 33).

equation 33 $$FeO + R^{'} - S - R^{''} \rightarrow FeS + R^{'} - O - R^{''}$$

$$FeO + H_2S \rightarrow FeS + H_2O$$

Corrosion in the bulk is clearly a function of dissolved iron c_{Fe++} and sulphur c_{Sb}. [Wang and Watkinson 2011] suggest the following reaction form, see equation 34. It was assumed that reaction order a or b obtain the values of either one or two.

equation 34 $$r_{FeS,b} = k_{FeS} \cdot {c_{Sb}}^{a} \cdot {c_{Fe++}}^{b}$$

Corrosion on the surface of the heat exchanger and in the film will result from interaction of soluble sulphur in the fluid with the carbon of the steel surface. The concentration of metal in the wall is constant and therefore part of the rate constant. Corrosion on the surface is clearly a function of the concentration of sulphur on the surface c_{Ss} as well as in the film c_{fs}. First or second order reaction may be assumed, see equation 35.

equation 35 $$r_{FeS,s} = k_{FeS,s} \cdot {c_{Ss}}^{a}$$

$$r_{FeS,f} = k_{FeS,f} \cdot {c_{Sf}}^{a}$$

Chapter 6.4.1 to 6.4.3 describe the development of fouling kinetic for corrosion in the bulk, the film and on the surface.

6.4.1 Corrosion in the bulk is rate controlling

If corrosion takes place in the fluid bulk, a reaction rate per unit surface area cannot be applied. The reaction rate in the bulk $r_{FeS,b}$ has to be multiplied with the surface area per reactor volume a_s, see equation 36.

equation 36 $$r_{FeS} = \frac{r_{FeS,b}}{a_S} = r_{FeS,b} \cdot \frac{V}{A}$$

The rate of corrosion in the bulk $r_{FeS,b}$ for different numbers of reaction order a and b are summarized in table 22.

a=1, b=1	a=1, b=2	a=2, b=1	a=2, b=2
$r_{FeS,b} = k_{FeS,b} \cdot c_{Sb} \cdot c_{Fe++}$	$r_{FeS,b} = k_{FeS,b} \cdot c_{Sb} \cdot c_{Fe++}^{2}$	$r_{FeS,b} = k_{FeS,b} \cdot c_{Sb}^{2} \cdot c_{Fe++}$	$r_{FeS,b} = k_{FeS,b} \cdot c_{Sb}^{2} \cdot c_{Fe++}^{2}$

table 39: rate of corrosion in the bulk $r_{ReS,b}$ for different numbers of reaction order a and b

In case corrosion in the bulk is controlling the overall fouling rate r_f per unit surface area is equal to the rate of corrosion in the bulk r_{FeS} per unit surface area (equation 37).

equation 37 $$r_f = r_{FeS} = r_{FeS,b} \cdot \frac{V}{A}$$

Therefore, the fouling rate dR_f/dt can be expressed like summarized in table 40.

a=1, b=1	a=1, b=2	a=2, b=1	a=2, b=2
$\frac{dR_f}{dt} = A_{FeS,b} \cdot exp\left(\frac{-E}{R \cdot T_b}\right) \cdot c_{Sb} \cdot c_{Fe++} \cdot \frac{M_f}{\rho_f \cdot \lambda_f} \cdot \frac{V}{A}$	$\frac{dR_f}{dt} = A_{FeS,b} \cdot exp\left(\frac{-E}{R \cdot T_b}\right) \cdot c_{Sb} \cdot c_{Fe++}^{2} \cdot \frac{M_f}{\rho_f \cdot \lambda_f} \cdot \frac{V}{A}$	$\frac{dR_f}{dt} = A_{FeS,b} \cdot exp\left(\frac{-E}{R \cdot T_b}\right) \cdot c_{Sb}^{2} \cdot c_{Fe++} \cdot \frac{M_f}{\rho_f \cdot \lambda_f} \cdot \frac{V}{A}$	$\frac{dR_f}{dt} = A_{FeS,b} \cdot exp\left(\frac{-E}{R \cdot T_b}\right) \cdot c_{Sb}^{2} \cdot c_{Fe++}^{2} \cdot \frac{M_f}{\rho_f \cdot \lambda_f} \cdot \frac{V}{A}$

table 40: fouling rate dR_f/dt for fouling limited by corrosion in the bulk, for different numbers of reaction order a and b

6.4.1.1 Temperature dependency of fouling controlled by corrosion in the bulk

Assuming constant velocity and concentration the temperature dependency of fouling controlled by corrosion in the bulk can be described with the equations developed in table 41. The equations for temperature dependency are the same for all different numbers of reaction orders a and b. Temperature effects are plotted in figure 25.

a=1, b=1	a=1, b=2	a=2, b=1	a=2, b=2
$\frac{dR_{f,2}}{dt} \sim \frac{dR_{f,1}}{dt} \cdot \frac{exp(\frac{-E}{R \cdot T_{b,2}})}{exp(\frac{-E}{R \cdot T_{b,1}})}$	$\frac{dR_{f,2}}{dt} \sim \frac{dR_{f,1}}{dt} \cdot \frac{exp(\frac{-E}{R \cdot T_{b,2}})}{exp(\frac{-E}{R \cdot T_{b,1}})}$	$\frac{dR_{f,2}}{dt} \sim \frac{dR_{f,1}}{dt} \cdot \frac{exp(\frac{-E}{R \cdot T_{b,2}})}{exp(\frac{-E}{R \cdot T_{b,1}})}$	$\frac{dR_{f,2}}{dt} \sim \frac{dR_{f,1}}{dt} \cdot \frac{exp(\frac{-E}{R \cdot T_{b,2}})}{exp(\frac{-E}{R \cdot T_{b,1}})}$
$\frac{dR_{f,2}}{dt} \sim \frac{dR_{f,1}}{dt} \cdot exp\left[\frac{E}{R} \cdot \left(\frac{1}{T_{b,1}} - \frac{1}{T_{b,2}}\right)\right]$	$\frac{dR_{f,2}}{dt} \sim \frac{dR_{f,1}}{dt} \cdot exp\left[\frac{E}{R} \cdot \left(\frac{1}{T_{b,1}} - \frac{1}{T_{b,2}}\right)\right]$	$\frac{dR_{f,2}}{dt} \sim \frac{dR_{f,1}}{dt} \cdot exp\left[\frac{E}{R} \cdot \left(\frac{1}{T_{b,1}} - \frac{1}{T_{b,2}}\right)\right]$	$\frac{dR_{f,2}}{dt} \sim \frac{dR_{f,1}}{dt} \cdot exp\left[\frac{E}{R} \cdot \left(\frac{1}{T_{b,1}} - \frac{1}{T_{b,2}}\right)\right]$

table 41: temperature dependency of fouling rate dR_f/dt of fouling controlled by corrosion in the bulk, for different numbers of reaction order a and b

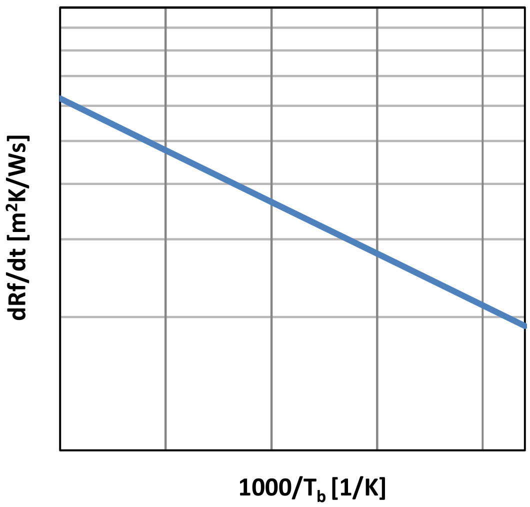

figure 25: temperature dependency of fouling rate dR_f/dt of fouling controlled by corrosion in the bulk

6.4.1.2 Velocity dependency of fouling controlled by corrosion in the bulk

The rate dependency of fouling controlled by corrosion in the bulk can be developed by integrating the rate law. For the reaction of iron oxide with organic sulphur or H_2S the sulphur concentration is correlated with the concentration of dissolved iron (equation 38). The result of the integrated rate law is summarized in table 42.

equation 38 $\quad c_S = v * c_{Fe++}$

a=1, b=1	a=1, b=2	a=2, b=1	a=2, b=2
$r_{FeS,b} = k_{FeS,b} \cdot c_{Sb} \cdot c_{Fe++b}$	$r_{FeS,b} = k_{FeS,b} \cdot c_{Sb} \cdot c_{Fe++b}^2$	$r_{FeS,b} = k_{FeS,b} \cdot c_{Sb}^2 \cdot c_{Fe++b}$	$r_{FeS,b} = k_{FeS,b} \cdot c_{Sb}^2 \cdot c_{Fe++b}^2$
$-\frac{dc_{Sb}}{dt} = k_{FeS,b} \cdot v \cdot c_{Sb}^2$	$-\frac{dc_{Sb}}{dt} = k_{FeS,b} \cdot v^2 \cdot c_{Sb}^3$	$-\frac{dc_{Sb}}{dt} = k_{FeS,b} \cdot v \cdot c_{Sb}^3$	$-\frac{dc_{Sb}}{dt} = k_{FeS,b} \cdot v \cdot c_{Sb}^4$
$\int_{c_{Sb0}}^{c_{Sb}} \frac{dc_{Sb}}{c_{Sb}^2} = -k_{FeS,b} \cdot v \cdot \int_0^t dt$	$\int_{c_{Sb0}}^{c_{Sb}} \frac{dc_{Sb}}{c_{Sb}^3} = -k_{FeS,b} \cdot v^2 \cdot \int_0^t dt$	$\int_{c_{Sb0}}^{c_{Sb}} \frac{dc_{Sb}}{c_{Sb}^3} = -k_{FeS,b} \cdot v \cdot \int_0^t dt$	$\int_{c_{Sb0}}^{c_{Sb}} \frac{dc_{Sb}}{c_{Sb}^3} = -k_{FeS,b} \cdot v \cdot \int_0^t dt$
$-\frac{1}{c_{Sb}} /_{c_{Sb0}}^{c_{Sb}} = -k_{FeS,b} \cdot v \cdot t /_0^t$ $\frac{1}{c_{Sb}} - \frac{1}{c_{Sb0}} = k_{FeS,b} \cdot v \cdot t$ $c_{Sb} = \frac{c_{Sb0}}{c_{Sb0} \cdot k_{FeS,b} \cdot v \cdot t + 1}$	$-\frac{1}{c_{Sb}^2} /_{c_{Sb0}}^{c_{Sb}} = -k_{FeS,b} \cdot v^2 \cdot t /_0^t$ $\frac{1}{c_{Sb}^2} - \frac{1}{c_{Sb0}^2} = k_{FeS,b} \cdot v^2 \cdot t$ $c_{Sb} = \sqrt{\frac{c_{Sb0}^2}{c_{Sb0} \cdot k_{FeS,b} \cdot v^2 \cdot t + 1}}$	$-\frac{1}{c_{Sb}^2} /_{c_{Sb0}}^{c_{Sb}} = -k_{FeS,b} \cdot v \cdot t /_0^t$ $\frac{1}{c_{Sb}^2} - \frac{1}{c_{Sb0}^2} = k_{FeS,b} \cdot v \cdot t$ $c_{Sb} = \sqrt{\frac{c_{Sb0}^2}{c_{Sb0} \cdot k_{FeS,b} \cdot v \cdot t + 1}}$	$-\frac{1}{c_{Sb}^3} /_{c_{Sb0}}^{c_{Sb}} = -k_{FeS,b} \cdot v \cdot t /_0^t$ $\frac{1}{c_{Sb}^3} - \frac{1}{c_{Sb0}^3} = k_{FeS,b} \cdot v \cdot t$ $c_{Sb} = \sqrt[3]{\frac{c_{Sb0}^3}{c_{Sb0} \cdot k_{FeS,b} \cdot v \cdot t + 1}}$

table 42: integrated rate laws for different numbers of reaction order a and b

For liquid flow the velocity can be assumed to be constant, time t can be expressed in terms of the length of the pipe l and the velocity u in the pipe. This leads to the equations stated in table 51. Velocity effects are plotted in figure 26.

a=1, b=1	a=1, b=2	a=2, b=1	a=2, b=2
$\frac{dR_f}{dt} = k_{FeS,b} \cdot v \cdot \frac{M_f}{\rho_f \cdot \lambda_f} \cdot \frac{V}{A} \cdot \left(\frac{c_{Sb0}}{c_{Sb0} \cdot k_{FeS,b} \cdot v \cdot \frac{l}{u} + 1} \right)^2$	$\frac{dR_f}{dt} = k_{FeS,b} \cdot v^2 \cdot \frac{M_f}{\rho_f \cdot \lambda_f} \cdot \frac{V}{A} \cdot \left(\frac{c_{Sb0}}{c_{Sb0} \cdot k_{FeS,b} \cdot v^2 \cdot \frac{l}{u} + 1} \right)^{\frac{3}{2}}$	$\frac{dR_f}{dt} = k_{FeS,b} \cdot v \cdot \frac{M_f}{\rho_f \cdot \lambda_f} \cdot \frac{V}{A} \cdot \left(\frac{c_{Sb0}}{c_{Sb0} \cdot k_{FeS,b} \cdot v \cdot \frac{l}{u} + 1} \right)^{\frac{3}{2}}$	$\frac{dR_f}{dt} = k_{FeS,b} \cdot v \cdot \frac{M_f}{\rho_f * \lambda_f} \cdot \frac{V}{A} \cdot \left(\frac{c_{Sb0}}{c_{Sb0} \cdot k_{FeS,b} \cdot v \cdot \frac{l}{u} + 1} \right)^{\frac{4}{3}}$
$\frac{dR_{f,2}}{dt} \sim \frac{dR_{f,1}}{dt} \cdot \left(\frac{\frac{c_{Sb0}}{c_{Sb0} \cdot k_{FeS,b} \cdot v \cdot \frac{l}{u_2} + 1}}{\frac{c_{Sb0}}{c_{Sb0} \cdot k_{FeS,b} \cdot v \cdot \frac{l}{u_1} + 1}} \right)^2$ $\frac{dR_{f,2}}{dt} \sim \frac{dR_{f,1}}{dt} \cdot \left(\frac{c_{Sb0} \cdot k_{FeS,b} \cdot v \cdot \frac{l}{u_1} + 1}{c_{Sb0} \cdot k_{FeS,b} \cdot v \cdot \frac{l}{u_2} + 1} \right)^2$	$\frac{dR_{f,2}}{dt} \sim \frac{dR_{f,1}}{dt} \cdot \left(\frac{\frac{c_{Sb0}}{c_{Sb0} \cdot k_{FeS,b} \cdot v \cdot \frac{l}{u_2} + 1}}{\frac{c_{Sb0}}{c_{Sb0} \cdot k_{FeS,b} \cdot v^2 \cdot \frac{l}{u_1} + 1}} \right)^{\frac{3}{2}}$ $\frac{dR_{f,2}}{dt} \sim \frac{dR_{f,1}}{dt} \cdot \left(\frac{c_{Sb0} \cdot k_{FeS,b} \cdot v^2 \cdot \frac{l}{u_1} + 1}{c_{Sb0} \cdot k_{FeS,b} \cdot v^2 \cdot \frac{l}{u_2} + 1} \right)^{\frac{3}{2}}$	$\frac{dR_{f,2}}{dt} \sim \frac{dR_{f,1}}{dt} \cdot \left(\frac{\frac{c_{Sb0}}{c_{Sb0} \cdot k_{FeS,b} \cdot v \cdot \frac{l}{u_2} + 1}}{\frac{c_{Sb0}}{c_{Sb0} \cdot k_{FeS,b} \cdot v \cdot \frac{l}{u_1} + 1}} \right)^{\frac{3}{2}}$ $\frac{dR_{f,2}}{dt} \sim \frac{dR_{f,1}}{dt} \cdot \left(\frac{c_{Sb0} \cdot k_{FeS,b} \cdot v \cdot \frac{l}{u_1} + 1}{c_{Sb0} \cdot k_{FeS,b} \cdot v \cdot \frac{l}{u_2} + 1} \right)^{\frac{3}{2}}$	$\frac{dR_{f,2}}{dt} \sim \frac{dR_{f,1}}{dt} \cdot \left(\frac{\frac{c_{Sb0}}{c_{Sb0} \cdot k_{FeS,b} \cdot v \cdot \frac{l}{u_2} + 1}}{\frac{c_{Sb0}}{c_{Sb0} \cdot k_{FeS,b} \cdot v \cdot \frac{l}{u_1} + 1}} \right)^{\frac{4}{3}}$ $\frac{dR_{f,2}}{dt} \sim \frac{dR_{f,1}}{dt} \cdot \left(\frac{c_{Sb0} \cdot k_{FeS,b} \cdot v \cdot \frac{l}{u_1} + 1}{c_{Sb0} \cdot k_{FeS,b} \cdot v \cdot \frac{l}{u_2} + 1} \right)^{\frac{4}{3}}$

table 43: velocity dependency of fouling rate dR_f/dt of fouling controlled by corrosion in the bulk

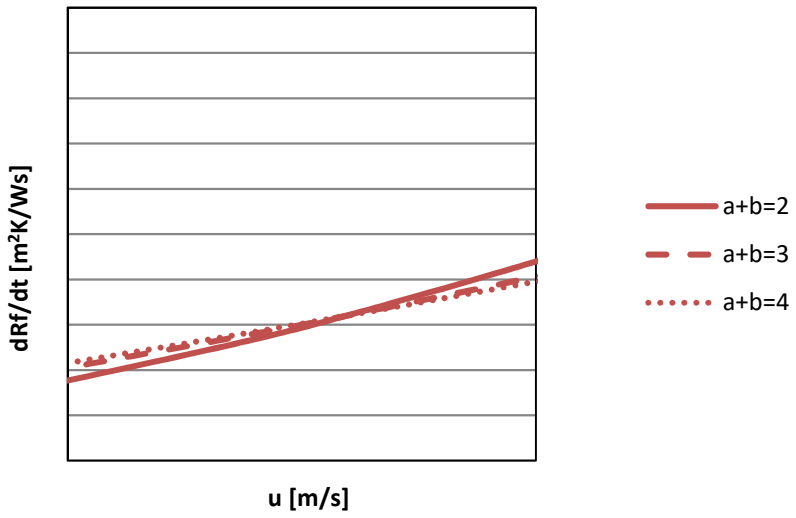

figure 26: velocity dependency of fouling rate dR_f/dt of fouling controlled by corrosion in the bulk

Initial fouling is not rate dependent, see table 42 and figure 27.

a=1, b=1	a=1, b=2	a=2, b=1	a=2, b=2
$\frac{dR_{f,2}}{dt} \sim \frac{dR_{f,1}}{dt}$	$\frac{dR_{f,2}}{dt} \sim \frac{dR_{f,1}}{dt}$	$\frac{dR_{f,2}}{dt} \sim \frac{dR_{f,1}}{dt}$	$\frac{dR_{f,2}}{dt} \sim \frac{dR_{f,1}}{dt}$

table 44: velocity dependency of fouling rate dR_f/dt of fouling controlled by corrosion in the bulk, for different numbers of reaction order a and b

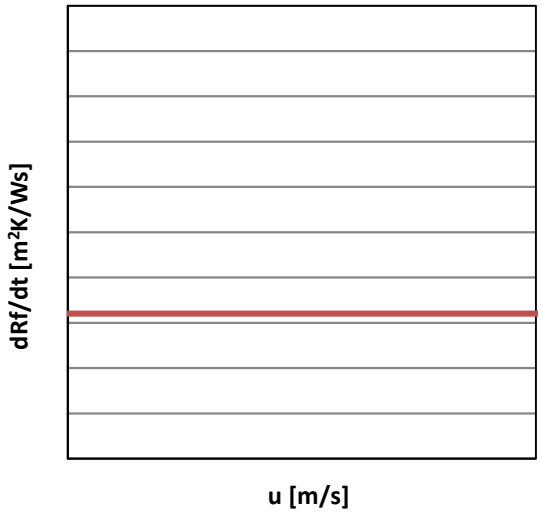

figure 27: velocity dependency of fouling rate R_f/dt of fouling controlled by corrosion in the bulk, for initial fouling

6.4.1.3 Discussion

According to the validity of the Arrhenius Law fouling rate for fouling controlled by corrosion in the bulk increases strongly with bulk temperature, because of the temperature sensitivity of reaction processes.

At low velocity (elevated residence time) the fluid spends more time in the heat exchanger and the concentration of sulphur and dissolved iron in the bulk depletes while the fluid passes the heat exchanger.

For initial fouling, before concentration in the bulk has changed, there is no dependency of concentration and therefore of velocity.

6.4.2 Corrosion in the film is rate controlling

The rate of corrosion in the film $r_{FeS,f}$ for first and second order reactions are summarized in table 45.

First order reaction	Second order reaction
$r_{FeS,f} = k_{FeS,f,1} \cdot c_{Sf}$	$r_{FeS,f} = k_{FeS,f,2} \cdot c_{Sf}^2$

table 45: rate of corrosion in the film $r_{ReS,f}$ for first and second order reaction

In case corrosion in the film is controlling the overall fouling rate r_f per unit surface area is equal to the rate of corrosion in the film $r_{FeS,f}$ per unit surface area (equation 39).

equation 39 $$r_f = r_{FeS,f}$$

Therefore, the fouling rate dR_f/dt can be expressed like summarized in table 46.

First order reaction	Second order reaction
$\frac{dR_f}{dt} = A_{FeS,f,1} \cdot exp\left(\frac{-E}{R \cdot T_f}\right) \cdot c_{Sf} \cdot \frac{M_f}{\rho_f \cdot \lambda_f}$	$\frac{dR_f}{dt} = A_{FeS,f,2} \cdot exp\left(\frac{-E}{R \cdot T_f}\right) \cdot c_{Sf}^2 \cdot \frac{M_f}{\rho_f \cdot \lambda_f}$

table 46: fouling rate dR_f/dt for fouling limited by corrosion in the film for first and second order reaction

6.4.2.1 Temperature dependency of fouling controlled by corrosion in the film

Assuming constant velocity and concentration the temperature dependency of fouling controlled by corrosion in the film can be described with the equations developed in table 47. The equations for temperature dependency are the same for first and second order reaction. Temperature effects are plotted in figure 28.

First order reaction	Second order reaction
$\frac{dR_{f,2}}{dt} \sim \frac{dR_{f,1}}{dt} \cdot \frac{exp(\frac{-E}{R \cdot T_{f,2}})}{exp(\frac{-E}{R \cdot T_{f,1}})}$	$\frac{dR_{f,2}}{dt} \sim \frac{dR_{f,1}}{dt} \cdot \frac{exp(\frac{-E}{R \cdot T_{f,2}})}{exp(\frac{-E}{R \cdot T_{f,1}})}$
$\frac{dR_{f,2}}{dt} \sim \frac{dR_{f,1}}{dt} \cdot exp\left[\frac{E}{R} \cdot \left(\frac{1}{T_{f,1}} - \frac{1}{T_{f,2}}\right)\right]$	$\frac{dR_{f,2}}{dt} \sim \frac{dR_{f,1}}{dt} \cdot exp\left[\frac{E}{R} \cdot \left(\frac{1}{T_{f,1}} - \frac{1}{T_{f,2}}\right)\right]$

table 47: temperature dependency of fouling rate dR_f/dt of fouling controlled by corrosion in the film, for first and second order reactions

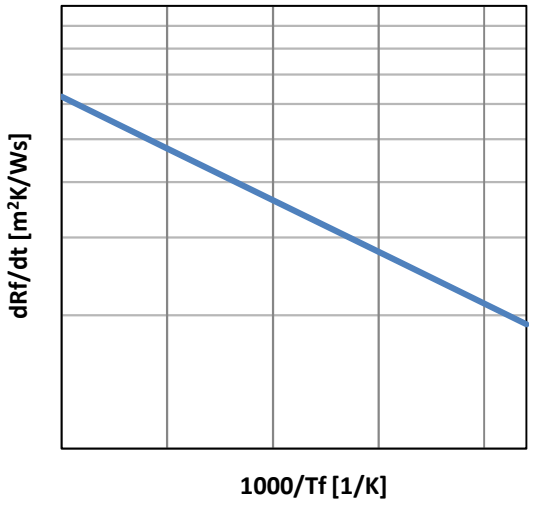

figure 28: temperature dependency of fouling rate dR_f/dt of fouling controlled by corrosion in the film

6.4.2.2 Velocity dependency of fouling controlled by corrosion in the film

The rate dependency of fouling controlled by corrosion in the film can be developed by integrating the rate law, see table 48.

First order reaction	Second order reaction
$-\frac{V}{A}\cdot\frac{dc_{Sf}}{dt} = k_{FeS,f,1}\cdot\frac{V}{A}\cdot c_{Sf}$ $-\frac{dc_{Sb}}{dt} = k_{FeS,f,1}\cdot c_{Sb}$	$-\frac{V}{A}\cdot\frac{dc_{Sf}}{dt} = k_{FeS,f,2}\cdot\left(\frac{V}{A}\right)^2\cdot c_{Sf}^2$ $-\frac{dc_{Sb}}{dt} = k_{FeS,f,2}\cdot c_{Sb}^2\cdot\frac{V}{A}$
$\int_{c_{Sb0}}^{c_{Sb}}\frac{dc_{Sb}}{c_{Sb}} = -k_{FeS,f,1}\cdot\int_0^t dt$	$\int_{c_{Sb0}}^{c_{Sb}}\frac{dc_{Sb}}{c_{Sb}^2} = -k_{FeS,f,2}\cdot\frac{V}{A}\cdot\int_0^t dt$
$\ln c_{Sb}/_{c_{Sb0}}^{c_{Sb}} = -k_{FeS,f,1}\cdot t/_0^t$ $\ln c_{Sb} - \ln c_{Sb0} = -k_{FeS,f,1}\cdot t$ $\ln\frac{c_{Sb}}{c_{Sb}} = -k_{FeS,f,1}\cdot t$ $c_{Sb} = c_{Sb0}\cdot exp(-k_{FeS,f,1}\cdot t)$	$-\frac{1}{c_{Sb}}/_{c_{Sb}}^{c_{Sb}} = -k_{FeS,f,2}\cdot\frac{V}{A}\cdot t/_0^t$ $\frac{1}{c_{Sb}} - \frac{1}{c_{Sb0}} = k_{FeS,f,2}\cdot\frac{V}{A}\cdot t$ $c_{Sb} = \frac{c_{Sb}}{c_{Sb0}\cdot k_{FeS,f,2}\cdot\frac{V}{A}\cdot t+1}$

table 48: integrated rate laws for first order and second order reaction

Time t can be expressed in terms of the length of the pipe l and the velocity u in the pipe. This leads to the equations stated in table 51. Velocity effects are plotted in figure 29.

First order reaction	Second order reaction
$\frac{dR_f}{dt} = exp\left(\frac{-E}{R*T_s}\right) \cdot c_{Sb0} \cdot exp(-k_{FeS,f,1} \cdot \mathrm{t}) \cdot \left(\frac{V}{A}\right) \cdot \frac{M_f}{\rho_f \cdot \lambda_f}$	$\frac{dR_f}{dt} = exp\left(\frac{-E}{R \cdot T_s}\right) \cdot \left(\frac{c_{Sb0}}{c_{Sb0} \cdot k_{FeS,f,2} \cdot \frac{V}{A} \cdot \mathrm{t}+1} \cdot \frac{\mathrm{V}}{\mathrm{A}}\right)^2 \cdot \frac{M_f}{\rho_f \cdot \lambda_f}$
$\frac{dR_{f,2}}{dt} \sim \frac{dR_{f,1}}{dt} \cdot \frac{exp(\frac{-A_{FeS,s} \cdot k_{FeS,f,1} \cdot l}{u_2})}{exp(\frac{-A_{FeS,s} \cdot k_{FeS,f,1} \cdot l}{u_1})}$ $\frac{dR_{f,2}}{dt} \sim \frac{dR_{f,1}}{dt} \cdot exp\left[k_{FeS,f,1} \cdot l \cdot \left(\frac{1}{u_1} - \frac{1}{u_2}\right)\right]$	$\frac{dR_{f,2}}{dt} \sim \frac{dR_{f,1}}{dt} \cdot \left(\frac{\frac{c_{Sb0}}{c_{Sb0} \cdot k_{FeS,f,2} \cdot \frac{V}{A} \cdot \frac{l}{u_2}+1}}{\frac{c_{Sb}}{c_{Sb0} \cdot k_{FeS,f,2} \cdot \frac{V}{A} \cdot \frac{l}{u_1}+1}}\right)^2$ $\frac{dR_{f,2}}{dt} \sim \frac{dR_{f,1}}{dt} \cdot \left(\frac{c_{Sb0} \cdot k_{FeS,f,2} \cdot \frac{V}{A} \cdot \frac{l}{u_1}+1}{c_{Sb0} \cdot k_{FeS,f,2} \cdot \frac{V}{A} \cdot \frac{l}{u_2}+1}\right)^2$

table 49: velocity dependency of fouling rate dR_f/dt of fouling controlled by corrosion in the film

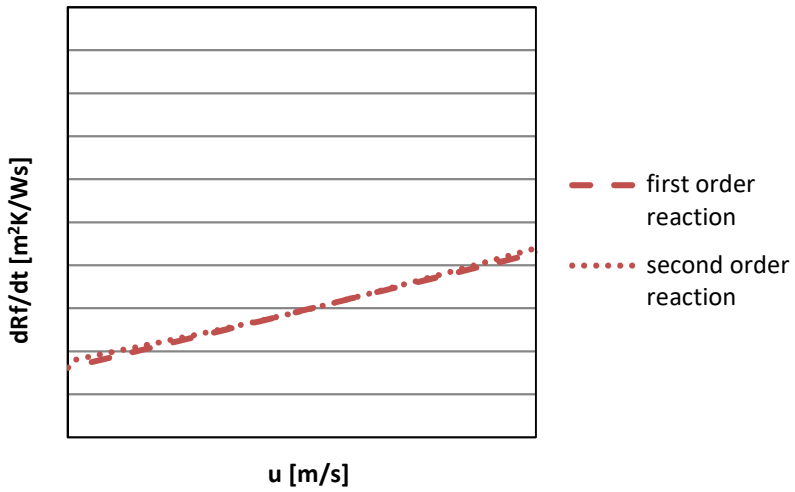

figure 29: velocity dependency of fouling rate dR_f/dt of fouling controlled by chemical reaction in the film

Initial fouling is not rate dependent, see table 50 and figure 30.

First order reaction	Second order reaction
$\frac{dR_{f,2}}{dt} \sim \frac{dR_{f,1}}{dt}$	$\frac{dR_{f,2}}{dt} \sim \frac{dR_{f,1}}{dt}$

table 50: velocity dependency of fouling rate dR_f/dt of fouling controlled by corrosion in the film, for first and second order reactions, for initial fouling

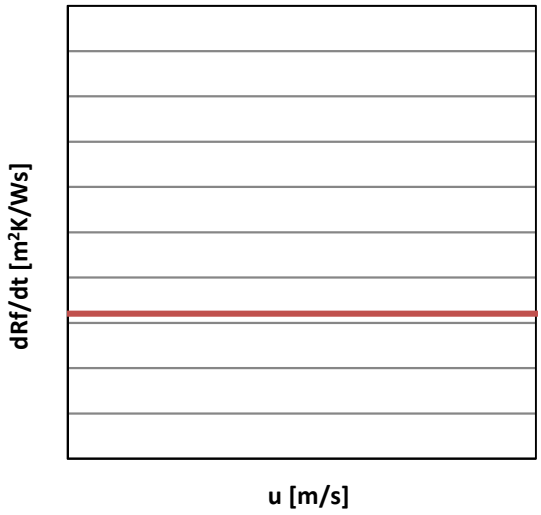

figure 30: velocity dependency of fouling rate R_f/dt of fouling controlled by corrosion in the film, for first and second order reactions, for initial fouling

6.4.2.3 Discussion

According to validity of the Arrhenius Law fouling rate for fouling controlled by corrosion in the film increases strongly with surface temperature, because of the temperature sensitivity of reaction processes.

At low velocity (elevated residence time) the fluid spends more time in the heat exchanger and the concentration of sulphur and dissolved iron in the bulk depletes while the fluid passes the heat exchanger.

For initial fouling, before concentration in the bulk has changed, there is no dependency of concentration and therefore of velocity.

6.4.3 Corrosion on the surface is rate controlling

The fouling rate dR_f/dt for fouling controlled by corrosion on the surface can be developed analogous to fouling controlled by corrosion in the film, see table 51.

First order reaction	Second order reaction
$\frac{dR_f}{dt} = \mathrm{A_{FeS,s,1}} \cdot exp\left(\frac{-E}{R \cdot T_s}\right) \cdot \mathrm{c_{Ss}} \cdot \frac{M_f}{\rho_f \cdot \lambda_f}$	$\frac{dR_f}{dt} = \mathrm{A_{FeS,s,2}} \cdot exp\left(\frac{-E}{R \cdot T_s}\right) \cdot \mathrm{c_{Ss}}^2 \cdot \frac{M_f}{\rho_f \cdot \lambda_f}$

table 51: fouling rate dR_f/dt for fouling limited by corrosion on the surface for first and second order reaction

6.4.3.1 Temperature dependency of fouling controlled by corrosion on the surface

Assuming constant velocity and concentration the temperature dependency of fouling controlled by corrosion on the surface can be described with the equations developed in table 52. The equations for temperature dependency are the same for first and second order reaction. Temperature effects are plotted in figure 31.

First order reaction	Second order reaction
$\frac{dR_{f,2}}{dt} \sim \frac{dR_{f,1}}{dt} \cdot \frac{exp(\frac{-E}{R \cdot T_{s,2}})}{exp(\frac{-E}{R \cdot T_{s,1}})}$	$\frac{dR_{f,2}}{dt} \sim \frac{dR_{f,1}}{dt} \cdot \frac{exp(\frac{-E}{R \cdot T_{s,2}})}{exp(\frac{-E}{R \cdot T_{s,1}})}$
$\frac{dR_{f,2}}{dt} \sim \frac{dR_{f,1}}{dt} \cdot exp\left[\frac{E}{R} \cdot \left(\frac{1}{T_{s,1}} - \frac{1}{T_{s,2}}\right)\right]$	$\frac{dR_{f,2}}{dt} \sim \frac{dR_{f,1}}{dt} \cdot exp\left[\frac{E}{R} \cdot \left(\frac{1}{T_{s,1}} - \frac{1}{T_{s,2}}\right)\right]$

table 52: temperature dependency of fouling rate dR_f/dt of fouling controlled by corrosion on the surface, for first and second order reactions

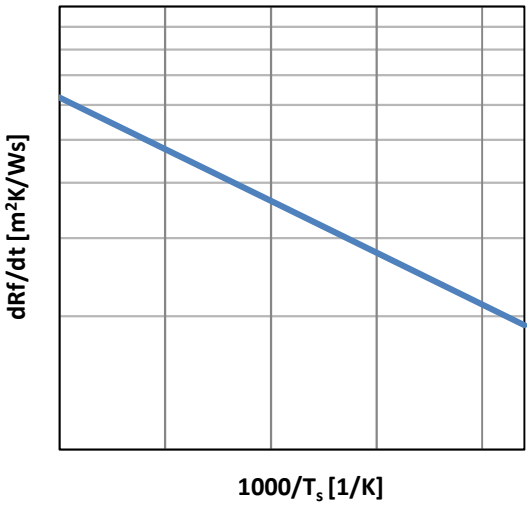

figure 31: temperature dependency of fouling rate dR_f/dt of fouling controlled by corrosion on the surface

6.4.3.2 Velocity dependency of fouling controlled by corrosion on the surface

The rate of fouling per unit surface area $r_{FeS,s}$ for developed fouling can be developed analogous to fouling controlled by corrosion in the film, see table 53. Velocity effects are plotted in figure 32.

First order reaction	Second order reaction
$\frac{dR_{f,2}}{dt} \sim \frac{dR_{f,1}}{dt} \cdot exp\left[k_{FeS,s,1} \cdot l \cdot \left(\frac{1}{u_1} - \frac{1}{u_2}\right)\right]$	$\frac{dR_{f,2}}{dt} \sim \frac{dR_{f,1}}{dt} \cdot \left(\frac{c_{Sb0} \cdot k_{FeS,s,2} \cdot \frac{V}{A} \cdot \frac{l}{u_1} + 1}{c_{Sb0} \cdot k_{FeS,s,2} \cdot \frac{V}{A} \cdot \frac{l}{u_2} + 1}\right)^2$

table 53: velocity dependency of fouling rate dR_f/dt of fouling controlled by corrosion on the surface

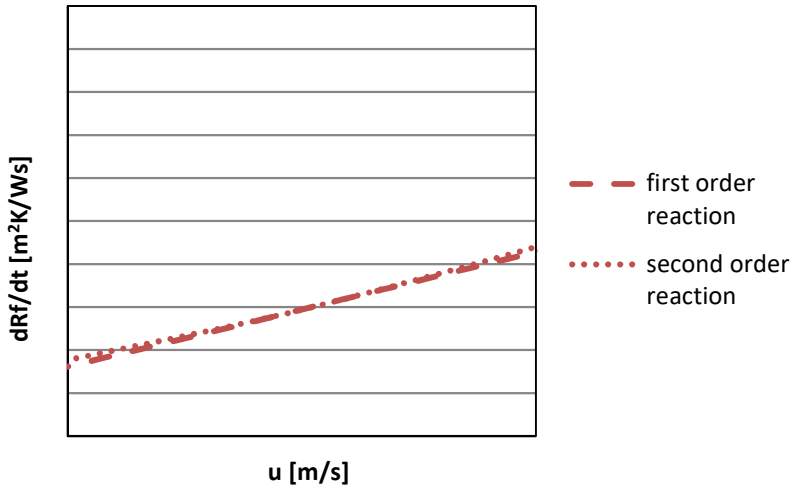

figure 32: velocity dependency of fouling rate dR_f/dt of fouling controlled by corrosion on the surface

Initial fouling is not rate dependent, see table 54 and figure 33.

First order reaction	Second order reaction
$\frac{dR_{f,2}}{dt} \sim \frac{dR_{f,1}}{dt}$	$\frac{dR_{f,2}}{dt} \sim \frac{dR_{f,1}}{dt}$

table 54: velocity dependency of fouling rate dR_f/dt of fouling controlled by corrosion on the surface, for first and second order reactions, for initial fouling

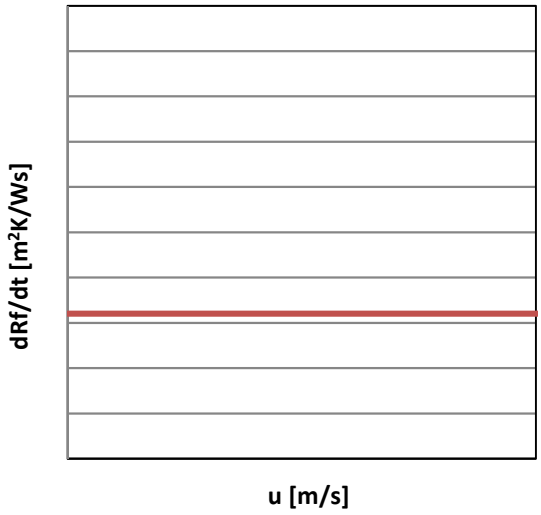

figure 33: velocity dependency of fouling rate R_f/dt of fouling controlled by corrosion on the surface, for first and second order reactions, for initial fouling

6.4.3.3 Discussion

According to validity of the Arrhenius Law, fouling rate for fouling controlled by corrosion on the surface increases strongly with surface temperature, because of the temperature sensitivity of reaction processes.

At low velocity (elevated residence time) the fluid spends more time in the heat exchanger and the concentration of sulphur and dissolved iron in the bulk depletes while the fluid passes the heat exchanger.

For initial fouling, before concentration in the bulk has changed, there is no dependency of concentration and therefore of velocity.

6.5 Asphaltene precipitation is rate controlling

The solubility of asphaltenes increases with temperature, therefore higher temperatures cause less fouling for fouling controlled by asphaltene precipitation. Precipitation of asphaltenes is assumed to follow crystallization mechanisms of solids from saturated liquids. For a solid-liquid equilibrium, the fugacity in both phases is the same, see equation 40, with f_a representing the fugacity of the precipitated asphaltenes and f_a^b the fugacity of the asphaltenes in the bulk liquid.

equation 40 $$f_a = f_a^{\,b}$$

The fugacity of the precipitated asphaltenes is assumed to be $f_a = {f_a}^0 = 1$, this simplifies the calculation of the phase equilibrium, see equation 41, with f_a^0 representing the standard fugacity of the precipitated asphaltenes; f_a^{0b} the standard fugacity of asphaltenes in the bulk, γ_a^b the fugacity coefficient and x_a^b the concentration of asphaltenes in the bulk liquid; $h_{m,a}$ the melting enthalpy and $T_{m,a}$ the melting temperature.

equation 41 $$f_a = {f_a}^0 = {f_a}^b = {x_a}^b \cdot {\gamma_a}^b \cdot {f_a}^{0b}$$

$$ln({x_a}^b \cdot {\gamma_a}^b) = ln\left(\frac{{f_a}^0}{{f_a}^{0b}}\right)$$

$$ln({x_a}^b \cdot {\gamma_a}^b) = -\frac{\mathrm{h_{m,a}}}{R \cdot T} * \left(1 - \frac{T}{T_{m,a}}\right)$$

Assuming a constant activity coefficient γ_a^b equation 41 can be transformed to equation 42, which gives the molar fraction of asphaltenes in the bulk x_a^b as a function of temperature T.

equation 42 $${x_a}^b = {\gamma_a}^b \cdot exp\left(-\frac{\mathrm{h_{m,a}}}{R \cdot T} \cdot \left(1 - \frac{T}{T_{m,a}}\right)\right) = {\gamma_a}^b \cdot exp\left(\frac{\mathrm{h_{m,a}}}{R \cdot T_{m,a}} - \frac{\mathrm{h_{m,a}}}{R \cdot T}\right) = {\gamma_a}^b \cdot \frac{exp\left(\frac{\mathrm{h_{m,a}}}{R \cdot T_{m,a}}\right)}{exp\left(\frac{\mathrm{h_{m,a}}}{R \cdot T}\right)}$$

The molar flow of precipitated asphaltenes in the bulk $\dot{N}_a^{\ b}$ can be described with equation 43 and is a function of temperature T.

equation 43 $${\dot{N}_a}^b = {x_a}^b \cdot \dot{N} = {\gamma_a}^b \cdot \frac{exp\left(\frac{\mathrm{h_{m,a}}}{R \cdot T_{m,a}}\right)}{exp\left(\frac{\mathrm{h_{m,a}}}{R \cdot T}\right)} \cdot \dot{N} = \frac{C_1}{exp\left(\frac{C_2}{T}\right)} \cdot \dot{N}$$

The molar flow of precipitated asphaltenes $\dot{N}_a$ can be expressed as difference between the molar flow of asphaltenes in the bulk at temperature T_{sb}, with all asphaltenes being dissolved, and the molar flow of asphaltenes in the bulk phase at a lower temperature T, being subject of precipitation, according to equation 44.

equation 44 $$\dot{N}_a(T) = \dot{N}_a(T_{sb})^b - \dot{N}_a(T)^b$$

$$\dot{N}_a = \left(\frac{C_1}{exp\left(\frac{C_2}{T_{sb}}\right)} - \frac{C_1}{exp\left(\frac{C_2}{T}\right)}\right) \cdot \dot{N} = C_1 \cdot \left(\frac{1}{exp\left(\frac{C_2}{T_{sb}}\right)} - \frac{1}{exp\left(\frac{C_2}{T}\right)}\right) \cdot \dot{N}$$

By assuming constant molar volume V_m and constant cross section A_q, equation 45, which gives the molar flow of precipitated asphaltenes as a function of temperature T and velocity u, can be developed.

equation 45 $$\dot{N}_a = C_1 \cdot \left(\frac{1}{exp\left(\frac{C_2}{T_{sb}}\right)} - \frac{1}{exp\left(\frac{C_2}{T}\right)}\right) \cdot \frac{u \cdot A_q}{V_m} = C_3 \cdot \left(\frac{1}{exp\left(\frac{C_2}{T_{sb}}\right)} - \frac{1}{exp\left(\frac{C_2}{T}\right)}\right) \cdot u$$

The molar flow of precipitated asphaltenes $\dot{N}_a$ divided by the surface area A, for adsorption (precipitation) of asphaltenes, gives the fouling rate per unit surface area r_a, see equation 46.

equation 46 $$r_a = \frac{\dot{N}_a}{A} = C_3 \cdot \left(\frac{1}{exp\left(\frac{C_2}{T_{sb}}\right)} - \frac{1}{exp\left(\frac{C_2}{T}\right)} \right) \cdot \frac{u}{A} = C_4 \cdot \left(\frac{1}{exp\left(\frac{C_2}{T_{sb}}\right)} - \frac{1}{exp\left(\frac{C_2}{T}\right)} \right) \cdot u$$

$$r_f = r_a$$

Asphaltene precipitation can take place either in the bulk, the film or on the surface, see table 55.

Asphaltene precipitation in the bulk	**Asphaltene precipitation in the film**	**Asphaltene precipitation on the surface**
$\frac{dR_f}{dt} = C_4 \cdot \left(\frac{1}{exp\left(\frac{C_2}{T_{sb}}\right)} - \frac{1}{exp\left(\frac{C_2}{T_b}\right)} \right) \cdot u \cdot \frac{M_f}{\rho_f \cdot \lambda_f}$	$\frac{dR_f}{dt} = C_4 \cdot \left(\frac{1}{exp\left(\frac{C_2}{T_{sb}}\right)} - \frac{1}{exp\left(\frac{C_2}{T_f}\right)} \right) \cdot u \cdot \frac{M_f}{\rho_f \cdot \lambda_f}$	$\frac{dR_f}{dt} = C_4 \cdot \left(\frac{1}{exp\left(\frac{C_2}{T_{sb}}\right)} - \frac{1}{exp\left(\frac{C_2}{T_s}\right)} \right) \cdot u \cdot \frac{M_f}{\rho_f \cdot \lambda_f}$
$C_2 = \frac{\mathrm{h_{m,a}}}{R}$; $C_4 = {\gamma_a}^b \cdot exp\left(\frac{\mathrm{h_{m,a}}}{R \cdot T_{m,a}}\right) \cdot \frac{A_q}{V_m \cdot A}$		

table 55: fouling rate dR_f/dt for fouling controlled by asphaltene precipitation

6.5.1 Temperature dependency of fouling controlled by asphaltene precipitation

For constant velocity table 56 summarizes the temperature dependency of asphaltene precipitation in the bulk, the film and on the surface. The three are alike, just differ by the temperatures.

Asphaltene precipitation in the bulk	Asphaltene precipitation in the film	Asphaltene precipitation on the surface
$\frac{dR_{f,2}}{dt} = \frac{dR_{f,1}}{dt} \cdot \frac{\left(\frac{1}{exp\left(\frac{C_2}{T_{sb}}\right)} - \frac{1}{exp\left(\frac{C_2}{T_{b2}}\right)}\right)}{\left(\frac{1}{exp\left(\frac{C_2}{T_{sb}}\right)} - \frac{1}{exp\left(\frac{C_2}{T_{b1}}\right)}\right)}$	$\frac{dR_{f,2}}{dt} = \frac{dR_{f,1}}{dt} \cdot \frac{\left(\frac{1}{exp\left(\frac{C_2}{T_{sb}}\right)} - \frac{1}{exp\left(\frac{C_2}{T_{f2}}\right)}\right)}{\left(\frac{1}{exp\left(\frac{C_2}{T_{sb}}\right)} - \frac{1}{exp\left(\frac{C_2}{T_{f1}}\right)}\right)}$	$\frac{dR_{f,2}}{dt} = \frac{dR_{f,1}}{dt} \cdot \frac{\left(\frac{1}{exp\left(\frac{C_2}{T_{sb}}\right)} - \frac{1}{exp\left(\frac{C_2}{T_{s2}}\right)}\right)}{\left(\frac{1}{exp\left(\frac{C_2}{T_{sb}}\right)} - \frac{1}{exp\left(\frac{C_2}{T_{s1}}\right)}\right)}$
$C_2 = \frac{\mathrm{h_{m,a}}}{R}$		

table 56: temperature dependency of fouling rate dR_f/dt for fouling controlled by asphaltene precipitation

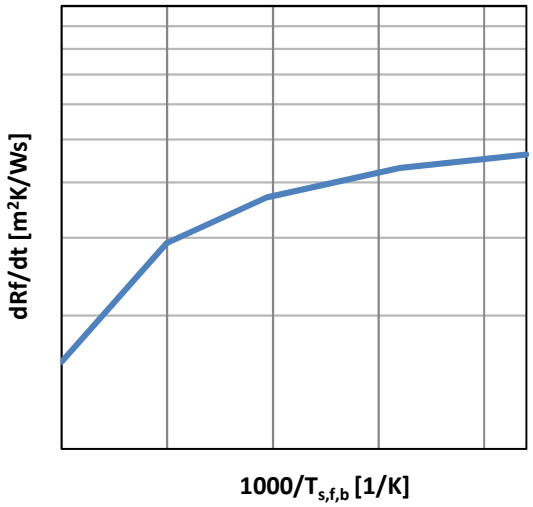

figure 34: temperature dependency of fouling rate dR_f/dt of fouling controlled by asphaltene precipitation

6.5.2 Velocity dependency of fouling controlled by asphaltene precipitation

For constant temperatures the dependency of the fouling rate of fouling controlled by asphaltene precipitation is summarized in table 62. Fouling rates are the same for asphaltene precipitation in the bulk, the film and on the surface.

Asphaltene precipitation in the bulk	Asphaltene precipitation in the film	Asphaltene precipitation on the surface
$\frac{dR_{f,2}}{dt} = \frac{dR_{f,1}}{dt} \cdot \frac{u_2}{u_1}$	$\frac{dR_{f,2}}{dt} = \frac{dR_{f,1}}{dt} \cdot \frac{u_2}{u_1}$	$\frac{dR_{f,2}}{dt} = \frac{dR_{f,1}}{dt} \cdot \frac{u_2}{u_1}$

table 57: velocity dependency of fouling rate dR_f/dt for fouling controlled by asphaltene precipitation

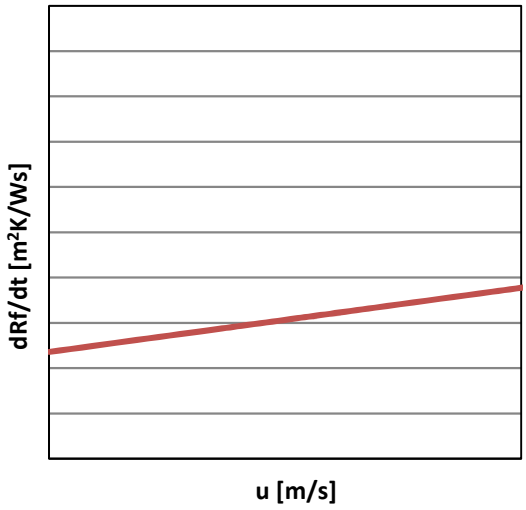

figure 35: velocity dependency of fouling rate dR_f/dt of fouling controlled by asphaltene precipitation

6.5.3 Discussion

Fouling rate for fouling controlled by asphaltene precipitation in the bulk, the film and on the surface depletes with either bulk, film or surface temperature because solubility of asphaltenes increases with temperature.

Fouling rates increase linearly with velocity, the higher the velocity the higher is the bulk flow with a certain amount of asphaltenes which can precipitate at a specific temperature.

6.6 Kinetic modelling summary

As described in previous chapters a number of equations can be developed to describe fouling rate dR_f/dt as a function of temperature T and velocity u. These equations are summarized in dependency of the controlling step in table 58 and table 59 for temperature and velocity effects.

The developed equations can be used to determine the controlling step of fouling by comparing experimental data with the model. Furthermore, once the controlling step is identified the equations can be used to predict fouling rates dRf/dt for different conditions or to optimize design of heat exchangers by the minimization of fouling.

The approach has a restriction. Removal of the fouling layer because of shear stress can't be reproduced, as mechanical abrasion is not accessible in the kinetic model. Furthermore, the kinetic model neglects the influence of surface roughness and changes in surface roughness.

The fouling layer is considered to be homogeneous and the shape of deposits isn't considered. Changes in flow velocity with changing cross-sectional area due to fouling are neglected.

Chemical reaction in the bulk	$\frac{dR_{f,2}}{dt} \sim \frac{dR_{f,1}}{dt} \cdot exp\left[\frac{E}{R} \cdot \left(\frac{1}{T_{b,1}} - \frac{1}{T_{b,2}}\right)\right]$	
Corrosion in the bulk	$\frac{dR_{f,2}}{dt} \sim \frac{dR_{f,1}}{dt} \cdot exp\left[\frac{E}{R} \cdot \left(\frac{1}{T_{b,1}} - \frac{1}{T_{b,2}}\right)\right]$	
Asphaltene precipitation in the bulk	$\frac{dR_{f,2}}{dt} = \frac{dR_{f,1}}{dt} \cdot \frac{\left(\frac{1}{exp\left(\frac{\mathrm{h_{m,a}}}{R \cdot T_{sb}}\right)} - \frac{1}{exp\left(\frac{\mathrm{h_{m,a}}}{R \cdot T_{b2}}\right)}\right)}{\left(\frac{1}{exp\left(\frac{\mathrm{h_{m,a}}}{R \cdot T_{sb}}\right)} - \frac{1}{exp\left(\frac{\mathrm{h_{m,a}}}{R \cdot T_{b1}}\right)}\right)}$	
Transport (diffusion)	Fully developed laminar flow in pipes: $\frac{dR_{f,2}}{dt} \sim \frac{dR_{f,1}}{dt}$	Fully developed turbulent flow in pipes: $\frac{dR_{f,2}}{dt} \sim \frac{dR_{f,1}}{dt} \cdot \left(\frac{T_{f,2}}{T_{f,1}}\right)^{0.6} \cdot \left(\frac{917-0.833*T_{f,2}}{917-0.833*T_{f,1}}\right)^{0.4} \cdot \left(\exp\left(\frac{406}{T_{f,1}} - \frac{406}{T_{f,2}}\right)\right)^{0.2}$
Chemical reaction in the film	$\frac{dR_{f,2}}{dt} \sim \frac{dR_{f,1}}{dt} \cdot exp\left[\frac{E}{R} \cdot \left(\frac{1}{T_{f,1}} - \frac{1}{T_{f,2}}\right)\right]$	
Corrosion in the film	$\frac{dR_{f,2}}{dt} \sim \frac{dR_{f,1}}{dt} \cdot exp\left[\frac{E}{R} \cdot \left(\frac{1}{T_{f,1}} - \frac{1}{T_{f,2}}\right)\right]$	
Asphaltene precipitation in the film	$\frac{dR_{f,2}}{dt} = \frac{dR_{f,1}}{dt} \cdot \frac{\left(\frac{1}{exp\left(\frac{\mathrm{h_{m,a}}}{R \cdot T_{sb}}\right)} - \frac{1}{exp\left(\frac{\mathrm{h_{m,a}}}{R \cdot T_{f2}}\right)}\right)}{\left(\frac{1}{exp\left(\frac{\mathrm{h_{m,a}}}{R \cdot T_{sb}}\right)} - \frac{1}{exp\left(\frac{\mathrm{h_{m,a}}}{R \cdot T_{f1}}\right)}\right)}$	

Adsorption	$\frac{dR_{f,2}}{dt} \sim \frac{dR_{f,1}}{dt} \cdot exp\left[\frac{E}{R} \cdot \left(\frac{1}{T_{s,1}} - \frac{1}{T_{s,2}}\right)\right]$	
Chemical reaction on the heat transfer surface	$\frac{dR_{f,2}}{dt} \sim \frac{dR_{f,1}}{dt} \cdot exp\left[\frac{E}{R} \cdot \left(\frac{1}{T_{s,1}} - \frac{1}{T_{s,2}}\right)\right]$	
Corrosion on the surface	$\frac{dR_{f,2}}{dt} \sim \frac{dR_{f,1}}{dt} \cdot exp\left[\frac{E}{R} \cdot \left(\frac{1}{T_{s,1}} - \frac{1}{T_{s,2}}\right)\right]$	
Asphaltene precipitation on the surface	$\frac{dR_{f,2}}{dt} = \frac{dR_{f,1}}{dt} \cdot \frac{\left(\frac{1}{exp\left(\frac{\mathrm{h_{m,a}}}{\frac{R}{T_{sb}}}\right)} - \frac{1}{exp\left(\frac{\mathrm{h_{m,a}}}{\frac{R}{T_{s2}}}\right)}\right)}{\left(\frac{1}{exp\left(\frac{\mathrm{h_{m,a}}}{\frac{R}{T_{sb}}}\right)} - \frac{1}{exp\left(\frac{\mathrm{h_{m,a}}}{\frac{R}{T_{s1}}}\right)}\right)}$	
Desorption of the fouling product	$-\frac{dR_{f,2}}{dt} \sim -\frac{dR_{f,1}}{dt} \cdot exp\left[\frac{E}{R} \cdot \left(\frac{1}{T_{s,1}} - \frac{1}{T_{s,2}}\right)\right]$	
Transport (back diffusion)	Fully developed laminar flow in pipes: $-\frac{dR_{f,2}}{dt} \sim -\frac{dR_{f,1}}{dt}$	Fully developed turbulent flow in pipes: $-\frac{dR_{f,2}}{dt} \sim -\frac{dR_{f,1}}{dt} \cdot \left(\frac{T_{f,2}}{T_{f,1}}\right)^{0.6} * \left(\frac{917-0.833*T_{f,2}}{917-0.833*T_{f,1}}\right)^{0.4} \cdot \left(\exp\left(\frac{406}{T_{f,1}} - \frac{406}{T_{f,2}}\right)\right)^{0.2}$

table 58: Summary of temperature dependency of equations developed by kinetic modelling, depending on the controlling step

<table>
<tr><td rowspan="2">Chemical reaction in the bulk</td><td>Pseudo zero order chemical reaction:
$\frac{dR_{f,2}}{dt} \sim \frac{dR_{f,1}}{dt}$</td><td>First order chemical reaction:
$\frac{dR_{f,2}}{dt} \sim \frac{dR_{f,1}}{dt} \cdot exp\left[\mathrm{k_{b1}} \cdot \mathrm{l} \cdot \left(\frac{1}{u_1} - \frac{1}{u_2}\right)\right]$</td><td>Second order chemical reaction:
$\frac{dR_{f,2}}{dt} \sim \frac{dR_{f,1}}{dt} \cdot \left(\frac{c_{Ab0} \cdot \mathrm{k_{b2}} \cdot \frac{\mathrm{l}}{u_1} + 1}{c_{Ab0} \cdot \mathrm{k_{b2}} \cdot \frac{\mathrm{l}}{u_2} + 1}\right)^2$</td></tr>
<tr><td colspan="3">Initial fouling:
$\frac{dR_{f,2}}{dt} \sim \frac{dR_{f,1}}{dt}$</td></tr>
<tr><td rowspan="2">Corrosion in the bulk</td><td>second order reaction (a=1, b=1):
$\frac{dR_{f,2}}{dt} \sim \frac{dR_{f,1}}{dt} \cdot \left(\frac{c_{Sb0} \cdot \mathrm{k_{FeS,b}} \cdot \mathrm{v} \cdot \frac{\mathrm{l}}{u_1} + 1}{c_{Sb0} \cdot \mathrm{k_{FeS,b}} \cdot \mathrm{v} \cdot \frac{\mathrm{l}}{u_2} + 1}\right)^2$</td><td>third order reaction (a=1, b=2):
$\frac{dR_{f,2}}{dt} \sim \frac{dR_{f,1}}{dt} \cdot \left(\frac{c_{Sb0} \cdot \mathrm{k_{FeS,b}} \cdot \mathrm{v}^2 \cdot \frac{\mathrm{l}}{u_1} + 1}{c_{Sb0} \cdot \mathrm{k_{FeS,b}} \cdot \mathrm{v}^2 \cdot \frac{\mathrm{l}}{u_2} + 1}\right)^{\frac{3}{2}}$</td><td>third order reaction (a=2, b=1):
$\frac{dR_{f,2}}{dt} \sim \frac{dR_{f,1}}{dt} \cdot \left(\frac{c_{Sb0} \cdot \mathrm{k_{FeS,b}} \cdot \mathrm{v} \cdot \frac{\mathrm{l}}{u_1} + 1}{c_{Sb0} \cdot \mathrm{k_{FeS,b}} \cdot \mathrm{v} \cdot \frac{\mathrm{l}}{u_2} + 1}\right)^{\frac{3}{2}}$</td><td>fourth order reaction (a=2, b=2):
$\frac{dR_{f,2}}{dt} \sim \frac{dR_{f,1}}{dt} \cdot \left(\frac{c_{Sb0} \cdot \mathrm{k_{FeS,b}} \cdot \mathrm{v} \cdot \frac{\mathrm{l}}{u_1} + 1}{c_{Sb0} \cdot \mathrm{k_{FeS,b}} \cdot \mathrm{v} \cdot \frac{\mathrm{l}}{u_2} + 1}\right)^{\frac{4}{3}}$</td></tr>
<tr><td colspan="4">Initial fouling, before concentration has changed:
$\frac{dR_{f,2}}{dt} \sim \frac{dR_{f,1}}{dt}$</td></tr>
<tr><td>Asphaltene precipitation in the bulk</td><td colspan="4">$\frac{dR_{f,2}}{dt} = \frac{dR_{f,1}}{dt} \cdot \frac{u_2}{u_1}$</td></tr>
<tr><td>Transport (diffusion)</td><td colspan="2">Fully developed laminar flow in pipes:
$\frac{dR_{f,2}}{dt} \sim \frac{dR_{f,1}}{dt}$</td><td colspan="2">Fully developed turbulent flow in pipes:
$\frac{dR_{f,2}}{dt} \sim \frac{dR_{f,1}}{dt} \cdot \left(\frac{u_2}{u_1}\right)^{0.8}$</td></tr>
</table>

<table>
<tr><td rowspan="2">Chemical reaction in the film</td><td>Developed fouling, pseudo zero order chemical reaction:
$\frac{dR_{f,2}}{dt} \sim \frac{dR_{f,1}}{dt}$</td><td>Developed fouling, first order chemical reaction:
$\frac{dR_{f,2}}{dt} \sim \frac{dR_{f,1}}{dt} \cdot exp\left[\mathrm{k_{f1}} \cdot \mathrm{l} \cdot \left(\frac{1}{u_1} - \frac{1}{u_2}\right)\right]$</td><td>Developed fouling, second order chemical reaction:
$\frac{dR_{f,2}}{dt} \sim \frac{dR_{f,1}}{dt} \cdot \left(\frac{c_{Abo} \cdot \mathrm{k_{f2}} \cdot \frac{V}{A} \cdot \frac{\mathrm{l}}{u_1} + 1}{c_{Abo} \cdot \mathrm{k_{f2}} \cdot \frac{V}{A} \cdot \frac{\mathrm{l}}{u_2} + 1}\right)^2$</td></tr>
<tr><td colspan="3">Initial fouling:
$\frac{dR_{f,2}}{dt} \sim \frac{dR_{f,1}}{dt}$</td></tr>
<tr><td>Corrosion in the film</td><td colspan="3">Initial fouling, before concentration has changed:
$\frac{dR_{f,2}}{dt} \sim \frac{dR_{f,1}}{dt}$</td></tr>
<tr><td rowspan="2">Corrosion in the film</td><td>First order chemical reaction:
$\frac{dR_{f,2}}{dt} \sim \frac{dR_{f,1}}{dt} \cdot exp\left[k_{FeS,f,1} \cdot \mathrm{l} \cdot \left(\frac{1}{u_1} - \frac{1}{u_2}\right)\right]$</td><td colspan="2">Second order chemical reaction:
$\frac{dR_{f,2}}{dt} \sim \frac{dR_{f,1}}{dt} \cdot \left(\frac{c_{Sbo} \cdot k_{FeS,f,2} \cdot \frac{V}{A} \cdot \frac{\mathrm{l}}{u_1} + 1}{c_{Sbo} \cdot k_{FeS,f,2} \cdot \frac{V}{A} \cdot \frac{\mathrm{l}}{u_2} + 1}\right)^2$</td></tr>
<tr><td colspan="3">Initial fouling:
$\frac{dR_{f,2}}{dt} \sim \frac{dR_{f,1}}{dt}$</td></tr>
<tr><td>Asphaltene precipitation in the film</td><td colspan="3">$\frac{dR_{f,2}}{dt} = \frac{dR_{f,1}}{dt} \cdot \frac{u_2}{u_1}$</td></tr>
<tr><td>Adsorption</td><td>Pseudo first order adsorption model:
$\frac{dR_{f,2}}{dt} \sim \frac{dR_{f,1}}{dt} \cdot \exp\left(k_{AD1} \cdot c_{As} \cdot l \cdot \left(\frac{1}{u_2} - \frac{1}{u_1}\right)\right)$</td><td colspan="2">Pseudo second order adsorption model:
$\frac{dR_{f,2}}{dt} \sim \frac{dR_{f,1}}{dt} \cdot \left(\frac{1 - k_{AD2} \cdot c_{As} \cdot c_{t,o} \cdot \frac{l}{u_1}}{1 - k_{AD} \cdot c_{As} \cdot c_{t,o} \cdot \frac{l}{u_2}}\right)^2$</td></tr>
</table>

Chemical reaction on the heat transfer surface	Pseudo zero order chemical reaction: $\frac{dR_{f,2}}{dt} \sim \frac{dR_{f,1}}{dt}$	First order chemical reaction: $\frac{dR_{f,2}}{dt} \sim \frac{dR_{f,1}}{dt} \cdot exp\left[\mathrm{k_{f1}} \cdot \mathrm{l} \cdot \left(\frac{1}{u_1} - \frac{1}{u_2}\right)\right]$	Second order chemical reaction: $\frac{dR_{f,2}}{dt} \sim \frac{dR_{f,1}}{dt} \cdot \left(\frac{c_{Ab0} \cdot \mathrm{k_{b2}} \cdot \frac{V}{A} \cdot \frac{1}{u_1} + 1}{c_{Ab0} \cdot \mathrm{k_{b2}} \cdot \frac{V}{A} \cdot \frac{1}{u_2} + 1}\right)^2$
	Initial fouling: $\frac{dR_{f,2}}{dt} \sim \frac{dR_{f,1}}{dt}$		
Corrosion on the surface	Developed fouling, first order chemical reaction: $\frac{dR_{f,2}}{dt} \sim \frac{dR_{f,1}}{dt} \cdot exp\left[k_{FeS,s,1} \cdot \mathrm{l} \cdot \left(\frac{1}{u_1} - \frac{1}{u_2}\right)\right]$	Developed fouling, second order chemical reaction: $\frac{dR_{f,2}}{dt} \sim \frac{dR_{f,1}}{dt} \cdot \left(\frac{c_{Sb0} \cdot k_{FeS,s,2} \cdot \frac{V}{A} \cdot \frac{1}{u_1} + 1}{c_{Sb0} \cdot k_{FeS,s,2} \cdot \frac{V}{A} \cdot \frac{1}{u_2} + 1}\right)^2$	
	Initial fouling: $\frac{dR_{f,2}}{dt} \sim \frac{dR_{f,1}}{dt}$		
Asphaltene precipitation on the surface	$\frac{dR_{f,2}}{dt} = \frac{dR_{f,1}}{dt} \cdot \frac{u_2}{u_1}$		
Desorption of the fouling product	$-\frac{dR_{f,2}}{dt} \sim -\frac{dR_{f,1}}{dt}$		
Transport (back diffusion)	Fully developed laminar flow in pipes: $-\frac{dR_{f,2}}{dt} \sim -\frac{dR_{f,1}}{dt}$	Fully developed turbulent flow in pipes: $-\frac{dR_{f,2}}{dt} \sim -\frac{dR_{f,1}}{dt} \cdot \left(\frac{u_2}{u_1}\right)^{0.8}$	

table 59: Summary of velocity dependency of rate equations developed by kinetic modelling, depending on the controlling step

7 Comparison with experimental data

The developed rate equations can be used to compare the models with experimental data from literature. In chapter 7.1 to 7.3 experimental data from different sources ([Watkinson 2005], [Scarborough et al. 1979], [Yang et al. 2011]) was used.

No matter, what the fouling mechanism was, asphaltene precipitation, particulate fouling, corrosion fouling or chemical reaction fouling, the effects of velocity and temperature on fouling rates dR_f/dt could best be described with the developed equations from kinetic modelling for fouling controlled by adsorption. This leads to the assumption, that either single steps or binary combinations of steps affect the fouling process, with adsorption always being a decisive step.

7.1 Comparison with experimental data from [Watkinson 2005]

[Watkinson 2005] published a series of initial fouling rates dR_f/dt as a function of temperature and velocity for different crude oils. [Watkinson 2005] tested eight crude oils and blends, three of them light and medium oils with fouling being assumed to be caused by particulates (seeding) initially present in the oil, crude oil for which fouling was assumed to be caused by autoxidation, three blends with fouling being assumed to be caused by asphaltene precipitation and one crude oil with fouling being assumed to be caused by corrosion, see table 60.

	Oil	Fouling caused by:
GPS	light	paticulates, solids initially present in the oil
CSK	light	paticulates, solids initially present in the oil
SSB	light	autoxidation
BHO	medium	paticulates, solids initially present in the oil
LSB	medium	corrosion
HOP	heavy blend	asphaltene precipitation
VR/PFX	heavy blend	asphaltene precipitation
ATB/PFX	heavy blend	asphaltene precipitation

table 60: crude oils and blends tested by [Watkinson 2005]

[Watkinson 2005] minimized the role of bulk fluid chemical reactions by maintaining bulk temperatures significantly below surface temperature. Therefore, chemical reaction as well as corrosion can basically take place in the boundary layer or on the heat transfer surface and chemical reaction and corrosion in the bulk can be ruled out.

[Watkinson 2005] tested the oils and blends at either constant temperature or constant velocity to get a closer insight into their impact on fouling rates.

[Watkinson 2005] used the film temperature T_f for the light and medium oils to correlate fouling rates, as he assumed reaction and adsorption processes to be the controlling steps. For the heavy oil blends, for which asphaltene precipitation is assumed to be responsible for fouling, the surface temperature T_s was used to correlate fouling rates.

7.1.1 Transport (diffusion) in the film and to the heat transfer surface is rate controlling

The effect of velocity and temperature on the initial fouling rates dR_f/dt for fouling controlled by diffusion are illustrated in figure 36 to figure 38.

Diffusion is influenced by film temperature T_f, therefore no comparison could be done for the heavy blends, which were correlated by [Watkinson 2005] with surface temperature T_s.

The comparison between experimental data and the developed kinetic model shows, that transport is not likely to be the controlling step.

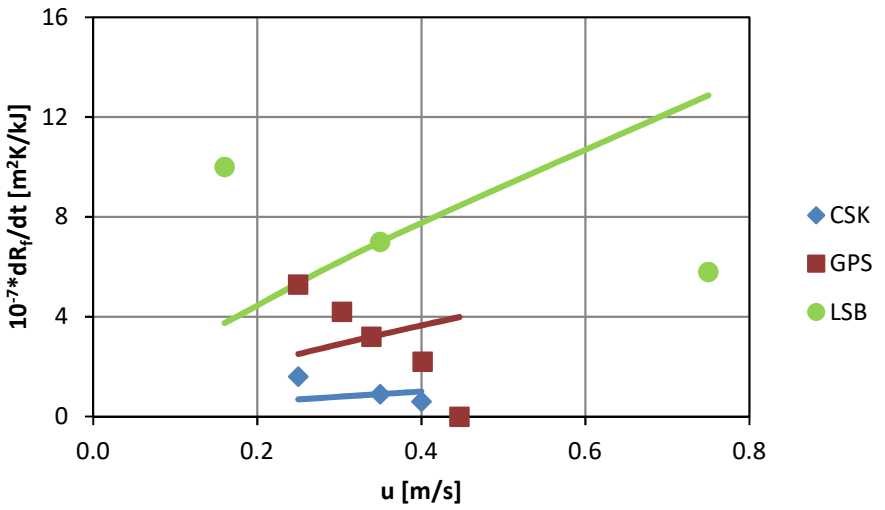

figure 36: Effect of velocity u on the initial fouling rates dR_f/dt, experimental data from [Watkinson 2005], compared with equations developed by kinetic modelling, with fouling controlled by transport (diffusion); dots: experiment; lines: model

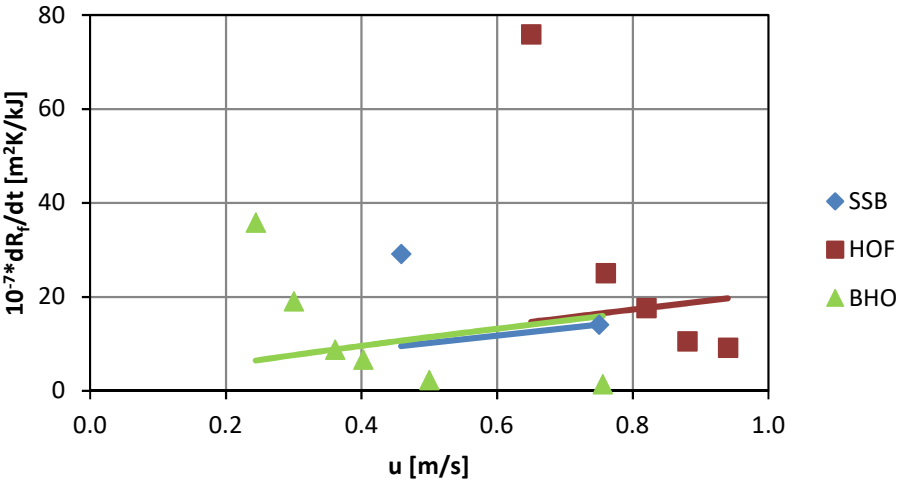

figure 37: Effect of velocity u on the initial fouling rates dR_f/dt, experimental data from [Watkinson 2005], compared with equations developed by kinetic modelling, with fouling controlled by transport (diffusion); dots: experiment; lines: model

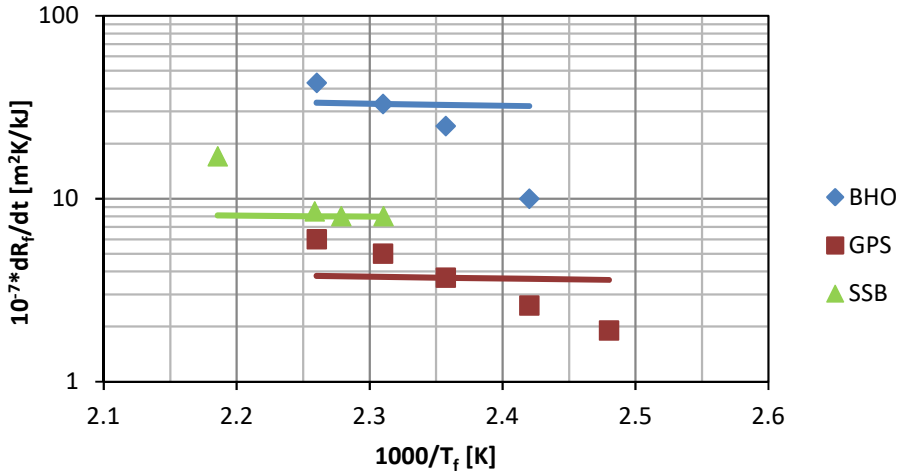

figure 38: Effect of film temperature T_f on the initial fouling rates dR_f/dt, experimental data from [Watkinson 2005], compared with equations developed by kinetic modelling, with fouling controlled by transport (diffusion); dots: experiment; lines: model

7.1.2 Adsorption is rate controlling

The effect of velocity and temperature on the initial fouling rates dR_f/dt for fouling controlled by adsorption are illustrated in figure 39 to figure 41.

Adsorption is influenced by surface temperature T_s, therefore no comparison could be done for the light and medium oils, which were correlated by [Watkinson 2005] with film temperature T_f.

For the modelling of kinetics, the equations developed for fouling controlled by adsorption (pseudo first order adsorption) compare best with the experimental data.

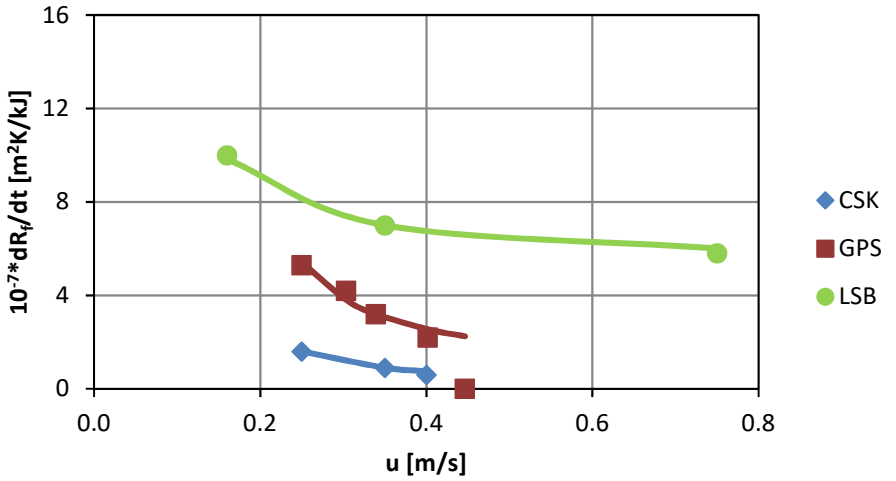

figure 39: Effect of velocity u on the initial fouling rates dR_f/dt, experimental data from [Watkinson 2005], compared with equations developed by kinetic modelling, with fouling controlled by adsorption (pseudo first order adsorption; dots: experiment; lines: model

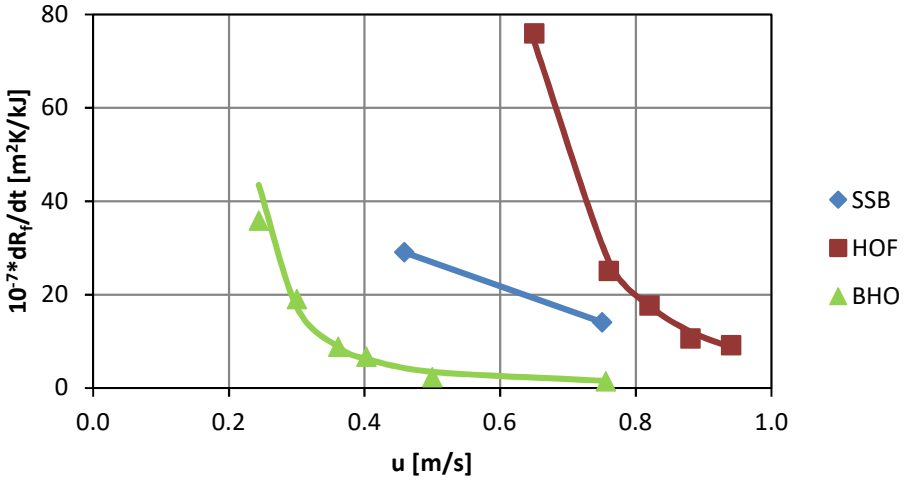

figure 40: Effect of velocity u on the initial fouling rates dR_f/dt, experimental data from [Watkinson 2005], compared with equations developed by kinetic modelling, with fouling controlled by adsorption (pseudo first order adsorption); dots: experiment; lines: model

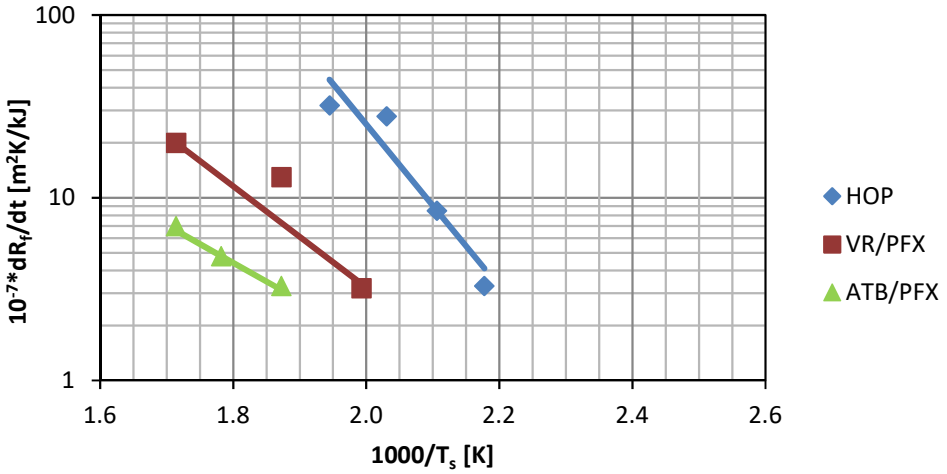

	E [kJ/mol]
VR/PFX	53.0
HOP	85.0
ATB/PFX	39.2

figure 41: Effect of surface temperature T_s on the initial fouling rates dR_f/dt, experimental data from [Watkinson 2005], compared with equations developed by kinetic modelling, with fouling controlled by adsorption (pseudo first order adsorption); dots: experiment; lines: model

7.1.3 Chemical reaction is rate controlling

[Watkinson 2005] tried to rule out bulk chemical reaction in his experiments by keeping bulk temperatures significantly below surface temperature. Measured initial fouling rates dR_f/dt were only compared with calculated data for fouling controlled by film chemical reaction and chemical reaction on the surface.

The effect of velocity and temperature on the initial fouling rates dR_f/dt for chemical reaction as controlling step are illustrated in figure 42 to figure 45. As the experimental data is given for initial fouling rates, no effect of velocity is determinable. The comparison between experimental data and the developed kinetic model shows, that chemical reaction is not likely to be the controlling step.

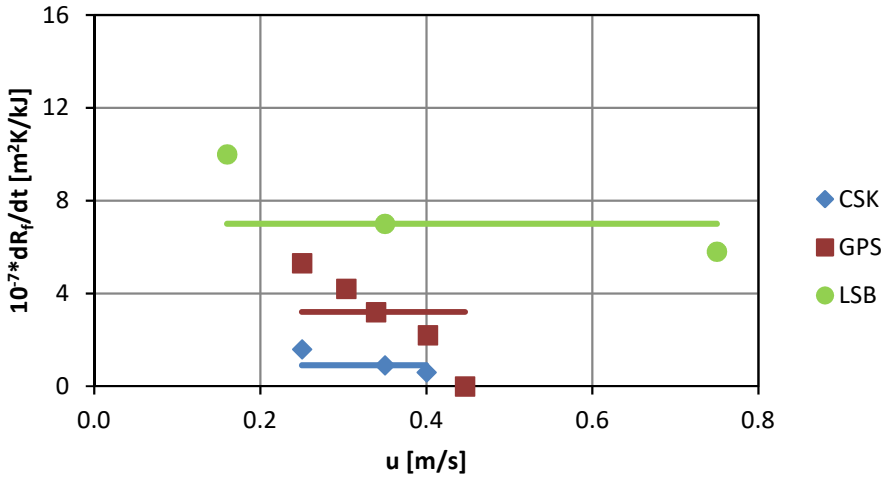

figure 42: Effect of velocity u on the initial fouling rates dR_f/dt, experimental data from [Watkinson 2005], compared with equations developed by kinetic modelling, with fouling controlled by chemical reaction in the film or on the surface. Initial fouling rates, before concentration has changed; dots: experiment; lines: model

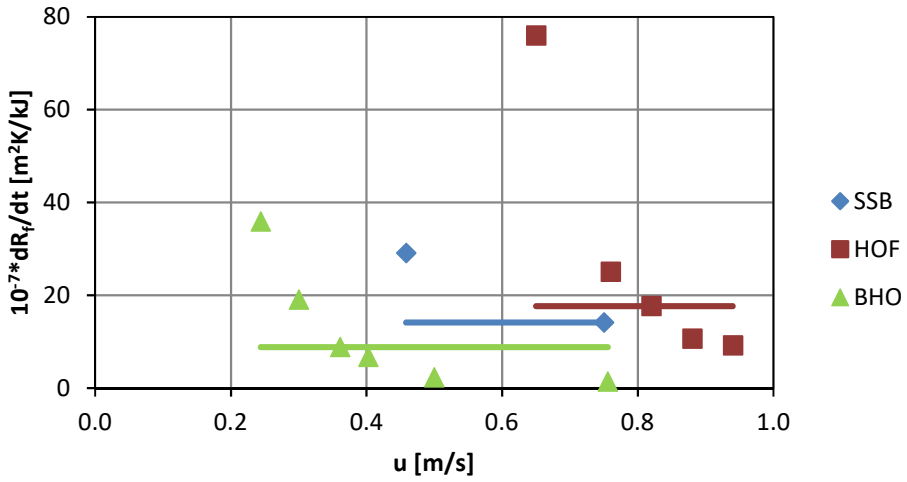

figure 43: Effect of velocity u on the initial fouling rates dR_f/dt, experimental data from [Watkinson 2005], compared with equations developed by kinetic modelling, with fouling controlled by chemical reaction in the film or on the surface. Initial fouling rates, before concentration has changed; dots: experiment; lines: model

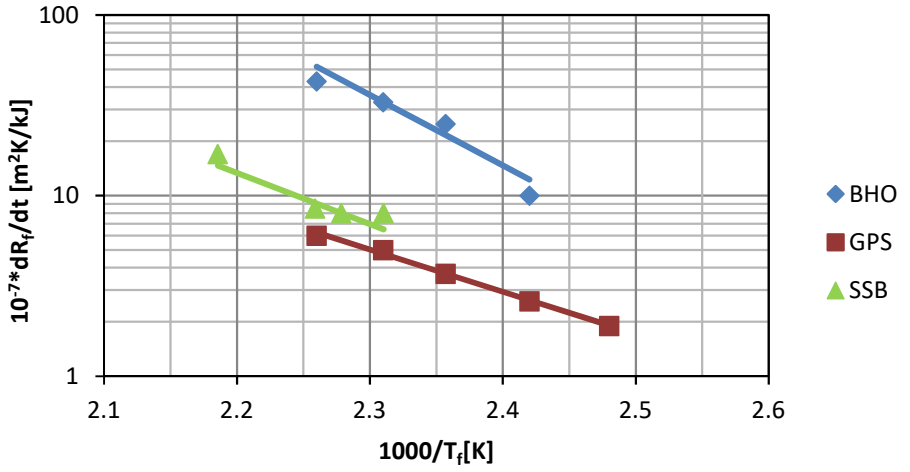

	E [kJ/mol]
BHO	74.7
GPS	44.7
SSB	54.2

figure 44: Effect of film temperature T_f on the initial fouling rates dR_f/dt, experimental data from [Watkinson 2005], compared with equations developed by kinetic modelling, with fouling controlled by chemical reaction in the film; dots: experiment; lines: model

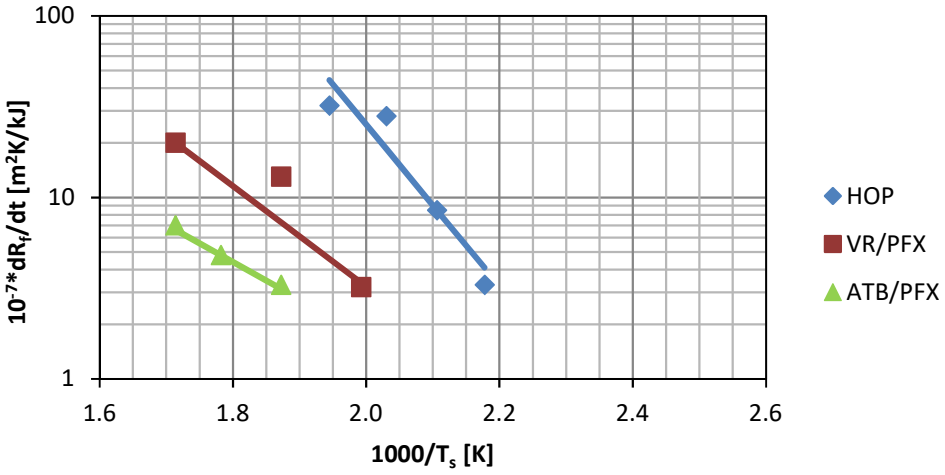

	E [kJ/mol]
VR/PFX	53.0
HOP	85.0
ATB/PFX	39.2

figure 45: Effect of surface temperature T_s on the initial fouling rates dR_f/dt, experimental data from [Watkinson 2005], compared with equations developed for kinetic modelling, with fouling controlled by chemical reaction on the surface; dots: experiment; lines: model

7.1.4 Corrosion is rate controlling

[Watkinson 2005] tried to rule out bulk chemical reaction and therefore corrosion in his experiments as well by keeping bulk temperatures significantly below surface temperature. Therefore, measured initial fouling rates dR_f/dt were only compared with calculated data for fouling controlled by corrosion in the film and on the surface.

The effect of velocity and temperature on the initial fouling rates dR_f/dt for chemical reaction as controlling step are illustrated in figure 46 to figure 49. As the experimental data is given for initial

fouling rates, no effect of velocity is determinable. The comparison between experimental data and the developed kinetic model shows, that corrosion is not likely to be the controlling step.

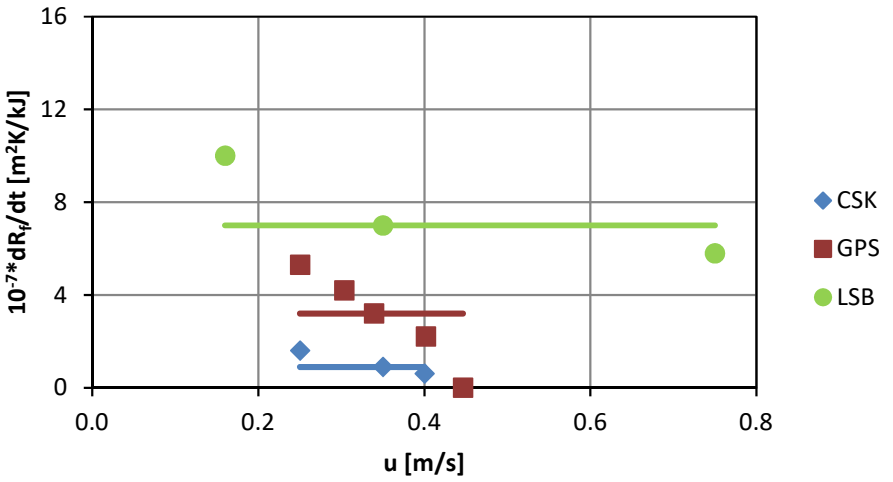

figure 46: Effect of velocity u on the initial fouling rates dR_f/dt, experimental data from [Watkinson 2005], compared with equations developed by kinetic modelling, with fouling controlled by corrosion in the film or on the surface. Initial fouling rates, before concentration has changed; dots: experiment; lines: model

figure 47: Effect of velocity u on the initial fouling rates dR_f/dt, experimental data from [Watkinson 2005], compared with equations developed by kinetic modelling, with fouling controlled by corrosion in the film or on the surface. Initial fouling rates, before concentration has changed; dots: experiment; lines: model

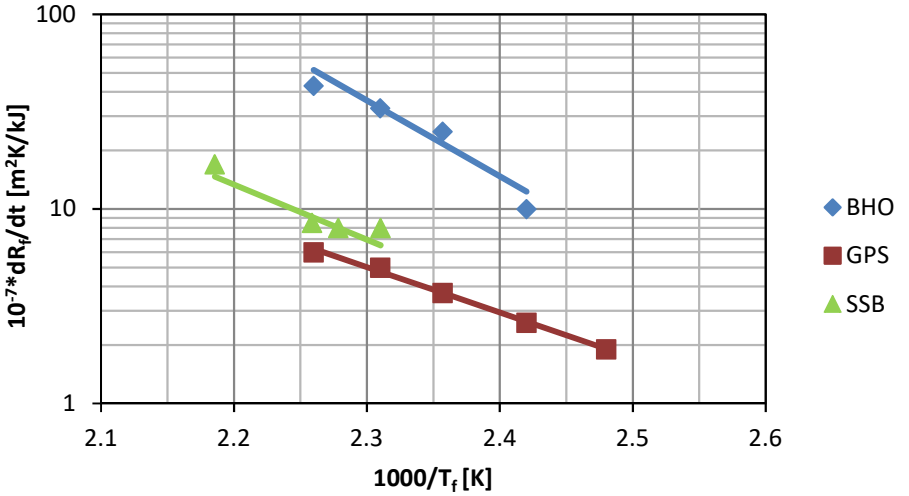

	E [kJ/mol]
BHO	74.7
GPS	44.7
SSB	54.2

figure 48: Effect of film temperature T_f on the initial fouling rates dR_f/dt, experimental data from [Watkinson 2005], compared with equations developed by kinetic modelling, with fouling controlled by corrosion in the film; dots: experiment; lines: model

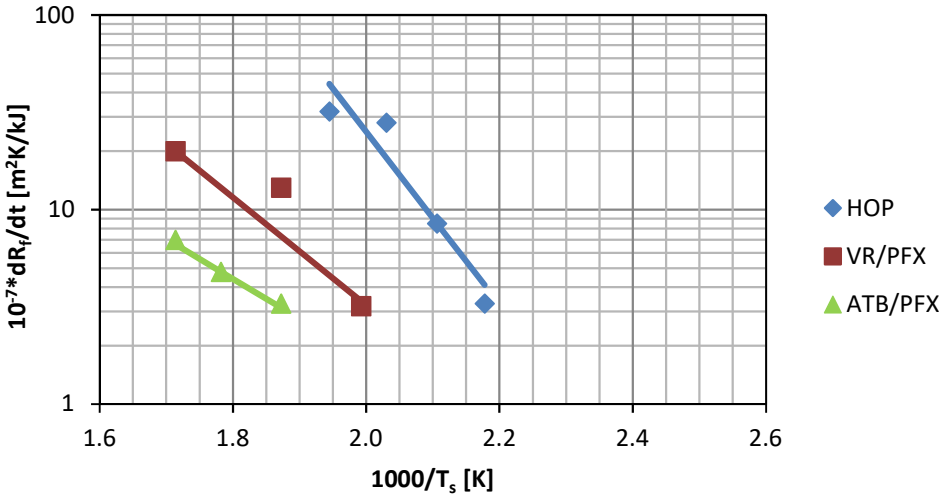

	E [kJ/mol]
VR/PFX	53.0
HOP	85.0
ATB/PFX	39.2

figure 49: Effect of surface temperature T_s on the initial fouling rates dR_f/dt, experimental data from [Watkinson 2005], compared with equations developed by kinetic modelling, with fouling controlled by corrosion in the film; dots: experiment; lines: model

7.1.5 Asphaltene precipitation is rate controlling

The effects of temperature and velocity on the initial fouling rates dR_f/dt for fouling controlled by asphaltene precipitation are illustrated in figure 50 to figure 53.

The comparison between experimental data and the developed kinetic model shows, that asphaltene precipitation is not likely to be the controlling step.

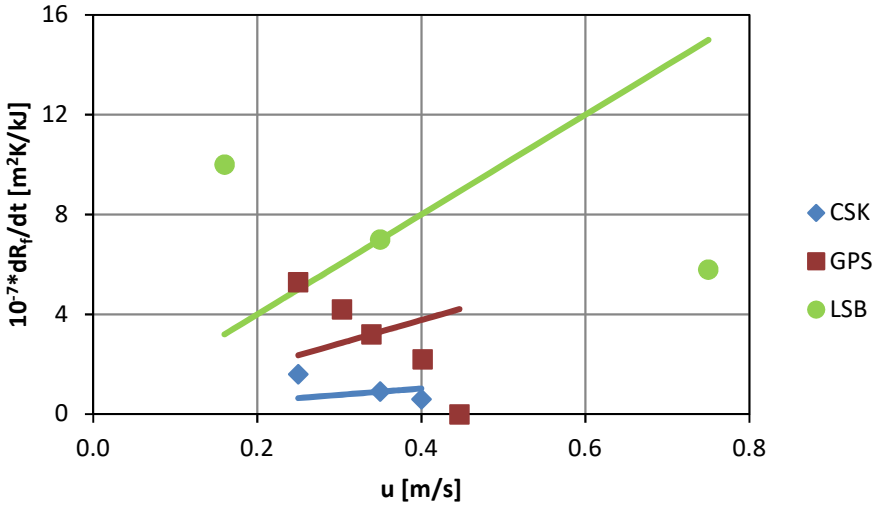

figure 50: Effect of velocity u on the initial fouling rates dR_f/dt, experimental data from [Watkinson 2005], compared with equations developed by kinetic modelling, with fouling controlled by asphaltene precipitation in the bulk, the film or on the surface; dots: experiment; lines: model

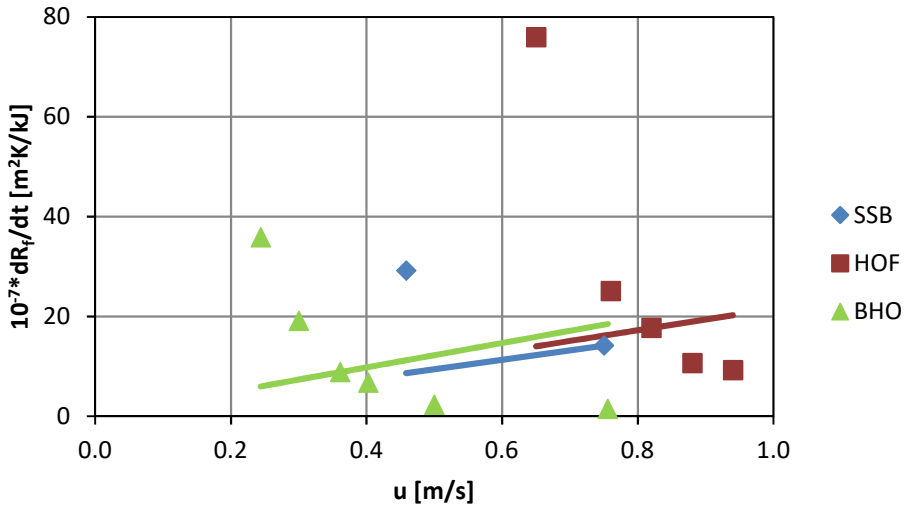

figure 51: Effect of velocity u on the initial fouling rates dR_f/dt, experimental data from [Watkinson 2005], compared with equations developed by kinetic modelling, with fouling controlled by asphaltene precipitation in the bulk, the film or on the surface; dots: experiment; lines: model

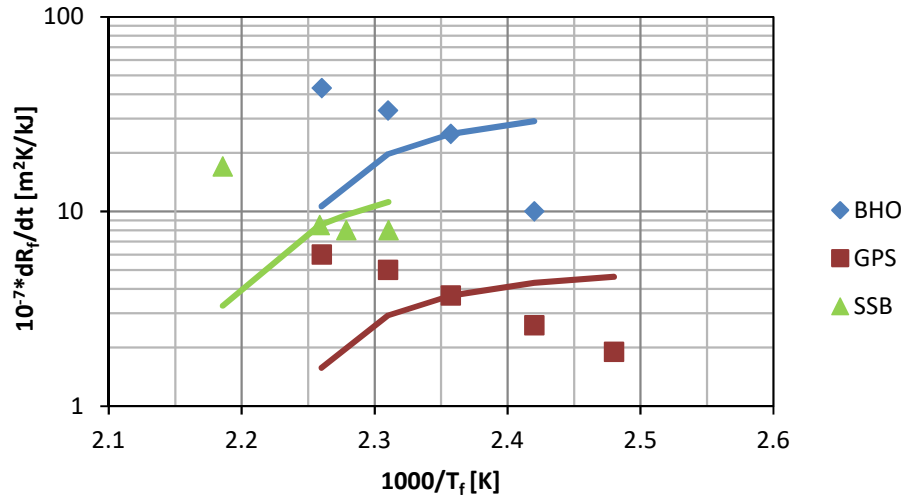

figure 52: Effect of film temperature T_f on the initial fouling rates dR_f/dt, experimental data from [Watkinson 2005], compared with equations developed by kinetic modelling, with fouling controlled asphaltene precipitation in the film; dots: experiment; lines: model

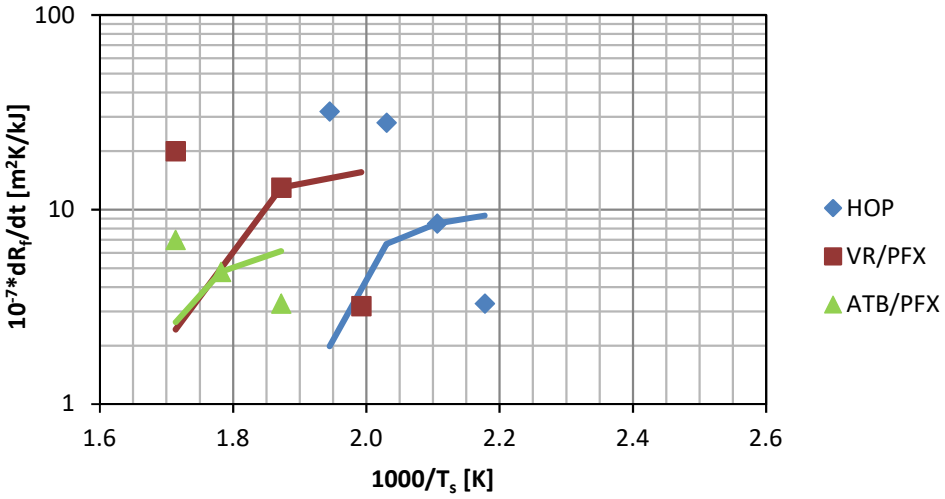

figure 53: Effect of surface temperature T_s on the initial fouling rates dR_f/dt, experimental data from [Watkinson 2005], compared with equations developed by kinetic modelling, with fouling controlled asphaltene precipitation on the surface; dots: experiment; lines: model

7.1.6 Desorption is rate controlling

The effects of temperature and velocity on the initial fouling rates dR_f/dt for fouling controlled by desorption are illustrated in figure 54 to figure 56. The comparison between experimental data and the developed kinetic model shows, that desorption is not likely to be the controlling step.

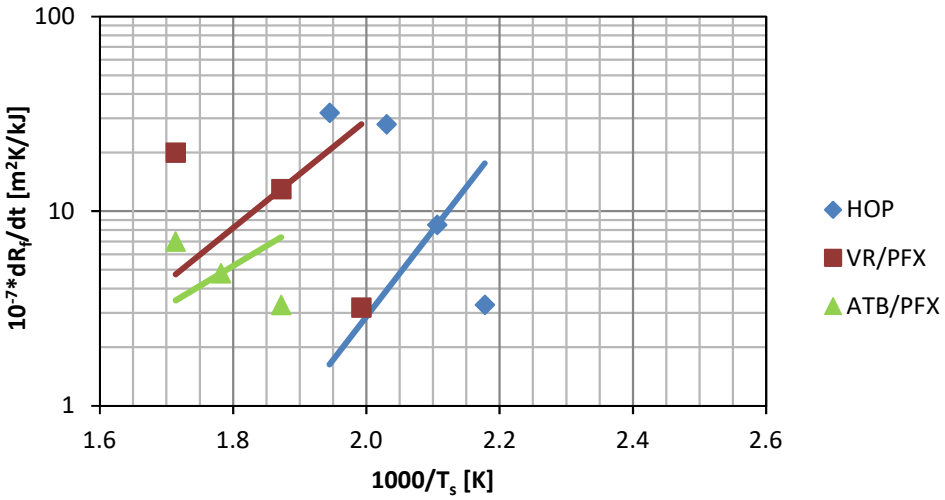

figure 54: Effect of surface temperature T_s on the initial fouling rates dR_f/dt, experimental data from [Watkinson 2005], compared with equations developed by kinetic modelling, with fouling controlled by desorption; dots: experiment; lines: model

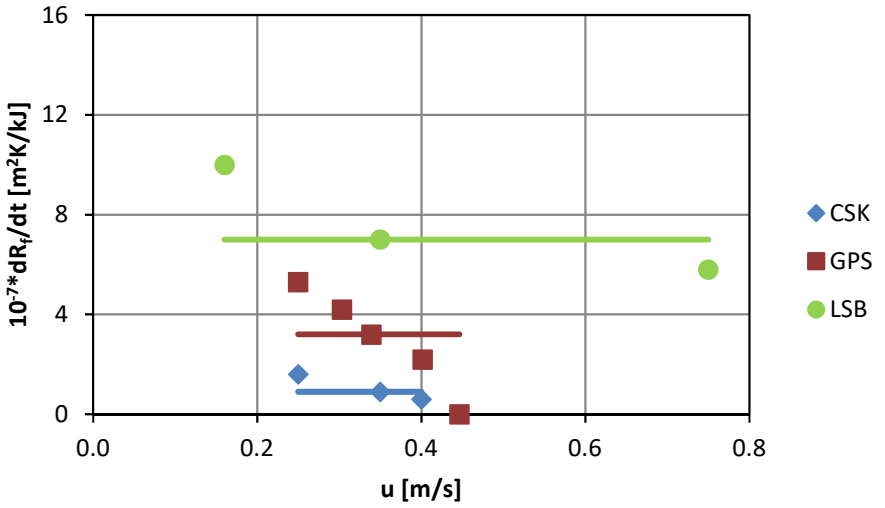

figure 55: Effect of velocity u on the initial fouling rates dR_f/dt, experimental data from [Watkinson 2005], compared with equations developed by kinetic modelling, with fouling controlled by desorption; dots: experiment; lines: model

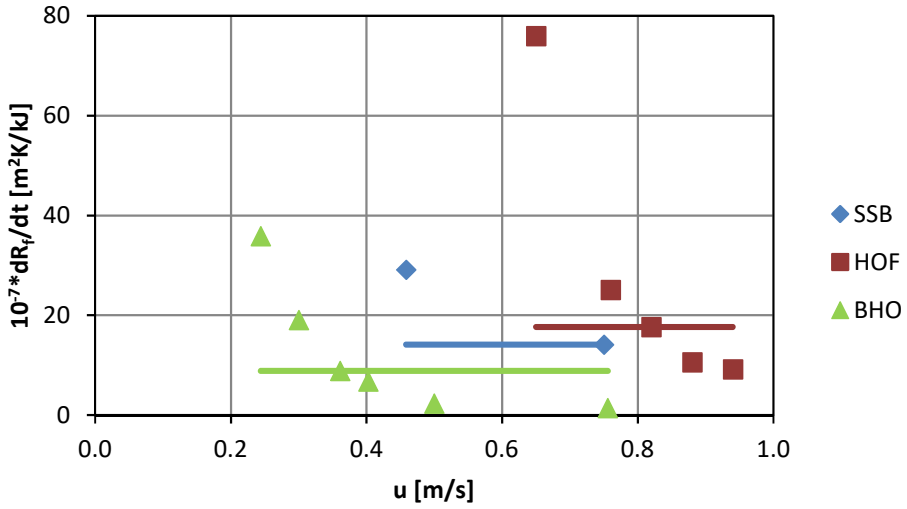

figure 56: Effect of velocity u on the initial fouling rates dR_f/dt, experimental data from [Watkinson 2005], compared with equations developed by kinetic modelling, with fouling controlled by desorption; dots: experiment; lines: model

7.1.7 Back diffusion is rate controlling

The effects of temperature and velocity on the initial fouling rates dR_f/dt for fouling controlled by back diffusion are illustrated in figure 57 to figure 59. The comparison between experimental data and the developed kinetic model shows, that back diffusion is not likely to be the controlling step.

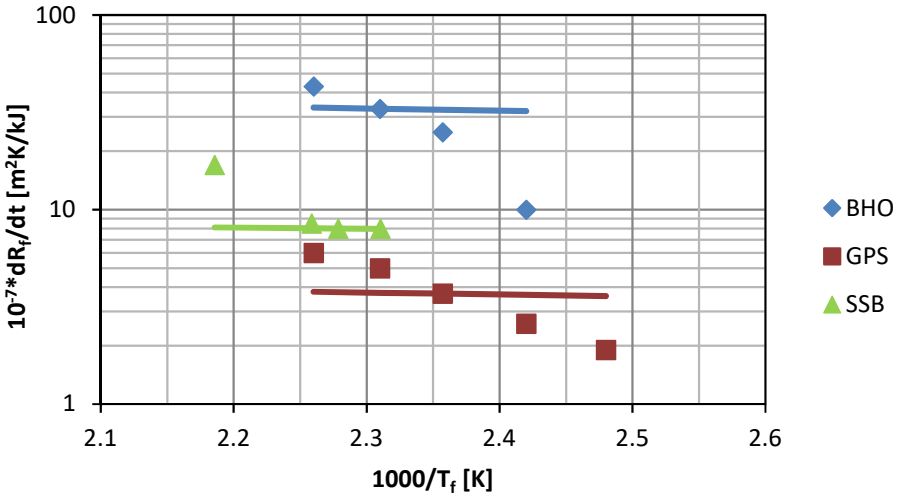

figure 57: Effect of film temperature T_f on the initial fouling rates dR_f/dt, experimental data from [Watkinson 2005], compared with equations developed by kinetic modelling, with fouling controlled by back diffusion; dots: experiment; lines: model

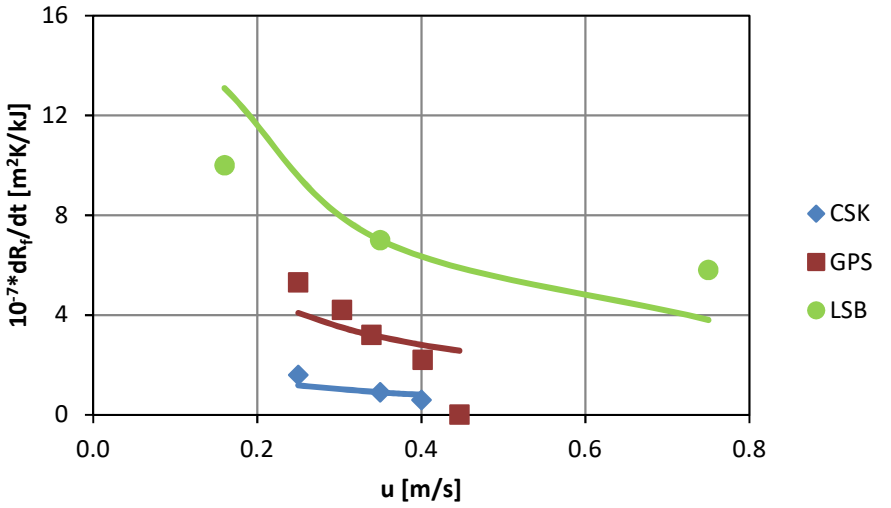

figure 58: Effect of velocity u on the initial fouling rates dR_f/dt, experimental data from [Watkinson 2005], compared with equations developed by kinetic modelling, with fouling controlled by back diffusion; dots: experiment; lines: model

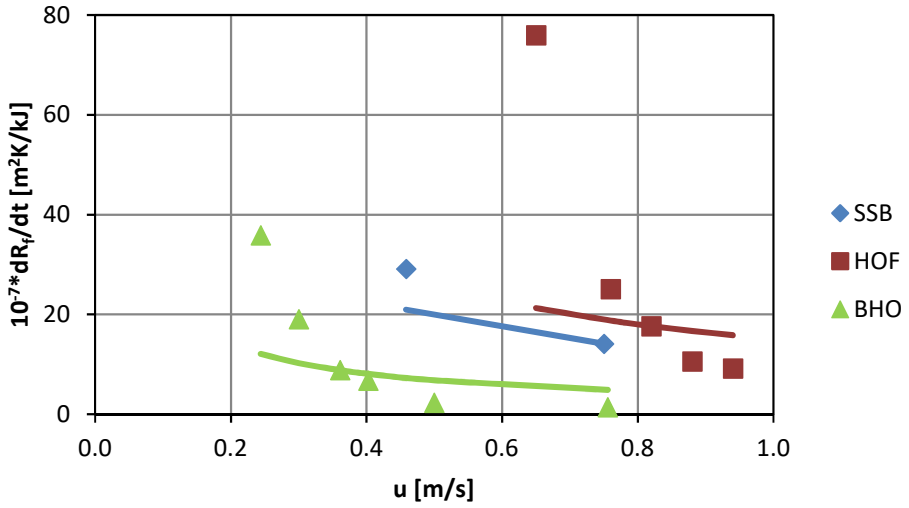

figure 59: Effect of velocity u on the initial fouling rates dR_f/dt, experimental data from [Watkinson 2005], compared with equations developed by kinetic modelling, with fouling controlled by back diffusion; dots: experiment; lines: model

7.2 Comparison with experimental data from [Scarborough et al. 1979]

[Scarborough et al. 1979] measured fouling rates dR_f/dt of coke formation (settling) in crude carrying tubes. Coking as fouling mechanism is relevant for very high temperatures only, therefore this experimental study considers temperatures up to 370°C. Nevertheless, the measured fouling rates were used to check the developed equations. To do this, the equations summarized in table 58 were used to describe the dependency from velocity u as well as from surface temperature T_s. The fouling rates dR_f/dt were compared with the equations for fouling controlled by adsorption (pseudo first order adsorption), with an activation energy of E = 58.6 kJ/mol. All other mechanisms did not match the experimental data. For results, see table 61.

[Polley et at. 2002] used the same set of data to evaluate a semi-empirical model, the calculated fouling rates R_f are mentioned in table 61 as well. The results from [Polley et al. 2002] matched the fouling rates dR_f/dt with a standard deviation of the ratio r (measured/predicted value) of 0.58, in comparison with a with a standard deviation of 0.21 for fouling controlled by adsorption.

		Experimental data, [Scarborough et al. 1979]	Calculated by [Poley et al. 2002]		Kinetic modeling: adsorption controlled		Adsorption, second order	adsortpion controlled, berechnet aus u un Ts
u	T_s	dR_f/dt	dR_f/dt	r	dR_f/dt	r	dRf/dt	dRf/dt
m s^{-1}	°C	10^{-6} m^2 K W^{-1} h^{-1}	10^{-6} m^2 K W^{-1} h^{-1}	-	10^{-6} m^2 K W^{-1} h^{-1}	-	10^{-6} m^2 K W^{-1} h^{-1}	10^{-6} m^2 K W^{-1} h^{-1}
2.48	414	3.2	4.0	0.80	4.4	0.73	4.8	4.4
1.25	467	20.1	37.3	0.54	20.1	1.00	20.1	20.1
2.48	397	2.8	1.6	1.75	3.4	0.83	3.7	3.4
1.25	432	11.4	23.9	0.48	12.5	0.91	12.5	12.5
1.25	401	7.9	14.8	0.53	7.9	1.00	7.9	7.9
1.29	374	5.6	8.4	0.67	4.9	1.15	4.8	4.9
2.53	404	4	2.2	1.82	3.7	1.09	4.0	3.7
2.53	376	1.2	0.0		2.4	0.51	2.6	2.4

table 61: Effect of surface temperature T_s and velocity u on fouling rates dR_f/dt, experimental data from [Scarborough et al. 1979], compared with 1) results from semi-empirical modelling from [Polley et al. 2002], 2) equations developed by kinetic modelling, with fouling controlled by adsorption (pseudo first order adsorption); table includes the ratio r (measured/predicted).

7.3 Comparison with experimental data from [Yang et al. 2011]

[Yang et al. 2011] used a stirred cell system to measure fouling rates dR_f/dt of crude oil at surface temperatures up to 400°C. He examined the effects of surface temperature and stirrer speed. [Yang et al. 2011] used the semi-empirical model developed by [Ebert and Panchal 1997] to correlate the measured fouling rates dR_f/dt. To get a good match of experiment and model he had to use different activation energies E for the different stirrer speed (122, 233 and 305 kJ/mol for stirrer speeds of 90, 160 and 300 rpm), strongly indicating the role of mass transfer. However, mass transfer control does not show E_A-numbers beyond 40 to 50 kJ/mol). Consequently, his approach does not reflect mass transfer control but anything else.

By applying adsorption (pseudo first order adsorption) the fouling rates dR_f/dt compare well with one activation energy E (208 kJ/mol) for a stirrer speed of 90 to 300 rpm, as shown in figure 60 and figure 61, with a standard deviation of the ratio r (measured/predicted values) of 0.28.

The results show, that fouling in this case is most likely controlled by adsorption.

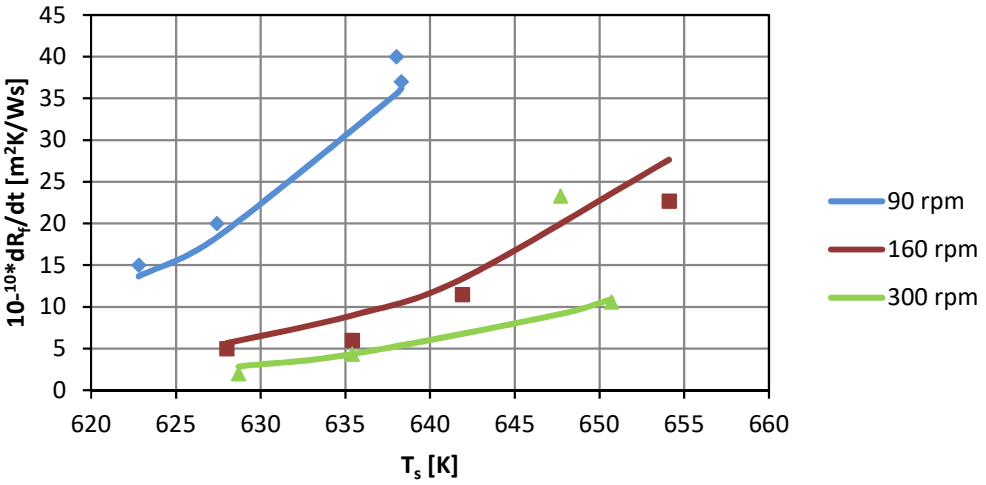

figure 60: Effect of surface temperature T_s and stirrer speed on fouling rates dR_f/dt, experimental data from [Yang et al. 2011], compared with equations developed by kinetic modelling, with fouling controlled by adsorption (pseudo first order adsorption); dots: experiment; lines: model

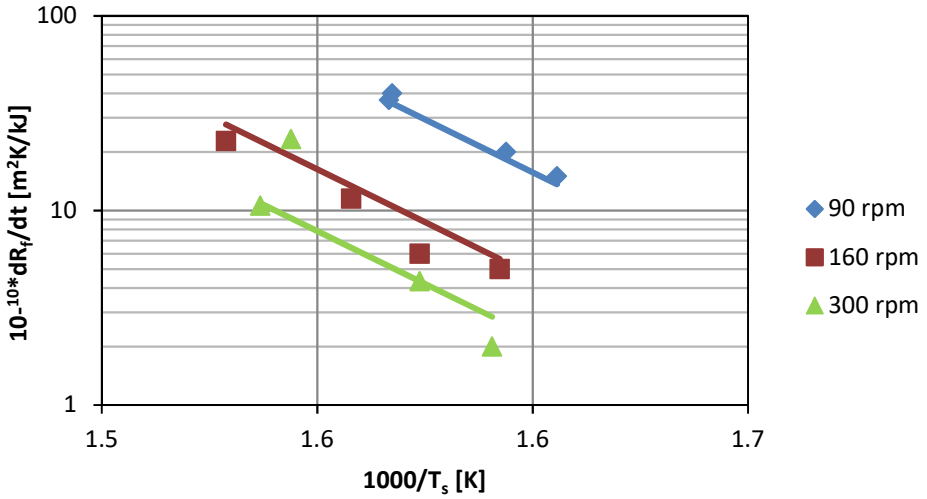

figure 61: Effect of surface temperature T_s and stirrer speed on fouling rates dR_f/dt, experimental data from [Yang et al. 2011], compared with equations developed by kinetic modelling, with fouling controlled by adsorption (pseudo first order adsorption); dots: experiment; lines: model

8 Comparison with semi-empirical models

A couple of semi-empirical models for the prediction of time dependent fouling in crude oil have been developed in recent years, see table 62. Several of these models are modifications of the original model from [Ebert and Panchal 1997].

These models generally consist of a deposition and a suppression term, see equation 47.

equation 47 $$\frac{dR_f}{dt} = deposition - suppression$$

[Wilson et al. 2015] summarized the models in the form of equation 48.

equation 48 $$\frac{dR_f}{dt} = \begin{Bmatrix} a_1 \cdot Re^{b_1} \\ a_2 . Re^{b_2} \cdot Pr^{0.33} \\ \frac{a_3}{h_{film}} \end{Bmatrix} . \begin{Bmatrix} exp\left(\frac{-E}{R \cdot T_f}\right) \\ exp\left(\frac{-E}{R \cdot T_s}\right) \end{Bmatrix} - \begin{Bmatrix} c_1 \cdot \tau_w \\ c_2 \cdot Re^{d_2} \\ c_3 \cdot u^{d_3} \end{Bmatrix}$$

The last term of equation 48 describes the reduction because of mechanical abrasion. In industrial application the net fouling resistance is strongly dependent on the removal of the fouling layer because of shear stress. This influence cannot be reproduced with the kinetic model, as mechanical abrasion is not accessible. Several of these models are summarized in table 63.

Source	Expression	Comments
[Watkinson and Epstein, 1970]	$\frac{dR_f}{dt} = \frac{a_0 e \cdot xp\left(\frac{-E}{R \cdot T_s}\right)}{u^{n_v}}$	
[Ebert and Panchal, 1997]	$\frac{dR_f}{dt} = \frac{a_1 \cdot exp\left(\frac{-E}{R \cdot T_f}\right)}{Re^{b_1}} - c_1 \cdot u^2$	
[Panchal et al., 1999]	$\frac{dR_f}{dt} = a_2 \cdot Re^{-0,66} Pr^{-0,33} exp\left(\frac{-E}{R \cdot T_f}\right) - c_2 \cdot \tau_w$	Adaption of [Ebert and Panchal, 1997]
[Polley et al., 2002]	$\frac{dR_f}{dt} = a_3 \cdot Re^{-0,8} Pr^{-0,33} exp\left(\frac{-E}{R \cdot T_s}\right) - c_3 \cdot Re^{0,8}$	
[Saleh et al., 2003]	$\frac{dR_f}{dt} = a_4 \cdot P^{b_4} \cdot u^d \cdot exp\left(\frac{-E}{RT_f}\right) - c_3 \cdot u^{0,8}$	
[Yeap et al., 2004]	$\frac{dR_f}{dt} = \frac{a_5 \cdot f \cdot u \cdot {T_s}^{2/3} \cdot \rho^{2/3} \cdot \mu^{-4/3}}{1 + e \cdot u^3 \cdot f^2 \cdot \rho^{-1/3} \cdot \mu^{-1/3} \cdot {T_s}^{2/3} \cdot exp\left(\frac{E}{R \cdot T_s}\right)} - c_5 \cdot u^{0,8}$	
[Nasr and Givi, 2006]	$\frac{dR_f}{dt} = a_6 \cdot Re^{b_6} \cdot exp\left(\frac{-E}{R \cdot T_f}\right) - c_6 \cdot Re^{0,8}$	Modification of [Polley et al., 2002]
[Polley, 2010]	$\frac{dR_f}{dt} = \frac{a_7}{h_{film}} \cdot exp\left(\frac{-E}{R \cdot T_f}\right) - S_p(\tau_w)$	
[Polley et al., 2011]	$\frac{dR_f}{dt} = \frac{a_8}{h_{film}} \cdot exp\left(\frac{-E}{R \cdot T_f}\right) - a_8 \cdot \tau_w$	Modification of [Panchal et al., 1999]
[Yang and Crittenden, 2012]	$\frac{dR_f}{dt} = \frac{a_9 \cdot f \cdot u \cdot {T_s}^{2/3} \cdot \rho^{2/3} \cdot \mu^{-4/3}}{1 + e \cdot u^3 \cdot f^2 \cdot \rho^{-1/3} \cdot \mu^{-1/3} \cdot {T_s}^{2/3} \cdot exp\left(\frac{E}{R \cdot T_s}\right)} - c_9 \cdot \tau_w$	Modification of [Yeap et al., 2004]

table 62: Fouling models in chronological order

For simplification, these models neglect the influence of surface roughness and changes in surface roughness aren't considered. Only chemical reaction fouling is considered. The fouling layer is considered to be homogeneous and the shape of deposits isn't considered. Changes in flow velocity with changing cross-sectional area due to fouling are neglected.

8.1 Development of effects of velocity and temperature on fouling rate for different semi-empirical models

Five semi-empirical models were used to compare the results of the developed kinetic model. The influence of shear stress is not described by the developed kinetic model. In order to compare them with semi-empirical models the suppression term in semi-empirical models is neglected.

To make it possible to compare the semi-empirical models with the developed equations the effects of velocity and temperature had to be determined, these are summarized in table 63 and table 64 for the selected models.

Source	[Watkinson and Epstein, 1970]	[Ebert and Panchal 1997]	[Polley et al. 2002]
Expression	$\frac{dR_f}{dt} = \frac{a_0 . exp\left(\frac{-E}{R \cdot T_S}\right)}{u^{n_v}}$	$\frac{dR_f}{dt} = a_1 \cdot Re^{b_1} \cdot exp\left(\frac{-E}{R \cdot T_f}\right)$	$\frac{dR_f}{dt} = a_3 \cdot Re^{-0,8} \cdot Pr^{-0,33} \cdot exp\left(\frac{-E}{R \cdot T_S}\right)$
Effect of velocity	$\frac{dR_{f,2}}{dt} \sim \frac{dR_{f,1}}{dt} \cdot \left(\frac{u_1}{u_2}\right)^{n_v}$	$\frac{dR_{f,2}}{dt} \sim \frac{dR_{f,1}}{dt} \cdot \left(\frac{u_1}{u_2}\right)^{b_1}$	$\frac{dR_{f,2}}{dt} \sim \frac{dR_{f,1}}{dt} \cdot \left(\frac{u_1}{u_2}\right)^{0,8}$
Effect of temperature	$\frac{dR_{f,2}}{dt} \sim \frac{dR_{f,1}}{dt} \cdot exp\left[\frac{E}{R} \cdot \left(\frac{1}{T_{S,1}} - \frac{1}{T_{S,2}}\right)\right]$	$\frac{dR_{f,2}}{dt} \sim \frac{dR_{f,1}}{dt} \cdot exp\left[\frac{E}{R} \cdot \left(\frac{1}{T_{f,1}} - \frac{1}{T_{f,2}}\right)\right]$	$\frac{dR_{f,2}}{dt} \sim \frac{dR_{f,1}}{dt} \cdot exp\left[\frac{E}{R} \cdot \left(\frac{1}{T_{S,1}} - \frac{1}{T_{S,2}}\right)\right]$

table 63: Effects of velocity and temperature for the semi-empirical models from [Watkinson and Epstein, 1970], [Ebert and Panchal, 1997] and [Polley et al. 2002]

Source	[Yeap et al. 2004]	[Polley et al. 2011]
Expression	$\frac{dR_f}{dt} = \frac{a_5 \cdot f \cdot u \cdot {T_s}^{2/3} \cdot \rho^{2/3} \cdot \mu^{-4/3}}{1+e \cdot u^3 \cdot f^2 \cdot \rho^{-1/3} \cdot \mu^{-1/3} \cdot {T_s}^{2/3} \cdot exp\left(\frac{E}{R \cdot T_s}\right)}$	$\frac{dR_f}{dt} = \frac{a_8}{h_{film}} \cdot exp\left(\frac{-E}{R \cdot T_f}\right)$
Effect of velocity	$\frac{dR_{f,2}}{dt} \sim \frac{dR_{f,1}}{dt} \cdot \frac{u_2}{u_1} \cdot \frac{1+e \cdot {u_1}^3 \cdot f^2 \cdot \rho^{-1/3} \cdot \mu^{-1/3} \cdot {T_s}^{2/3} \cdot exp\left(\frac{E}{R \cdot T_s}\right)}{1+e \cdot {u_2}^3 \cdot f^2 \cdot \rho^{-1/3} \cdot \mu^{-1/3} \cdot {T_s}^{2/3} \cdot exp\left(\frac{E}{R \cdot T_s}\right)}$	$\frac{dR_{f,2}}{dt} \sim \frac{dR_{f,1}}{dt}$
Effect of temperature	$\frac{dR_{f,2}}{dt} \sim \frac{dR_{f,1}}{dt} * \frac{1+e \cdot u^3 \cdot f^2 \cdot \rho^{-1/3} \cdot \mu^{-1/3} \cdot {T_{s,1}}^{2/3} \cdot exp\left(\frac{E}{R \cdot T_{s,1}}\right)}{1+e \cdot u^3 \cdot f^2 \cdot \rho^{-1/3} \cdot \mu^{-1/3} \cdot {T_{s,2}}^{2/3} \cdot exp\left(\frac{E}{R \cdot T_{s,2}}\right)}$	$\frac{dR_{f,2}}{dt} \sim \frac{dR_{f,1}}{dt} \cdot exp\left[\frac{E}{R} \cdot \left(\frac{1}{T_{s,1}} - \frac{1}{T_{s,2}}\right)\right]$

table 64: Effects of velocity and temperature for the semi-empirical models from [Yeap et al. 2004] and [Polley et al. 2011]

8.2 Comparison with experimental data from [Watkinson 2005]

For different crude oils and blends [Watkinson 2005] published a series of initial fouling rates as a function of temperature and velocity. These data were compared with the kinetic model equations.

To compare semi-empirical models with the equations obtained by kinetic modelling the parameters n_v and b_1 were fitted. For the kinetic modelling it was assumed, that adsorption (pseudo first order adsorption) is the controlling step. The results for semi-empirical models from [Watkinson and Epstein, 1970], [Ebert and Panchal, 1997], [Polley et al. 2002], [Yeap et al. 2004] and [Polley 2011] can be seen in figure 62 to figure 65.

While the temperature dependency can be reproduced with good accuracy by all models and with the developed equation for fouling controlled by adsorption, the semi-empirical models described the dependency on the velocity only poorly. The equations obtained by kinetic modelling matched the dependency on the velocity quite good.

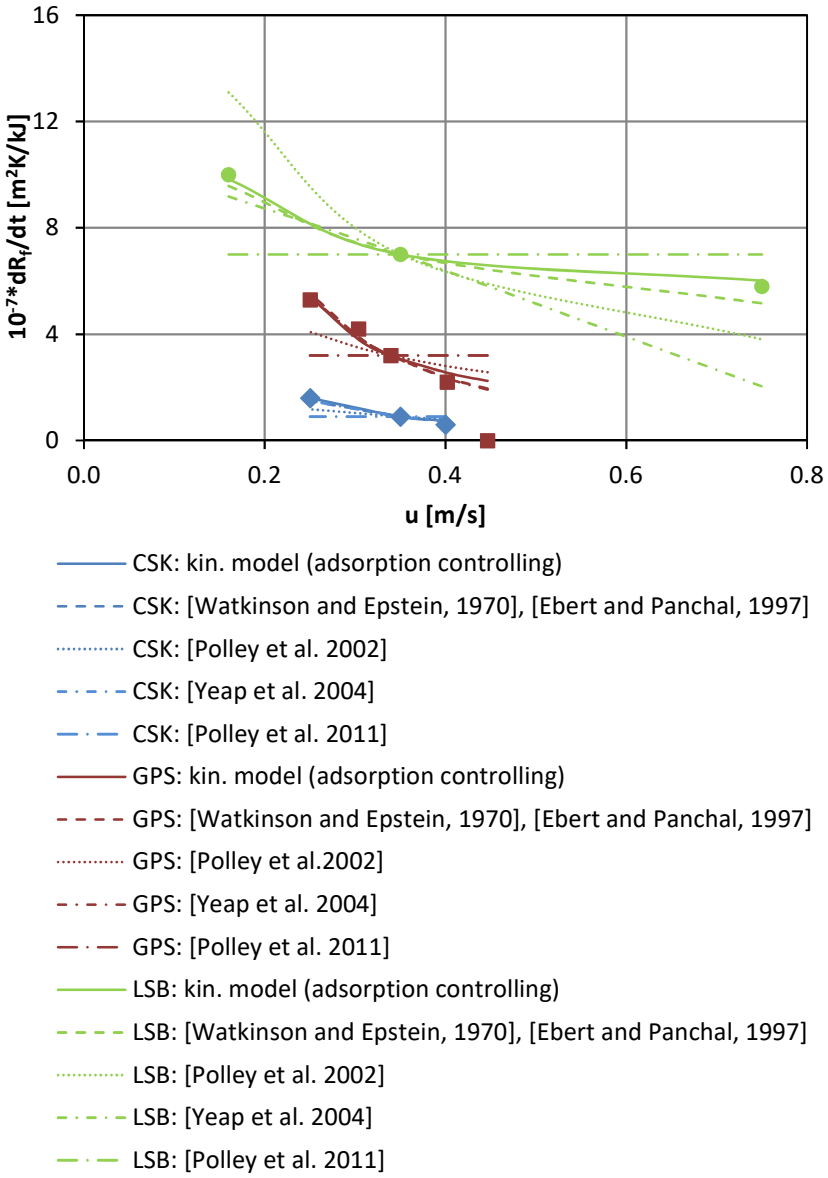

figure 62: Effect of velocity u on the initial fouling rate dR_f/dt, experimental data from [Watkinson 2005]. Compared with: 1) equations developed by kinetic modelling, for fouling controlled by adsorption (pseudo first order adsorption), 2) semi-empirical models; dots: experiment; lines: models

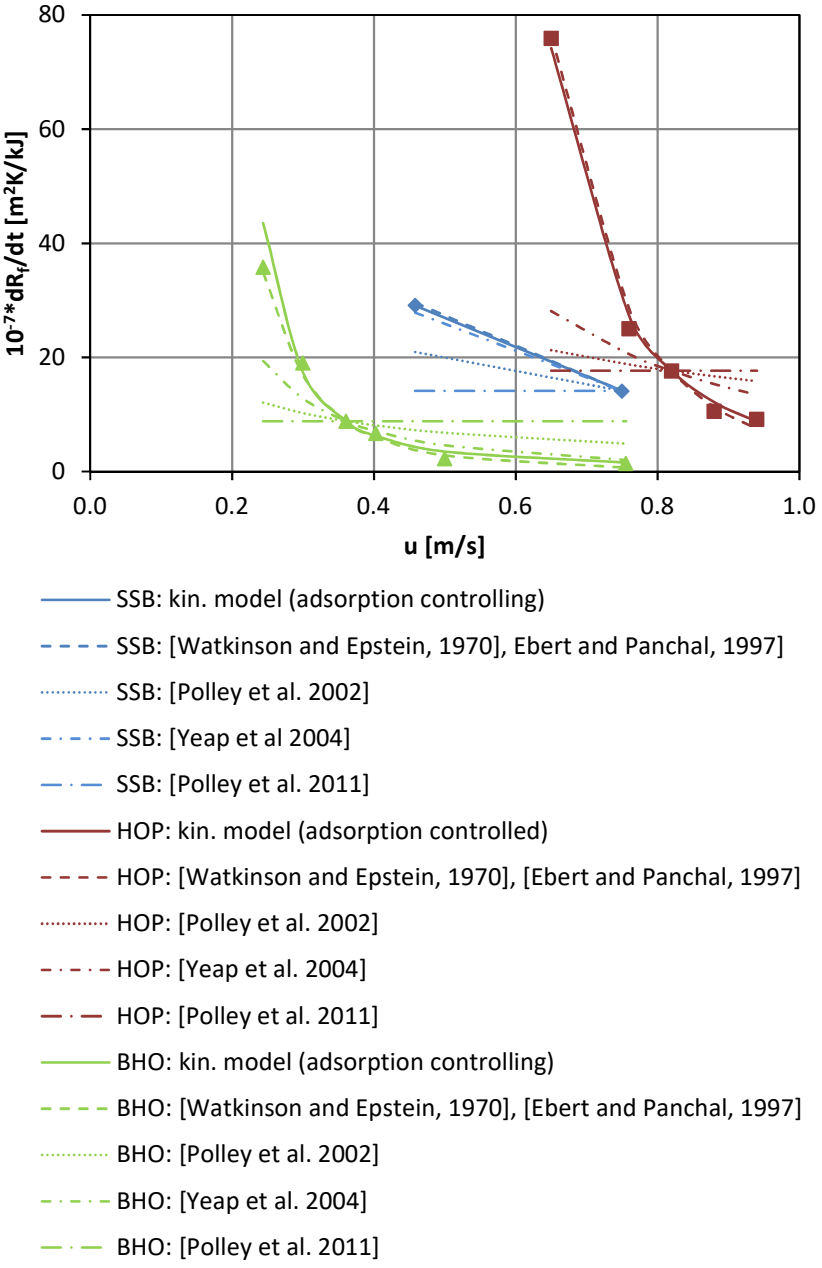

figure 63: Effect of velocity u on the initial fouling rate dR_f/dt, experimental data from [Watkinson 2005]. Compared with: 1) equations developed by kinetic modelling, for fouling controlled by adsorption (pseudo first order adsorption), 2) semi-empirical models; dots: experiment; lines: models

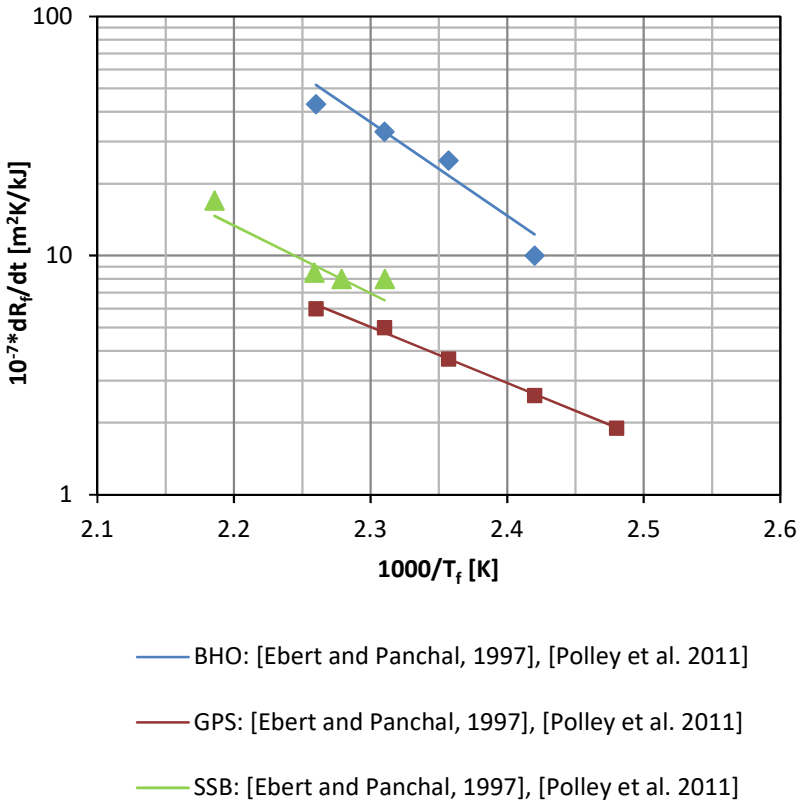

figure 64: Effect of surface temperature T_f on the initial fouling rate dR_f/dt, experimental data from [Watkinson 2005]. Compared with: semi-empirical models; dots: experiment; lines: models

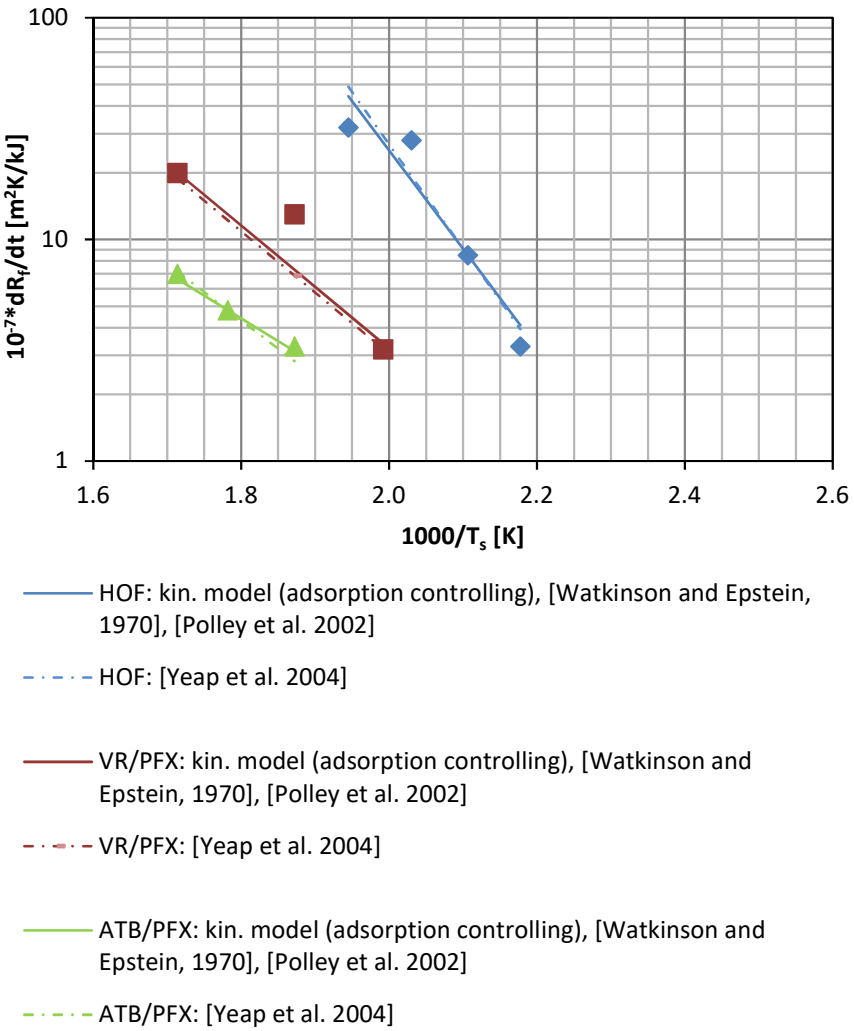

figure 65: Effect of surface temperature T_s on the initial fouling rate dR_f/dt, experimental data from [Watkinson 2005]. Compared with: 1) equations developed by kinetic modelling, for fouling controlled by adsorption (pseudo first order adsorption) 2) semi-empirical models; dots: experiment; lines: models

9 Variables affecting fouling

Chapter 9.1 to 9.4 summarize the variables affecting fouling, based on the finding gained above, that fouling is most likely an adsorption controlled process. If the adsorbed particles were not initially present in the oil, but were formed by either corrosion, asphaltene precipitation or chemical reaction, it is most likely to be controlled by a multistep process.

Removal seems to be relevant for all fouling mechanisms, see [Yiantsios and Karabelas 1994] and [Yang et al. 2014]. The steps influencing the fouling process for the different fouling mechanisms are summarized in table 65.

	Corrosion Fouling	Asphaltene Precipitation	Chemical Reaction Fouling			Particualte Fouling
			Autoxidation	Polymeri-zation	Thermal Cracking	
Reaction	**yes**	no	**yes**	**yes**	**yes**	no
Transport	no	no	no	no	no	no
Adsorption	**yes**	**yes**	**yes**	**yes**	**yes**	**yes**
Removal	**yes**	**yes**	**yes**	**yes**	**yes**	**yes**

table 65: Steps influencing fouling for the different fouling mechanisms

Reaction is strongly dependent on temperature, adsorption on velocity as well as temperature, removal on shear stress and therefore on velocity. Temperature and velocity are operating parameters which can be manipulated. Unlike, crude oil composition and impurities can't normally be influenced.

9.1 Crude oil composition

As a matter of fact, fouling is heavily influenced by the processed crude oil (see table 66). Crude oil composition and impurities can't normally be adjusted to specific target composition. For low sulphur light crude oils particulate fouling and autoxidation are the dominant fouling mechanism, fouling in medium sulphur crude oils is caused by corrosion and in unstable heavy oils by asphaltene precipitation [Watkinson 2005]. Sulfur content in heavy oils is quite high, therefore corrosion fouling could be expected to be a dominant fouling mechanism as well. However [Wang and Watkinson 2011] found, that for unstable heavy oil systems asphaltene precipitation is the major fouling mechanism. They suggest, that coke produced by aging effects from precipitated asphaltenes may protect metals from FeS formation.

Polymerization can be expected where cracked feedstocks have been added [Coletti and Hewitt 2015, S. 29].

Thermal cracking isn't a dominant fouling mechanism itself, as it starts at about 350°C and will therefore mainly occur in the crude distillation furnace. But thermal cracking still plays a role in the aging of deposits.

	Corrosion Fouling	Asphaltene Precipitation	Chemical Rection Fouling			Particualte Fouling
			Autoxidation	Polymeri-zation	Thermal Cracking	
Low sulphur light crude oil			x			x
Medium sulphur crude oil	x					
Unstable heavy oil systems		x				
Cracked feedstocks				x		

table 66: Dominant fouling mechanisms for different feedstocks

Several fouling mechanisms are influenced by impurities in the processed crude oil, see table 67.

Corrosion fouling is strongly affected by impurities in the processed crude oil. In particular oxygen, organic sulphur, hydrogen sulphide, nitrogen (normally from ammonia), chlorides, organic acids and corrosion products formed elsewhere can contribute to corrosion.

Autoxidation takes place in the presence of oxygen and can be catalysed by trace amounts of metal salts, especially of cobalt, manganese, iron, copper, chromium, lead and nickel.

Particulate fouling can occur when particles like dirt, clay or corrosion products formed elsewhere are transported with the crude oil.

	Corrosion Fouling	Asphaltene Precipitation	Chemical Rection Fouling			Particualte Fouling
			Autoxidation	Polymeri-zation	Thermal Cracking	
Metal salts (cobalt, manganese, iron, copper, chromium, lead and nickel)			x			
Oxygen	x		x			
Sulphur (organic sulphur or H_2S)	x					
Ammonia	x					
Chlorides	x					
Organic acids	x					
Dirt, clay						x
Corrosion products formed elsewhere	x					x

table 67: Fouling mechanisms influenced by impurities in the processed crude oil

9.2 Temperature

Fouling rates of all chemical fouling mechanisms and corrosion fouling increase as a function of temperature (see table 68). This can be easily explained with the Arrhenius equation (see equation 49), which describes the dependency of the rate constant from the temperature. It shows, that an increase in temperature leads to higher reaction rates.

equation 49 $r_c \sim \exp\left(\frac{-E}{R \cdot T}\right)$

Asphaltene precipitation doesn't lead to increased fouling at higher temperatures. The solubility of asphaltenes increases with temperature, asphaltene precipitation therefore decreases with higher temperatures.

The adsorption process of the suspended particles initially present or produced by corrosion, chemical reaction or asphaltene precipitation is favoured by higher temperature.
[Watkinson 2005] tested a number of oils and blends, including light and medium oils as well as heavy blends. The initial fouling rates had a high temperature dependency. He found, that for crude oils where particulate fouling is dominant, the dependency from temperature was less than for corrosion fouling and chemical reaction fouling dominated crude oils.

	Corrosion Fouling	Asphaltene Precipitation	Chemical Rection Fouling			Particualte Fouling
			Autoxidation	Polymeri-zation	Thermal Cracking	
Dependence of fouling from higher temperatures	Increases strongly	Decreases	Increases	Increases	Starts at about 350°C, increases strongly	Increases weakly

table 68: Dependency of fouling mechanisms from higher temperatures, found by [Watkinson 2005]

An increase in temperature also leads to a shorter induction period [Yang et al. 2011].

Thermal Cracking starts at about 350°C and increases strongly with temperature. In the preheat train usually 350°C are not reached. But thermal cracking still plays an important role in the aging of deposits [Wilson et al. 2009].

9.3 Velocity

Fouling rate for adsorption controlled fouling decreases with increasing velocity because of the limited contact time for adhesion to occur. Higher velocity increases shear stress and makes the adsorption step and therefore fouling deposition more difficult. It can even result in fouling removal.

Velocity has a second effect on fouling. Higher velocities lead to an increased convective heat transfer coefficient and reduce thermal resistance, which again leads to reduced wall temperatures. As wall temperatures corresponds with fouling, velocity has an additional effect on the fouling rate.

[Yang et al. 2014] simulated the dynamics and phase behaviour of crude-oil fouling. Higher bulk flow velocities resulted in strengthened interface wave propagation and braking and the entrainment of foulant droplets.

[Yiantsios and Karabelas 1994] set up a model for the removal kinetics of fouling of tube surfaces. They found in agreement with experimental results, that an increase in velocity results in a smaller asymptotic fouling resistance which is reached more rapidly.

9.4 Heat exchanger surface

Surface and surface conditions like roughness have a significant influence on the adsorption process. The smoother the surface, the less sites are available, where particles can be adsorbed.

[Hazelton et al. 2015] conducted experiments with different materials for heat transfer surfaces. For the crude oil and the temperature range they used, they suggested corrosion fouling and cracking to be the dominant fouling mechanisms. They found significant difference in the fouling behavior for 347 stainless steel, P91 steel and plain carbon steel. 347 stainless steel was the one who was most resistant to fouling, because it resists corrosion and therefore avoids corrosion fouling.

[Santos et al. 2004] and [Müller-Steinhagen and Zhao 1997] investigated modified surfaces of stainless steels by ion implementation. They found, that modifying the surfaces can lead to significant reduction of fouling.

Surface conditions (especially roughness) influence corrosion fouling. [Yeap et al. 2004] suggested, that surface roughness is responsible for the negative fouling resistance in the initial period which was reported by several experiments, see figure 66. After an initiation time in which no fouling occurs on the clean heat exchanger surface, a negative fouling resistance can occur because of the growing surface roughness which leads to higher turbulence level and to a higher heat transfer coefficient. [Coletti et al. 2011] were able to simulate the evolution of surface roughness and the negative fouling resistance for a single tube. They pointed out that roughness dynamics is important for pilot plant scale tests, because it has a small time scale.

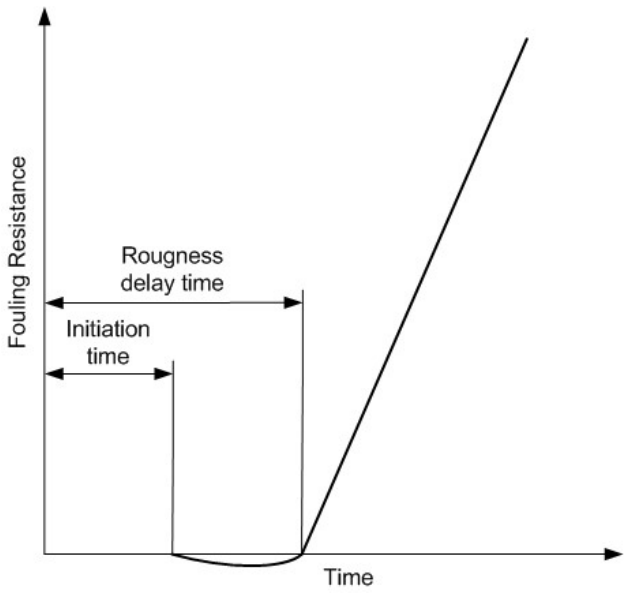

figure 66: After an initiation time in which no fouling occurs on the clean heat exchanger surface, a negative fouling resistance can occur because of the growing surface roughness

Several researchers investigated the impact of surface roughness. [Yang et al. 2014] showed, that shorter roughness delay time can be expected for initially not clean heat exchanger surfaces. [Herz et al. 2008] found that for rough surfaces the heat transfer coefficient decreases more rapidly than for smooth surfaces.

10 Fouling mitigation

Based on the finding gained above there are three possibilities, to mitigate fouling:

- prevention or restriction of adsorption;
- minimization of particles initially present in the oil and minimization of production of new particles by corrosion, chemical reaction or asphaltene precipitation;
- maximization of removal of adsorbed particles.

Therefore, several possible steps can be taken to mitigate fouling, see table 69.

	Corrosion Fouling	Asphaltene Precipitation	Chemical Rection Fouling			Particualte Fouling
			Autoxidation	Polymeri-zation	Thermal Cracking	
Elimination of inpurities	x		x			x
Higher velocity	x	x	x	x	x	x
Reduce surface temperatures	x		x	x	x	x
Use crude oils blends with low C.I.I.		x				
Use appropriate surface material	x	x	x	x	x	x
Chemical additives	x	x				x
Monitoring fouling and cleaning periodically	x	x	x	x	x	x

table 69: fouling mitigation

Chapter 10.1 to 10.8 summarize possibilities to mitigate fouling.

10.1 Elimination of impurities

Impurities present in the feed can lead to fouling, either by being absorbed on the heat exchanger surface itself or by being responsible for chemical reaction or corrosion.

Solid particles can be removed from the feed by feedstock pre-cleaning like filtration and sedimentation. It is recommended to provide adequate desalters, as desalters reduce trace metal contamination. Caustic scrubbing reduces sulfur compounds.

10.2 Higher velocities

Higher velocities reduce contact time for adsorption to take place and increase shear stress which leads to removal.

Higher velocities can be obtained by appropriate heat exchanger design, for example using less but longer tubes in standard shell and tube heat exchangers. In recent years alternative baffle types have been used, where baffles create a helical flow through the shell of the heat exchanger

(helichanger) and help avoid stagnant areas. Furthermore, alternative tube types, like corrugating tubes can be used to obtain higher velocities.

Several vendors sell tube inserts for crude oil shell and tube heat exchangers. The use of inserts in tubes, like Turbotal® or hiTRAN, who create shear stress by rotation of the fluid in the pipes, reduces fouling significantly.

All measures which increase shear stress and therefore reduce fouling lead to higher pressure drop over the heat exchangers.

Most crude oil heat exchangers are shell and tube type. Especially in the shell the fluid is not uniformly distributed, and stagnant areas with low velocities exist. Alternative heat exchanger design like plate type heat exchangers with more uniform flow would be a means to reduced fouling.

10.3 Reduced surface temperature

For all chemical fouling mechanisms, corrosion fouling, as well as the adsorption step of the particles on the surface of the heat exchanger, surface temperature has a considerable impact. Surface temperature is an operation parameter which can be influenced by a rearrangement of network structure and heat transfer-coefficients.

The crude preheat train consists of a set of heat exchangers which transfer energy from processed bottoms of the crude oil distillation column to the crude oil. By mixing different hot streams with different cold stream, the distribution of temperature in the network and therefore surface temperature of the individual heat exchangers can be influenced.

Several studies have been recently performed which deal with the network structure. [Yeap et al. 2004] developed a thermo-hydraulic model which includes a fouling model. With a modified temperature field plot it is possible to check potential network retrofits. [Coletti and Macchietto 2011] developed a dynamic, distributed thermo-hydraulic model undergoing fouling and aging. [Coletti et al. 2011] performed a case study for retrofit network design, which showed, that the steady state maximized energy recovery at steady state is not necessarily the best when fouling is considered. [Polley et al. 2013] undertook a case study for the retrofit of heat exchanger network with thermo-hydraulic simulation. [Wang and Smith 2013] developed an optimization algorithm for heat-exchanger networks and included a fouling model.

The heat transfer coefficient is influenced by velocity. Higher velocities lead to an increased convective heat transfer coefficient and reduce thermal resistance, which again leads to reduced wall temperatures. Therefore, all measures which enlarge velocity influence surface temperature as well.

10.4 Crude oil blends with low C.I.I.

Mixtures of incompatible crude oils are responsible for significant fouling due to asphaltene precipitation. By consequently using crude oil blends with C.I.I. less than 1 asphaltene precipitation cannot be completely ruled out, but strongly restricted.

10.5 Appropriate surface material

Surface roughness and surface material influence corrosion fouling and adsorption. By choosing appropriate surface material, fouling can be restricted.

This can be done by minimising surface roughness with surface coatings or surface treatment. Corrosion resistant material based on stainless steel or the use of non-corrosive materials like titanium can help avoid corrosion fouling.

10.6 Chemical additives

Chemical additives can improve stability of heavy fuel oils and therefore significantly reduce fouling caused by asphaltene precipitation.

Dispersants can keep particles in the bulk fluid and away from the surface and hinder adsorption, and corrosion fouling inhibitors can prevent corrosion fouling.

10.7 Online cleaning

Several measures like mechanical or acoustical vibration, pulsating flow, transport of cleaning devices through the tubes or thermal shocks can be seen as online cleaning, who hinder the formation of a fouling layer.

Cleaning devices can be sponge balls, brushes, chains or scrappers.

10.8 Monitoring fouling and cleaning periodically

A common way in dealing with fouling is to monitor fouling and to disassembly and manually clean the fouled heat exchangers. Mechanical cleaning like drills or scrappers, lances who produce liquid, steam or air jets and chemical cleaning methods are used.

In recent years several authors like [Bamrungsab and Siemanond 2016] published papers on the optimization of cleaning schedule.

11 Conclusion

By assuming the different steps of crude oil fouling like chemical reaction, corrosion, asphaltene precipitation, transport and adsorption to be rate controlling, fouling rate equations were developed which show the influence of the main variables fluid velocity and temperature on the fouling rate dR_f/dt. The proposed models, which show the influence of the main variables velocity and temperature on the fouling rate dRf/dt, in dependence of the controlling step for fouling, compare well with several experimental data from literature.

For all examined experimental data it turned out, that no matter, what the fouling mechanism was, asphaltene precipitation, particulate fouling, corrosion fouling or chemical reaction fouling, the effects of velocity and temperature on fouling rates dRf/dt could best be described with the developed equations from kinetic modelling for fouling controlled by adsorption. This leads to the assumption, that either single steps or binary combinations of steps control the fouling process, with adsorption always being involved.

The results of modelling were compared with five semi-empirical models for the prediction of time depending fouling in crude oil.

The findings from kinetic modelling can be used to mitigate fouling by prevention or restriction of adsorption, minimization of particles initially present in the oil and minimization of production of new particles by corrosion, chemical reaction or asphaltene precipitation.

List of references

Asomaning S., Watkinson A.P. (2000): "Petroleum stability and heteroatom species effects fouling of heat exchangers by asphaltenes"; Heat Transfer Engineering, 21 (3), 10–16

Bai Z.S., Wang H.L. (2007): "Crude oil desalting using hydrocyclones", Chemical Engineering Research and Design, 85, 1565-1579

Bamrungsab S., Siemanond K. (2016): "Heat exchanger network design with fouling effects", Proceedings of the 26th European Symposium on Computer Aided Process Engineering - ESCAPE 26, Elsevier B.V., Slovenia

Bott T.R. (1997): "Aspects of crystallization fouling", Experimental thermal and fluid science, 14, 356-360

Coletti F., Hewitt G.F. (2015): "Crude oil fouling. Deposit characterization, measurements, and modelling.", 1st edition, Gulf Professional Publishing, USA

Coletti F., Ishiyama E.M., Paterson W.R., Wilson D.I., Macchietto S. (2010): "Impact of Deposit Aging and Surface Roughness on Thermal Fouling: Distributed Model", AiChE Journal, Vol. 56, No. 12, 3257-3273

Coletti F., Macchietto S., (2011); "A Dynamic, Distributed Model of Shell-and-Tube Heat Exchangers Undergoing Crude Oil Fouling", Ind. Eng. Chem. Res., 50, 4515-4533

Coletti F., Macchietto S., Polley G.T., (2011): "Effects of fouling on performance of retrofitted heat exchanger networks: a thermo-hydraulic based analysis", Computers and Chemical Engineering 35, 907-917

Derakhshesh M., Eaton P., Newman B., Hoff A., Mitlin D., Gray M.R. (2013): "Effect of asphaltene stability on fouling at delayed coking process furnace conditions", Energy Fuels, 2013, 27, 1856-1864

Doug M. (2015): "Part 4: Atmospheric distillation", FQE Chemicals Blog über chemische Reinigung bei Fouling, Abrufdatum 04.12.2015, URL: http://blog.fqechemicals.com/atmospheric-distillation

Ebert W.A., Panchal C.B. (1997): " Analysis of exxon crude–oil–slip stream coking data", Proceedings of Fouling Mitigation of Industrial Heat–Exchange Equipment, 451-460, Begell House, New York

ESDU (2000): "Heat exchanger fouling in the pre-heat train of a crude oil distillation unit", Data Item 00013, ESDU International plc, London

Fogler H. S. (2006): "Elements of Chemical Reaction Engineering", 4th Edition, Prentice Hall Professonal Technical Refernece, USA

Hazelton M., Stephenson T., Lepore J., Subramani V., Mitlin D. (2015): "Sulfide promited chronic fouling in a refinery: a broad phenomenon spanning a range of heat transfer surfaces and oil types", Fuel, 160, 479-489

Herz A., Malayeri M.R., Müller-Steinhagen H. (2008): "Fouling of roughened stainless steel surfaces during convective heat transfer to aqueous solutions", Energy Conversion and Management, 49, 33841-3386

Karabelas A.J., Yiantsios S.G., Thonon B., Grillot J.M. (1997): "Liquid-side fouling of heat exchangers. An integrated R&D approach for conventional and novel designs", Applied thermal engineering, 17, 727-737

Levenspiel O. (1999): "Chemical Reaction Engineering", 3rd edition, John Wiley & Sons, USA

Mason T.G., Lin M.Y. (2003): "Asphaltene nanoparticle aggregation in mixtures of incompatible crude oils", Physical Review, 67, 050401-1-4

Melo L.F., Bott T.R. (1997): "Biofouling in water systems", Experimental thermal and fluid science, 14, 375-381

Morales-Fuentes A., Polley G.T., Picón-Núñez M., Martínez-Martínez S. (2012): "Modelling the thermo-hydraulic performance of direct fired heaters of crude processing", Applied thermal engineering, 39, 157-162

Müller-Steinhagen H., Malayeri H., Watkinson M.P. (2009): "Heat exchanger fouling: environmental impacts", Heat Transfer Engineering, 30 (10), 773-776

Müller-Steinhagen H., Zhao Q. (1997): "Investigation of low Fouling Surface Alloys made by Ion Implementation Technology", Chemical Engineering Science, Vol. 52, No. 19, 3321-3332

Nasr M.R.J, Givi M.M (2006): "Modelling of crude oil fouling in preheat exchangers of refinery distillation units", Applied Therm. Eng. Vol. 26, 1572-1577

Oliveira R. (1997): "Understanding adhesion: A means for preventing fouling", Experimental thermal and fluid science, 14, 316-322

Panchal C.B., Kuru W.C., Liao C.F., Ebert W.A., Palen J.W. (1999): "Treshold conditions for crude oil fouling", Understanding Heat Exchanger Fouling and its Mitigation, 273-279, Begell House, New York

Polley G.T., Wilson D.I., Yeap B.L., Pugh S.J. (2002): "Evaluation of laboratory crude oil treshold fouling data for application to refinery pre-heat trains", Applied Thermal Engineering 22, 777-788

Polley G.T. (2010): "Review of the development of models for the prediction of fouling rates in exchangers heating crude oil", Proc. 11th Annual Intl. Conf. Petroleum Phase Behaviour and Fouling, 13-17, Jersey City

Polley G.T., Tamakloe E., Picon-Nunez M. (2011): "Models for chemical reaction fouling", Aiche Spring Meeting, Chicago

Polley G.T., Tamakloe E., Nunez M.P., Ishiyama E.M., Wilson D.I. (2013): "Applying thermo-hydraulic simulation and heat exchanger analysis to the retrofit of heat recovery systems", Applied Thermal Engineering, 51, 137-143

Rautenbach R., Melin T. (2007): " Membranverfahren, Grundlagen der Modul- und Anlagenauslegung", 3rd edition, Springer, Berlin, Heidelberg

Saleh Z., Sheikholeslami R., Watkinson A.P. (2003): "Fouling characteristics of a light Australian crude oil", Proc. Heat Exchanger Fouling and Cleaning: Fundamentals and Applications, 225-223, Santa Fe, NM

Saleh Z.S., Sheikholeslami R., Watkinson A.P. (2005): "Blending effects on fouling of four crude oils", ECI symposium series, Volume RP2: Proceedings of 6th international conference on heat exchanger fouling and challenges and opportunities, Engineering conference international, Germany

Santos O., Nylander T., Rosmaninho R., Rizzo G., Yiantsios S., Andritsos N., Karabelas A., Müller-Steinhagen H., Melo L., Boulangé-Petermann L., Gabet C., Braem A., Trägårdh C., Paulsson M. (2004): "Modified stainless steel surfaces targeted to reduce fouling - surface characterization", Journal of Food Engineering 64, 63-79

Scarborough C.E., Cherringhton D.C., Diener R., Golan L.P. (1979): "Coking of crude oil at high heat flux levels", Chemical Engineering Progress 78, 41-46

Speight J.G. (2015): "Fouling in refineries", 1st edition, Gulf Professional Publishing, UK

Somerscales E.F.C. (1997): "Fundamentals of corrosion fouling", Experimental thermal and fluid science, 14, 335-355

TEMA (1999): "Standards of Tubular Exchanger Manufacturers Associaton", eight edition, Tubular Exchanger Manufacturers Association, Tarrytown, NY

VDI (2006): "VDI-Wärmeatlas", tenth edition, Verein Deutscher Ingenieure VDI-Gesellschaft Verfahrenstechnik und Chemieingenieurwesen (GVC), Berlin Heidelberg

Wang Y., Smith R. (2013): "Retrofit of a Heat-Exchanger Network by Considering Heat-Transfer Enhancement and Fouling", Ind. Eng. Chem. Res., 52, 8527-8537

Wang W., Watkinson A.P. (2011): "Iron sulphide and coke fouling from sour oils: review and initial experiments", Proceedings of international conference on heat exchanger fouling and cleaning, published online: www.heatexchanger-fouling.com

Watkinson A.P., Epstein N. (1970): "Particulate Fouling of Sensible Heat Exchangers", Proc. 4th Int'l Heat Transfer Conf. Vol. 1 paper, HE1.6 12pp

Watkinson A.P. (2005) : "Deposition from Crude Oils in Heat Exchangers", ECI symposium series, Volume RP2: Proceedings of 6th international conference on heat exchanger fouling and challenges and opportunities, Engineering conference international, Germany

Watkinson A.P., Wilson D.I. (1997): "Chemical Reaction Fouling: A Review", Experimental thermal and fluid science, 14, 361-374

Wauquier J.P. (1995): "Petroleum Refining, Volume 1: Crude Oil. Petroleum Products. Process Flowsheet.", Èdition Technip, Paris

Wiehe I.A., Kennedy R.J., Dickakian G. (2001): "Fouling of nearly incompatible oils", Energy Fuels, 15 (5), 1057–1058

Wilson D.I., Ishiyama E.M. Paterson W.R., Watkinson A.P. (2009): "Ageing: Looking Back and Looking Forwards", Proceedings of international conference on heat exchanger fouling and cleaning, published online: www.heatexchanger-fouling.com

Wilson D.I., Polley G.T., Pugh S.J. (2005): "Ten years of Ebert, Panchal and the 'Treshold Fouling' Concept", ECI symposium series, Volume RP2: Proceedings of 6th international conference on heat exchanger fouling and challenges and opportunities, Engineering conference international, Germany

Yang M., O'Meara A., Crittenden B.D. (2011): "Determination of Crude oil Fouling Tresholds", Proceedings of international conference on heat exchanger fouling and cleaning, published online: www.heatexchanger-fouling.com

Yang M., Young A., Niyetkaliyev A., Crittenden B. (2011): "Modelling fouling induction periods", International Journal of Thermal Science, 51, 175-183

Yang M. Crittenden B.D. (2012): "Fouling tresholds in bare tubes and tubes fitted with inserts", Applied Energy 89, 67-73

Yang J., Jimenez Serratos M.G., Fari-Arole D., Müller E.A., Matar O.K. (2014): "Crude Oil Fouling: Fluid Dynamics, Reactions and Phase Change", Procedia IUTAM, 15 186-193

Yeap B.L., Wilson D.Il, Polley G.T., Pugh S.J. (2004): "Mitigation of Crude Oil Refinery Heat Exchanger Fouling trough Retrofits based on thermo-hydraulic Fouling Models", Trans IChem E, Part A- 53-71

Yiantsios S.G., Karabelas A.J. (1994): "Fouling of Tube Surfaces: Modelling of Removal Kinetics", AiChE Journal, Vol. 40, No. 11, 1804-1813

Nomenclature

Romans

a	-	reaction order for corrosion fouling
a_s	$m^2\ m^{-3}$	surface area per reactor volume
a_i	$m^2\ K\ J^{-1}$	parameter in fouling model
A	m^2	reactor surface area
A_{AD1}	$m^2\ mol^{-1}\ s^{-1}$	constant in rate equation for first order adsorption
A_{AD2}	$m^4\ mol^{-2}\ s^{-1}$	constant in rate equation for second order adsorption
A_{b0}	$mol\ m^{-3}\ s^{-1}$	constant for pseudo zero order reaction in the bulk
A_{b1}	s^{-1}	constant for first order reaction in the bulk
A_{b2}	$m^3\ s^{-1}\ mol^{-1}$	constant for second order reaction in the bulk
A_q	m^2	reactor cross section
A_{De1}	s^{-1}	constant for first order desorption
A_{De2}	$m^2\ s^{-1}\ mol^{-1}$	constant for second order desorption
A_{f0}	$mol\ m^{-2}\ s^{-1}$	constant for pseudo zero order reaction in the film
A_{f1}	s^{-1}	constant for first order reaction in the film
A_{f2}	$m^2\ s^{-1}\ mol^{-1}$	constant for second order reaction in the film
$A_{FeS,b}$	$m^{3(a+b-1)}\ mol^{(a+b-1)}\ s^{-1}$	constant for corrosion fouling in the bulk
$A_{FeS,f,1}$	s^{-1}	constant for corrosion fouling in the film, first order
$A_{FeS,f,2}$	$m^4\ mol^{-2}\ s^{-1}$	constant for corrosion fouling in the film, 2nd order
$A_{FeS,s,1}$	s^{-1}	constant for corrosion fouling on the surface, first order
$A_{FeS,s,2}$	$m^4\ mol^{-2}\ s^{-1}$	constant for corrosion fouling on the surface, 2nd order
A_{s0}	$mol\ m^{-2}\ s^{-1}$	constant for pseudo zero order reaction on the surface
A_{s1}	s^{-1}	constant for first order reaction on the surface
A_{s2}	$m^2\ s^{-1}\ mol^{-1}$	constant for second order reaction on the surface
A_q	m^2	cross section area
b	-	reaction order for corrosion fouling
b_i	-	parameter in fouling model
c	K^{-1}	constant for asphaltene precipitation
c_a	$mol\ m^{-3}$	asphaltene concentration
c_{A*S}	$mol\ m^{-2}$	sites, occupied by A
c_{Ab}	$mol\ m^{-3}$	concentration of A in the bulk

c_{Ab0}	mol m^{-3}	concentration of A in the bulk at t=0
c_{Af}	mol m^{-2}	concentration of A in the film
c_{AS}	mol m^{-2}	concentration of A on the surface
c_{Fe++}	mol m^{-3}	concentration of dissolved iron
c_{Fb}	mol m^{-3}	concentration of F in the bulk
c_{Fs}	mol m^{-2}	concentration of F on the surface
c_{F*S}	mol m^{-2}	sites, occupied by F
c_i	dep. on model	parameter in fouling model
c_S	mol m^{-3}	sulfur concentration
c_{Sb}	mol m^{-3}	sulfur concentration in the bulk
c_{Sb0}	mol m^{-3}	sulfur concentration in the bulk at t=0
c_{Sf}	mol m^{-2}	sulfur concentration in the film
c_{Ss}	mol m^{-2}	sulfur concentration on the surface
c_t	mol m^{-2}	total number of sites
$c_{t,0}$	mol m^{-2}	total number of sites at t=0
c_v	mol m^{-2}	vacant sites
C	-	integration constant
d	m	pipe diameter
d_i	-	parameter in fouling model
D_{AB}	m^2 s^{-1}	diffusion coefficient
E	J mol^{-1}	activation energy
e	$m^{13/3}$ $s^{8/3}$ $kg^{2/3}$ $K^{-2/3}$	parameter in fouling model
f_a	Pa	fugacity of the precipitated asphaltenes
f_a^0	Pa	standard fugacity of the precipitated asphaltenes
f_a^b	Pa	fugacity of the asphaltenes in the bulk liquid
f_a^{0b}	Pa	standard fugacity of the asphaltenes in the bulk liquid
h_{film}	m^2 K W^{-1}	film transfer coefficient
$h_{m,a}$	J mol^{-1}	melting enthalpy of asphaltenes
k	W m^{-2} K^{-1}	heat transfer resistances
k_a	s^{-1}	rate constant for asphaltene precipitation
k_{AD1}	m^2 mol^{-1} s^{-1}	rate constant of first order adsorption
k_{AD2}	m^4 mol^{-2} s^{-1}	rate constant for second order adsorption

k_{b0}	mol m^{-3} s^{-1}	rate constant for pseudo zero order reaction in the bulk
k_{b1}	s^{-1}	rate constant for first order reaction in the bulk
k_{b2}	m^3 s^{-1} mol^{-1}	rate constant for second order reaction in the bulk
k_{De1}	s^{-1}	rate constant of first order desorption
k_{De2}	m^2 s^{-1} mol	rate constant for second order desorption
k_{Di}	m s^{-1}	mass transfer coefficient
k_{f0}	mol m^{-2} s^{-1}	rate constant for pseudo zero order reaction in the film
k_{f1}	s^{-1}	rate constant for first order reaction in the film
k_{f2}	m^2 s^{-1} mol	rate constant for second order reaction in the film
$k_{FeS,b}$	$m^{3(a+b-1)}$ $mol^{(1-a-b)}$ s^{-1}	rate constant for corrosion fouling in the bulk
$k_{FeS,f}$	$mol^{(1-a)}$ s^{-1}	rate constant for corrosion fouling in the film
$k_{FeS,f,1}$	s^{-1}	rate constant for corrosion fouling in the film, first order
$k_{FeS,f,2}$	m^2 s^{-1} mol^{-1}	rate constant for corrosion fouling in the film, 2nd order
$k_{FeS,s}$	$mol^{(1-a)}$ s^{-1}	rate constant for corrosion fouling on the surface
$k_{FeS,s,1}$	s^{-1}	rate constant for corrosion fouling on the surface, first order
$k_{FeS,s,2}$	m^2 s^{-1} mol^{-1}	rate constant for corrosion fouling on the surface, 2nd order
k_{s0}	mol m^{-2} s^{-1}	rate constant for pseudo zero order reaction on the surface
k_{s1}	s^{-1}	rate constant for first order reaction on the surface
k_{s2}	m^2 s^{-1} mol	rate constant for second order reaction on the surface
l	m	reactor (pipe) length
m	kg m^{-2}	deposit mass per area
$\dot{m}_f$	kg s^{-1}	mass flow of f
M_f	kg $kmol^{-1}$	molar mass of fouling deposit
n	kmol m^{-2}	deposit per area
n_v	-	velocity exponent for fouling model
$\dot{N}$	mol s^{-1}	molar flow in the bulk liquid
$\dot{N}_a$	mol s^{-1}	molar flow of precipitated asphaltenes
$\dot{N}_a{}^b$	mol s^{-1}	molar flow of asphaltenes in the bulk liquid
Nu	-	Nusselt number
Pr	-	Prandtl number
q_w	W m^{-2}	heat flow density
r_a	mol m^{-3} s^{-1}	rate of reaction for asphaltene precipitation
r_{Ad}	mol s^{-1} m^{-2}	rate of adsorption per unit surface area

$r_{Ad,1}$	mol s^{-1} m^{-2}	rate of adsorption per unit surface area, pseudo first order
$r_{Ad,2}$	mol s^{-1} m^{-2}	rate of adsorption per unit surface area, pseudo second order
r_{BDi}	mol s^{-1} m^{-2}	rate of back diffusion per unit surface area
r_c	mol m^{-3} s^{-1}	rate of reaction
r_{De}	mol m^{-2} s^{-1}	rate of desorption per unit surface area
$r_{De,1}$	mol m^{-2} s^{-1}	rate of desorption per unit surface area, pseudo first order
$r_{De,2}$	mol m^{-2} s^{-1}	rate of desorption per unit surface area, pseudo second order
r_{Di}	mol m^{-2} s^{-1}	rate of diffusion per unit surface area
r_{FeS}	mol m^{-2} s^{-1}	rate of corrosion per unit surface area
$r_{FeS,b}$	mol m^{-3} s^{-1}	rate of corrosion in the bulk
$r_{FeS,f}$	mol m^{-2} s^{-1}	rate of corrosion in the film per unit surface area
$r_{FeS,s}$	mol m^{-2} s^{-1}	rate of corrosion on the surface per unit surface area
r_{Re}	mol m^{-2} s^{-1}	reaction rate per unit surface area
$r_{Re,b}$	mol m^{-3} s^{-1}	reaction rate in the fluid bulk
$r_{Re,b,0}$	mol m^{-3} s^{-1}	reaction rate in the fluid bulk, pseudo zero order
$r_{Re,b,1}$	mol m^{-3} s^{-1}	reaction rate in the fluid bulk, pseudo first order
$r_{Re,b,2}$	mol m^{-3} s^{-1}	reaction rate in the fluid bulk, pseudo second order
$r_{Re,f}$	mol m^{-2} s^{-1}	reaction rate in the film per unit surface area
$r_{Re,f,0}$	mol m^{-2} s^{-1}	reaction rate (film) per unit surface area, pseudo zero order
$r_{Re,f,1}$	mol m^{-2} s^{-1}	reaction rate (film) per unit surface area, pseudo first order
$r_{Re,f,2}$	mol m^{-2} s^{-1}	reaction rate (film) per unit surface area, pseudo second order
r_f	mol m^{-2} s^{-1}	overall fouling rate per unit surface area
R	kg m^2 s^{-2} mol^{-1} K^{-1}	gas constant
R_f	m^2 K W^{-1}	fouling resistances
Re	-	Reynolds number
s	m	pipe thickness
S	-	surface site
s_f	m	deposit thickness
Sc	-	Schmidt number
Sh	-	Sherwood number
t	s	time
T	K	temperature
T_b	K	bulk temperature

T_f	K	film temperature
$T_{m,a}$	K	melting temperature of asphaltenes
T_s	K	surface temperature
T_{sb}	K	temperature, at which all asphaltenes are dissolved
u	$m\ s^{-1}$	mean velocity
v	-	proportional factor
V	m^3	reactor volume
V_m	$m^3\ mol^{-1}$	molar volume
x_a^b	-	molar concentration of asphaltenes in the bulk liquid

Greek

α	$W\ m^{-2}\ K^{-1}$	heat transfer coefficients
γ_a^b	-	fugacity coefficient of asphaltenes in the bulk liquid
λ	$W\ m^{-1}\ K^{-1}$	thermal conductivity
λ_f	$W\ m^{-1}\ K^{-1}$	thermal conductivity deposit
μ	$kg\ m^2\ s^{-1}$	dynamic viscosity
τ_w	Pa	wall shear stress
υ	$m^2\ s^{-1}$	kinematic viscosity
ρ	$kg\ m^{-3}$	density
ρ_f	$kg\ m^{-3}$	density of the fouling layer

Subscripts

i	inner
o	outer